Alma Mater Studiorum Universitá di Bologna
dipartimento di chimica fisica e inorganica

Dottorato di Ricerca in Scienze Chimiche XIX Ciclo
S.S.D. CHIM/02

Ab Initio Computation of Electric Properties and Intermolecular Forces

Supervisor:
Prof.
G. L. Bendazzoli

Presented by:
Dott.
Antonio Monari

PhD Coordinator:
Prof. V. Balzani

Bologna, March 2007

"What is number? What are space and time? What is mind, and what is matter? I do not say that we can here and now give definitive answers to all those ancient questions, but I do say that a method has been discovered by which we can make successive approximations to the truth, in which each new stage results from an improvement, not a rejection, of what has gone before. In the welter of conflicting fanaticism, one of the unifying forces is scientific truthfulness, by which I mean the habit of basing our beliefs upon observations and inferences as impersonal, and as much divested of local and temperamental bias, as is possible for human beings."

Bertrand Russell (1945)

Contents

List of Tables

List of Figures

Introduction

Intermolecular Forces and Electric Properties play a key role in the understanding of many physical and chemical phenomena and in the characterization of a molecular system [1].

Electric properties (mainly multipole moments and polarizabilities) directly reflect the electron density distribution of the system, influencing a significative amount of molecular (or intermolecular) properties. We recall, for instance, their role on many optical or spectroscopical properties, such as:

- refraction index
- absorption constant in optical spectroscopy
- selection rules in rotational and vibrational spectroscopy (Micro Wave, IR, Raman)
- optical activity
- non linear optical phenomena

It is clear that the determination of high quality value for those observables represents a valuable target for Quantum Chemistry in order to give useful parameters for the modeling of important systems both at micro and macro level.

Intermolecular Forces, on their side, show an analogous valuable importance in the fields of theoretical or applied chemistry. In this context for Intermolecular Forces we consider the forces, mainly due to electric type interactions, exercising among atoms or molecules, the latter considered, in a wider sense, as stable aggregates of nuclei and electrons (monomers). It is crucial to recall that Intermolecular Forces depend from the Electric Properties of the single monomers and from their relative orientation [2]. Other kinds of forces, such as gravitational, magnetic or nuclear, may be neglected due to their low intensity (the first two types) or to their very short range (the latter one). Although their intensity is some order of magnitude lower than the energy of the isolated molecules

or the binding energy, Intermolecular Forces are of great importance in describing the behavior of numerous systems in the fields of material science, catalysis, biochemistry. As an example we may cite:

- transport properties in real fluid
- cohesion properties in condensed systems
- liquid crystal behavior and their response to external perturbations
- enzyme-substrate interactions in biochemistry and drug chemistry
- interaction in heterogenous catalysis

This thesis shows the study and application of *high level ab initio* quantum chemistry methods (mainly Full CI and Coupled Cluster) to the determination of electric properties and intermolecular forces of small systems. Moreover since this kind of problems are computationally high demanding and require the use of different codes and software some emphasis will be put on the building of a common format allowing the interfacing of such codes, and ultimately on the moving towards grid computation.

Overview

The present thesis will be organized as follows:

- Chapters 1, 2 and 3 will be dedicated to the presentation of the theory of Intermolecular Forces and Electric Properties, of the common *ab initio* computational strategies and to the briefly recall of the computational machinery used in this work.
- Chapters 4, 5, 6, 7 and 8 will be devoted to the presentation and discussion of innovative methods implemented or applied in our laboratory together with original results.
- Chapters 9, 10 and 11 will be dedicated to the description of our proposal for a grid oriented common format for Quantum Chemistry problems and of the FORTRAN API and to the illustration of the first applications.

Part I

Intermolecular Forces and Electric Properties: Theory

Chapter 1

Theory of Intermolecular Forces

1.1 Introduction

In the conditions of validity of Born Oppenheimer approximation one can define intermolecular interaction energy, for fixed nuclei position, as the difference between the energy of the system $A + B$ in a given particular configuration and the energy resulting when A and B are brought to infinite separation. In that context assuming the distance is such that we can safely neglect internal separation [3]. The interaction energy will depend on the distance R defining the separation of the monomers and the Euler angle Ω specifying their relative orientation.

Intermolecular Energies are extremely small, their ratio with respect to the energy of the individual monomers being of the orders of 10^{-5} [1] (Table 1.1) .

It is clear that the required interaction energies are in general so small compared with the energies of the separated molecules that any attempt to calculate them at the *ab initio* method is bound to meet great difficulties, and requires the use of an high level of theory and of consistently large basis sets (possibly with diffuse and high angular momenta functions); this leads to a significative increase in the computational cost of the problem.

Two main approaches have been used in quantum chemistry to treat these phenomena:

1. Supramolecular approach
2. Perturbation Theory

[1] Here and elsewhere, except where differently stated atomic units are used: length Bohr $a_0 = 5.29177 \cdot 10^{-11}$ m, energy hartree $h = 4.35944 \cdot 10^{-18}$ J, electron charge e=1 a.u.=$1.60218 \cdot 10^{-19}$ C, multipole moments $\mu^l = ea_0^l$, multipole polarizabilities $\alpha_{l,l'} = e^2 a_0^{l+l'} h^{-1}$, intermolecular coefficients $C_n = a_0^{-n} h$.

Table 1.1: Well depths at the experimental geometries, total energy of the isolated molecules and their ratios for some small dimers [2]

Dimer	He_2	$(H_2)_2$	$(N_2)_2$	$(HF)_2$	$(H_2O)_2$
R	5.6	6.5	8.0	5.1	5.6
$E^{int} \cdot 10^{-3}$	-0.034	-0.117	-0.392	-7.76	-8.92
E_0	-5.807	-2.349	-218.768	-200.607	-152.877
$\frac{E^{int}}{E_0} \cdot 10^{-5}$	0.58	4.98	1.79	3.87	5.83

In the first one the energy of the dimer $A + B$ is computed for each geometry therefore directly obtaining an intermolecular potential energy hypersurface [4, 5].
In the second one the interaction is treated as a small perturbation via an extension of the common Rayleigh-Schrödinger perturbation theory [6, 7].

Both these approaches will be treated in this thesis in detail, while many original applications will be shown and discussed; in particular for the determination of long range dispersion interactions.

1.1.1 Classification of Intermolecular Forces

Intermolecular forces are repulsive at short range and attractive at large distances, we can identify a number of facts that are responsible for attraction and repulsion of molecular systems: this fact leads to a very well known classification of intermolecular forces contributes in term of their physical meaning.

Electrostatic (coulombic) energy: it gives the semiclassical interaction between rigid charge distribution of the two monomers. Strictly pairwise additive, it appears in first order of perturbation theory. For systems with permanent multipole moments it varies at long range as the R^{-n} (R being the intermolecular separation and n the order of the interaction), while at short range it decreases exponentially with the distance.

Induction (polarization) energy: it is the additive term resulting from the distortion of the charge distribution of one molecule by the mean electric field provided by the other, and vice versa. If one or both monomers possesses permanent multipole moments this will be a long range contribution. It is not pairwise additive and it is described in second order perturbation theory.

Dispersion energy: it describes the intermolecular electron correlation due to the instantaneous coupling of the density fluctuation mutually induced in each molecule. It is a long range interaction, pairwise additive and appears in second order perturbation theory. For neutral atom having spherical symmetry dispersion is more important than induction at large distances, but at short range the situation is reversed.

Exchange energy: it is the first order term arising from the antisymmetry requirement of the wave function. Attractive for closed shell it is a 2-electron contribution surviving even for zero-overlap.

Overlap (penetration) energy: it is the other first order contribution arising from the antisymmetry requirement, it describes the Pauli repulsion due to the interpenetration of the charge clouds of molecules having a closed shell structure. It comprises 1-electron and 2-electron terms, the first being larger but vanishing at zero overlap. Like the first one it is a non-classical contribution depending on the nature of the spin coupling of the interacting systems. Strictly non-additive it decays exponentially with the intermolecular separation.

Second order penetration energy: it is a second order contribution including exchange and overlap corrections to induction and dispersion, it implies intermolecular overlap between occupied orbitals of one molecule and vacant orbitals of the other. It is usually a very small term that can be neglected without a too much significant loss in accuracy.

1.2 Molecules in Static Electric Fields

1.2.1 Multipole Operators

As previously stated all the contributions to the intermolecular interaction energy derive ultimately from the Coulombic interactions between their particles (electrons). In order to derive a consistent theory we should be able to describe the way in which the charge is distributed in a molecule. For most purposes this is done in a simple and compact way using the so called multipole operators [1], and their expectation values the multipole moments.

Multipole operators and moments can be defined in two ways. One uses the mathematical language of cartesian tensors, while the other, the spherical tensors formulation, is based on the spherical harmonics. The latter is more flexible and powerful expecially

for more advanced works, but the first one is somehow easier to understand. In any case the two descriptions are closely related and in many applications it is possible to use either.

1.2.1.1 Cartesian Definition

In a formal way the first, and the simplest, multipole moment is the total charge $q = \sum_a e^a$, with the sum running over all the charged particles in the molecules. The next operator is the very famous dipole operator. The name derive from the fact that his moment (expectation value) can be considered as being generated by two charges of equal magnitude q separated by a distance d, in this case the magnitude of the moment is $q \cdot d$ and the vector conventionally goes from the negative charge to the positive one. More generally the operator for the z-component takes the form,

$$\hat{\mu}_z = \sum_a e^a a_z \tag{1.1}$$

and similarly for $\hat{\mu_x}$ and $\hat{\mu_y}$, where obviously the vector a has been used to describe the position of each charged particle. The corresponding dipole moment is obtained by the corresponding expectation value of the previous operator so for a system in the state $|n\rangle$

$$\begin{aligned} \mu_\alpha &= \langle n|\hat{\mu}_\alpha|n\rangle \\ &= \int \rho_n(r) r_\alpha dr \end{aligned} \tag{1.2}$$

where α is one of the coordinates and the second equation has been expressed in terms of molecular charges density ($\rho(r)$). If the integration is carried over the electron coordinates only (including anyway the nuclear charge) we get the dipole moment for a fixed nuclear geometry. In order to exactly match the experimental value we have to integrate over the nuclear coordinates too, this means perform a vibrational averaging of the dipole moment value.

The next of the multipole operators and moments is the quadrupole moment, the name again recalls the fact that this charge distribution can be obtained with two charges of equal magnitude, two positive and two negative. The operator is slightly more complicated and can take the general form

$$\hat{\Theta}_{\alpha\beta} = \sum_a e^a (\frac{3}{2} a_\alpha a_\beta - \frac{1}{2} a^2 \delta_{\alpha\beta}) \tag{1.3}$$

where δ is the Kronecker delta $\delta_{\alpha\beta} = 1$ if $\alpha = \beta$, $\delta_{\alpha\beta} = 0$ if $\alpha \neq \beta$. From the previous relation it follows that $\Theta_{xx} + \Theta_{yy} + \Theta_{zz} = 0$ giving rise to the well know traceless relation of quadrupole.

For the sake of simplicity we will skip the definition, in cartesian form, of the other multipole operators, for instance octupole, let us only generalise what we derived to any given rank: the multipole operator of rank n has n suffixes and takes the form:

$$\hat{\xi}^{(n)}_{\alpha\beta\ldots\nu} = \frac{(-1)^n}{n!} \sum_a e^a a^{2n+1} \frac{\partial}{\partial a_\nu} \cdots \frac{\partial}{\partial a_\beta} \frac{\partial}{\partial a_\alpha} \left(\frac{1}{a}\right) \tag{1.4}$$

from the previous definition it follows that $\hat{\xi}$ is symmetric with respect to the permutation of its suffixes, and it is traceless with respect of any pair of suffixes $\hat{\xi}_{\alpha\alpha\gamma\ldots\nu} = 0$, moreover the maximum number of independent component is equal to $2n + 1$

1.2.1.2 Spherical tensor definition

In many cases, expecially when dealing with advanced applications or high rank multipoles, it is convenient to express the operators using the spherical harmonics, in fact even if the corresponding formulae are sometimes more difficult to derive, their application and use is simplified with respect to the analogous cartesian formalism [8].

In terms of the regular spherical harmonics multipole operators are defined as:

$$\hat{Q}_{lm} = \sum_a e^a R_{lm}(a) \tag{1.5}$$

where $R_{lm}(a)$ are the corresponding spherical harmonics, in practice however it is usually more convenient to use the real form:

$$\hat{Q}_{lk} = \sum_a e^a R_{lk}(a) \tag{1.6}$$

It should be noted how the independent spherical harmonics of rank n are exactly $2n + 1$, so again for a given rank the independent multipole operator components are $2n+1$, in accordance with the result previously obtained using cartesian tensor formalism.

1.2.2 The energy of a molecule in a static electric field

We may consider a molecule in an external potential $V(r)$. This potential has an electric field associated, which formally may be defined as $F_\alpha = -\frac{\partial V}{\partial r_\alpha} = -\nabla_\alpha V$, consider moreover the field gradient $F_{\alpha\beta} = -\frac{\partial^2 V}{\partial r_\alpha \partial r_\beta} = -\nabla_\alpha \nabla_\beta V$. Let us use the simplified notation $V_\alpha = -\frac{\partial V}{\partial r_\alpha}$ and $V_{\alpha\beta} = -\frac{\partial^2 V}{\partial r_\alpha \partial r_\beta}$ in that case we will have $F_\alpha = -V_\alpha$ and $F_{\alpha\beta} = -V_{\alpha\beta}$.

If, after a suitable choice of the origin and the set of coordinates, we expand the potential in a Taylor series we get:

$$V(r) = V(0) + r_\alpha V_\alpha(0) + \frac{1}{2} r_\alpha r_\beta V_{\alpha\beta} + \frac{1}{3!} r_\alpha r_\beta r_\gamma V_{\alpha\beta\gamma} + \cdots \tag{1.7}$$

where we have used the Einstein sum rule: a repeated suffix implies summation over the three coordinates values (x,y,z) of that suffix. We are interested to find out the energy of the molecule in the presence of this potential, so the involved perturbation Hamiltonian operator is

$$\mathcal{H}' = \sum_a e^a \hat{V}(a) \tag{1.8}$$

where as usual sum is taken over all electrons and nuclei of the molecules, substituting we obtain:

$$\mathcal{H}' = V(0) \sum_a e^a + V_\alpha(0) \sum_a e^a a_\alpha + \frac{1}{2} V_{\alpha\beta}(0) \sum_a e^a a_\alpha a_\beta + \cdots \tag{1.9}$$

abbreviating for $V(0)$ to V and so on and introducing the zeroth $\hat{M}$, first $\hat{M}_\alpha$ and second $\hat{M}_{\alpha\beta}$ moment we may write the perturbation as:

$$H' = V\hat{M} + V_\alpha \hat{M}_\alpha + \frac{1}{2} V_{\alpha\beta} \hat{M}_{\alpha\beta} + \cdots \tag{1.10}$$

the zeroth moment is easily recognized as the charge operator q, as well as no difficulties arise in defining the first order moment as the dipole moment operator $\hat{\mu}_\alpha$, for the second order momentum some algebraical work is necessary in order to get it in a more recognizable form.

Let us define a new quantity $\hat{M}'_{\alpha\beta} = \hat{M}_{\alpha\beta} - k\delta_{\alpha\beta}$, where k is a constant an $\delta_{\alpha\beta}$ is the Kronecker delta tensor. Since we are only interested in the energy value it follows that:

$$\begin{aligned} \frac{1}{2} V_{\alpha\beta} \hat{M}'_{\alpha\beta} &= \frac{1}{2} V_{\alpha\beta} \hat{M}_{\alpha\beta} - \frac{1}{2} k \delta_{\alpha\beta} V_{\alpha\beta} \\ &= \frac{1}{2} V_{\alpha\beta} \hat{M}_{\alpha\beta} - \frac{1}{2} k V_{\alpha\alpha} \\ &= \frac{1}{2} V_{\alpha\beta} \hat{M}_{\alpha\beta} \end{aligned} \tag{1.11}$$

the last line follows from the Laplace equation: $V_{\alpha\alpha} = \sum_\alpha \frac{\partial^2 V}{\partial \alpha^2} = \nabla^2 V = 0$ and is obviously true for any value of k. We may therefore chose k so that it makes $\hat{M}'_{\alpha\beta}$ traceless $\hat{M}'_{\alpha\alpha} = \hat{M}'_{xx} + \hat{M}'_{yy} + \hat{M}'_{zz} = 0$ so being $\delta_{\alpha\alpha} = 3$ we have $\hat{M}_{\alpha\alpha} - 3k = 0$ and $k = \frac{1}{3}\hat{M}_{\alpha\alpha} = \frac{1}{3}\sum_a e^a a^2$ therefore we obtain:

$$\hat{M}'_{\alpha\beta} = \sum_a e^a (a_\alpha a_\beta - \frac{1}{3} a^2 \delta_{\alpha\beta}) = \frac{2}{3} \hat{\Theta}_{\alpha\beta} \tag{1.12}$$

We demonstrated how subtracting away the trace of the second moment, which, by the way, does not contribute to the electrostatic energy one arrives to the quadrupole moment, except for a numerical factor.

The higher momenta can be manipulated in a very similar way so we may generalise the expression for the electrostatic perturbation Hamiltonian as:

$$\mathcal{H}' = qV + \hat{\mu}_\alpha V_\alpha + \frac{1}{3}\hat{\Theta}_{\alpha\beta}V_{\alpha\beta} + \cdots + \frac{1}{(2n-1)!!}\hat{\xi}^{(n)}_{\alpha\beta\ldots\nu}V_{\alpha\beta\ldots\nu} + \cdots \tag{1.13}$$

where $(2n-1)!! = (2n-1)(2n-3)\cdots 5\cdot 3\cdot 1$ and n is an integer defining the rank of the multipole.

In term of the spherical tensor formulation the same expression can be written as:

$$\mathcal{H}' = \sum_{lm}(-1)^m \hat{Q}_{l,-m}V_{lm} \tag{1.14}$$

where $V_{lm} = [(2l-1)!!]^{-1}R_{lm}(\nabla)V|_{r=0}$, in this case by $R_{lm}(\nabla)$ we mean the regular spherical harmonic whose argument is the vector gradient operator ∇, i.e. for example $R_{10}(\nabla) = \nabla_z = \frac{\partial}{\partial z}$. We will not show in details here the proof of the result, since it is a little bit indirect and its derivation can be somehow cumbersome, the only point we will like to underline is, again, the equivalence between cartesian and spherical tensor formalism.

Moreover it is also possible to express the perturbation Hamiltonian in real, instead of regular, spherical harmonics, in this case the equation becomes

$$\mathcal{H}' = \sum_{lk}\hat{Q}_{lk}V_{lk} \tag{1.15}$$

obtaining a formulation which in many cases may be much more convenient.

1.2.2.1 First Order Energy

Once the perturbation Hamiltonian has been written in a convenient form it is trivial to find out the first order energy for a given state following standard perturbation theory.

If, for instance, one is interested in the energy for the zero state $|0\rangle$ the first order energy becomes simply $\langle 0|\mathcal{H}'|0\rangle$:

$$E' = qV + \mu_\alpha V_\alpha + \frac{1}{3}\Theta_{\alpha\beta}V_{\alpha\beta} + \frac{1}{15}\Omega_{\alpha\beta\gamma}V_{\alpha\beta\gamma} + \ldots \tag{1.16}$$

where as usual $\mu_\alpha = \langle 0|\hat{\mu}_\alpha|0\rangle$ and so on for higher order multipoles. The previous can be written in a more compact way following the spherical moments formalism as:

$$E' = \sum_{lk} Q_{lk}V_{lk} \tag{1.17}$$

where again $Q_{lk} = \langle 0|\hat{Q}_{lk}|0\rangle$.

It is important to underline how from the previous equations one can guess the energy due to the dipole components depends only on the electric field $F_\alpha = -V_\alpha$, while the energy due to the quadrupole involves only the field gradient $F_{\alpha\beta} = -V_{\alpha\beta}$.

1.2.2.2 Second Order Energy

The second order energy is again given, for the ground state, by the standard Rayleigh-Scrödinger perturbation theory. The involved quantities can be expressed via the usual some over the states and in this case we get:

$$E'' = -\sum_{n\neq 0} \frac{\langle 0|\mathcal{H}'|n\rangle\langle n|\mathcal{H}'|0\rangle}{E_n - E_0} \tag{1.18}$$

If we substitute in the previous equation the expression for the perturbation Hamiltonian we derived previously, we may define a set of polarizabilities as:

$$\alpha_{\alpha,\beta} = \sum_{n\neq 0} \frac{\langle 0|\hat{\mu}_\alpha|n\rangle\langle n|\hat{\mu}_\beta|0\rangle + \langle 0|\hat{\mu}_\beta|n\rangle\langle n|\hat{\mu}_\alpha|0\rangle}{E_n - E_0} \tag{1.19}$$

$$A_{\alpha,\beta\gamma} = \sum_{n\neq 0} \frac{\langle 0|\hat{\mu}_\alpha|n\rangle\langle n|\hat{\Theta}_{\beta\gamma}|0\rangle + \langle 0|\hat{\Theta}_{\beta\gamma}|n\rangle\langle n|\hat{\mu}_\alpha|0\rangle}{E_n - E_0} \tag{1.20}$$

$$C_{\alpha\beta,\gamma\delta} = \frac{1}{3}\sum_{n\neq 0} \frac{\langle 0|\hat{\Theta}_{\alpha\beta}|n\rangle\langle n|\hat{\Theta}_{\gamma\delta}|0\rangle + \langle 0|\hat{\Theta}_{\gamma\delta}|n\rangle\langle n|\hat{\Theta}_{\alpha\beta}|0\rangle}{E_n - E_0} \tag{1.21}$$

where the first equation represents the dipole-dipole polarizability, the second one the dipole-quadrupole polarizability and the last one the quadrupole-quadrupole polarizability.

With these definitions we may now express the second order energy as:

$$E'' = -\frac{1}{2}\alpha_{\alpha\beta}V_\alpha V_\beta - \frac{1}{3}A_{\alpha,\beta\gamma}V_\alpha V_{\beta\gamma} - \frac{1}{6}C_{\alpha\beta,\gamma\delta}V_{\alpha\beta}V_{\gamma\delta} + \cdots \tag{1.22}$$

It is important to notice how the zeroth order operator (the charge operator) drops from the energy equation even if the molecules is charged, this is due to the fact it is a constant and its matrix elements between different eigenstates are zero by orthogonality.

In the spherical tensor formalism, as well as we did for the first order momenta, we may define a generic polarizability $\alpha_{lk,l'k'}$as:

$$\alpha_{lk,l'k'} = \sum_{n\neq 0} \frac{\langle 0|\hat{Q}_{lk}|n\rangle\langle n|\hat{Q}_{l'k'}|0\rangle + \langle 0|\hat{Q}_{l'k'}|n\rangle\langle n|\hat{\Theta}_{lk}|0\rangle}{E_n - E_0} \tag{1.23}$$

in this case the second order energy takes the form:

$$E'' = -\frac{1}{2}\sum_{lk,l'k'} \alpha_{lk,l'k'} V_{lk} V_{l'k'} \tag{1.24}$$

1.2.2.3 Physical Interpretation

To get a deeper insight on the physical meaning of these properties, which so far have been described with a purely mathematical formalism it is useful to write down the complete expression for the energy (let us consider a neutral molecule for the sake of simplicity)

$$\begin{aligned} E &= E_0 + \mu_\alpha V_\alpha + \frac{1}{3}\Theta_{\alpha\beta} V_{\alpha\beta} + \frac{1}{15}\Omega_{\alpha\beta\gamma} V_{\alpha\beta\gamma} + \cdots \\ &\quad -\frac{1}{2}\alpha_{\alpha\beta} V_\alpha V_\beta - \frac{1}{3} A_{\alpha,\beta\gamma} V_\alpha V_{\beta\gamma} - \frac{1}{6} C_{\alpha\beta,\gamma\delta} V_{\alpha\beta} V_{\gamma\delta} - \cdots \end{aligned} \tag{1.25}$$

if we consider the derivative of the energy with respect to V_ξ(in physical words the variation of the energy due to the application of an electric field along ξ) we obtain

$$\begin{aligned} \frac{\partial E}{\partial v_\xi} &= \mu_\alpha \delta_{\alpha\xi} - \frac{1}{2}\alpha_{\alpha\beta}(V_\alpha \delta_{\beta\xi} + V_\beta \delta_{\alpha\xi}) - \frac{1}{3} A_{\alpha,\beta\gamma} \delta_{\alpha\xi} V_{\beta\gamma} - \cdots \\ &= \mu_\xi - \alpha_{\xi\beta} V_\beta - \frac{1}{3} A_{\xi,\beta\gamma} V_{\beta\gamma} - \cdots \end{aligned} \tag{1.26}$$

from the previous equation we can recognize that the the static dipole can be defined as:

$$\mu_\xi = \left(\frac{\partial E}{\partial V_\xi}\right)_{V\to 0} \tag{1.27}$$

this is, indeed maybe the most common, and surely most classical description, of dipole moment, and is also the basis for some simple methods of calculating it (see for instance the finite field technique). As the polarizability $\alpha_{\beta\xi}$ is concerned it is clear it defines the additional dipole induce by the application of an electric field $F_\beta = -V_\beta$, and the dipole-quadrupole polarizability $A_{\xi,\beta\gamma}$ the dipole induced by an applied field gradient $F_{\beta,\gamma} = -V_{\beta\gamma}$.

In the same way if we derive the energy with respect to a gradient potential $V_{\xi\eta}$ we get

$$3\frac{\partial E}{\partial V_{\xi\eta}} = \Theta_{\xi\eta} - A_{\alpha,\xi\eta} V_\alpha - C_{\alpha\beta,\xi\eta} V_{\alpha\beta} - \cdots \tag{1.28}$$

therefore the quadrupole moment, in analogy with the dipole moment is simply

$$\Theta_{\xi\eta} = \left(\frac{\partial E}{\partial V_{\xi\eta}}\right)_{V\to 0} \tag{1.29}$$

while A also describes the quadrupole moment induced by an electric field $F_\alpha = -V_\alpha$ and C describes the quadrupole moment induced by an electric field gradient $F_{\alpha\beta} = -V_{\alpha\beta}$.

1.2.3 Dependence from the origin

A slight complication in the study of electric properties arises when one takes into account the dependence from the origin of multipole moments and polarizabilities. In fact for a given molecule only the first non zero element in the series (charge, dipole, quadrupole) is invariant upon a translation of the coordinate system.

Let us consider for instance the dipole moment along z

$$\mu_z = \langle 0|\hat{\mu}_z|0\rangle = \sum_a \langle 0|e^a \cdot z|0\rangle \tag{1.30}$$

now if we apply a translation to the coordinate system such as $x^0, y^0, z^0 \to x^0, y^0, z^0 + c$ the dipole moment becomes:

$$\mu_z^C = \langle 0|\hat{\mu}_z|0\rangle + c \cdot \sum_a \langle 0|e^a|0\rangle = \mu_z^0 + c \cdot q \tag{1.31}$$

so if the molecule is charged ($q \neq 0$) the expectation value of the dipole moment varies with the choice of the origin.

For the quadrupole operator a similar relation can be derived, and considering as an example the Θ_{zz} component we have

$$\begin{aligned}
\hat{\Theta}_{zz}^C &= \sum_a e^a \left[\frac{3}{2}(a_z - c)^2 - \frac{1}{2}(a_x^2 + a_y^2 + (a_z + c)^2)\right] \\
&= \sum_a e^a \left[(\frac{3}{2}a_z^2 - \frac{1}{2}a^2) + 2a_z c + c^2\right] \\
&= \hat{\Theta}_{zz}^0 + 2c\hat{\mu_z}^0 + q\dot{c^2}
\end{aligned} \tag{1.32}$$

for the other components undergoing the same translation the following relations can be applied

$$\hat{\Theta}_{xx}^C = \hat{\Theta}_{xx}^0 - c\hat{\mu}_z^0 - \frac{c^2}{2} \tag{1.33}$$

$$\hat{\Theta}^C_{xz} = \hat{\Theta}^0_{xz} + \frac{3}{2} c \hat{\mu}^0_x \tag{1.34}$$

The same situation affects polarizabilities as well as multipole moments, with only one simplification: the matrix elements of the total charge that might occur in the sum over states are all zero, because q is a constant and states are orthogonal, so the dipole-dipole polarizability will be independent of origin even for charged ions. However higher rank polarizabilities will not be invariant and in general will depend on lower rank ones. So considering, for instance, a linear molecule we will have for dipole-quadrupole polarizabilities

$$A^C_{z,zz} = A^0_{z,zz} + 2c\alpha_z \tag{1.35}$$

$$A^C_{x,xz} = A^0_{x,xz} + \frac{3}{2} c\alpha_x \tag{1.36}$$

$$A^C_{z,xx} = A^0_{z,xx} - c\alpha_z \tag{1.37}$$

and for quadrupole polarizabilities one should consider the formulae

$$C^C_{zz,zz} = C^0_{zz,zz} + 4cA^0_{z,zz} + 4c^2\alpha_z \tag{1.38}$$

$$C^C_{xx,xx} = C^0_{xx,xx} - 2cA^0_{z,xx} + c^2\alpha_z \tag{1.39}$$

$$C^C_{xz,xz} = C^0_{xz,xz} + 3cA^0_{x,xz} + \frac{9}{4} c^2\alpha_x \tag{1.40}$$

1.3 Molecules in oscillating electric fields

If we apply to our molecule an electric field which oscillates with the time (for instance electromagnetic radiation), we should use time dependent perturbation theory to describe the response of the system. In fact the total Hamiltonian $\mathcal{H} = \mathcal{H}_0 + \mathcal{H}'$ consists of a time independent part $\mathcal{H}_0$ together with a time dependent perturbation $H' = \hat{V} f(t)$ which can be described as the product of a time independent operator $\hat{V}$ and a time factor $f(t)$.

Therefore the wave function can be written as

$$\Psi = \sum_k a_k(t)\psi_k(t) = \sum_k a_k \psi_k e^{-i\omega_k t} \tag{1.41}$$

assuming a small perturbation and considering the system is initially in a state $|n\rangle$ the coefficients $a_k(t)$ satisfy the following condition

$$\frac{\partial a_k(t)}{\partial t} = -\frac{i}{\hbar} v_{kn} f(t) e^{i\omega_{kn} t} \; k \neq n \tag{1.42}$$

integration from the tuning on of the field to the time t gives

$$a_k(t) = -\frac{i}{\hbar} v_{kn} \int_{-\infty}^{t} f(\tau) e^{i\omega_{kn}\tau} d\tau \tag{1.43}$$

If we are dealing with optical frequencies the wavelength can be considered to be so long, compared with the molecular size that electric field gradient and higher derivatives can be neglected, moreover if we put ourselves in the steady state response, the perturbation becomes

$$\mathcal{H}'(t) = 2\hat{V} e^{\varepsilon t} \cos(\omega t) = \hat{V}(e^{(\varepsilon+i\omega)t} + e^{(\varepsilon-i\omega)t}) = \hat{V} f(t) \tag{1.44}$$

with ε being an arbitrary small factor (later it will be allowed to tend to zero). Having factorized the perturbation we may directly substitute and integrate in order to find the evolution of the coefficient $a_k(t)$

$$\begin{aligned}
a_k(t) \quad &= \quad -\frac{i}{\hbar} v_{kn} \int_{-\infty}^{t} ((e^{(\varepsilon+i\omega_{kn}+i\omega)\tau} + e^{(\varepsilon+i\omega_{kn}-i\omega)\tau}) d\tau \\
&= \quad -\frac{V_{kn}}{\hbar} \left[\frac{e^{(\varepsilon+i\omega_{kn}+i\omega)\tau}}{\omega_{kn}+\omega-i\varepsilon} + \frac{e^{(\varepsilon+i\omega_{kn}-i\omega)\tau}}{\omega_{kn}-\omega-i\varepsilon} \right]_{-\infty}^{t} \\
\varepsilon \to 0 \quad &= \quad -\frac{V_{kn}}{\hbar} \left(\frac{e^{(\varepsilon+i\omega_{kn}+i\omega)\tau}}{\omega_{kn}+\omega-i\varepsilon} + \frac{e^{(\varepsilon+i\omega_{kn}-i\omega)\tau}}{\omega_{kn}-\omega-i\varepsilon} \right) \\
&= \quad -\frac{V_{kn}}{\hbar} \left(\frac{e^{i(\omega_{kn}+\omega)t}}{\omega_{kn}+\omega} + \frac{e^{i(\omega_{kn}-\omega)t}}{\omega_{kn}-\omega} \right)
\end{aligned} \tag{1.45}$$

We also note the coefficient $a_k(t)$ remains small provided that V_{kn} is small compared with $\hbar(\omega_{kn} \pm \omega)$.

We are now ready to evaluate the component μ_α of the dipole moment for the molecule in its ground state, in the presence of the perturbation $\mathcal{H}'(t) = 2\hat{V}\cos(\omega t) = -2\hat{\mu}_\beta F_\beta \cos(\omega t)$ due to an electromagnetic field polarized in the β direction.

At the first order we have

$$\begin{aligned}
\mu_\alpha(t) \quad &= \quad \langle \Psi_0 + \sum_{k\neq 0} a_k(t)\psi_k | \hat{\mu}_\alpha | \Psi_0 + \sum_{k\neq 0} a_k(t)\psi_k \rangle \\
&= \quad \langle 0|\hat{\mu}_\alpha|0\rangle + \left\{ \sum_{k\neq 0} a_k(t) \langle 0|\hat{\mu}_\alpha|k\rangle e^{i\omega_{0k}t} + c.c. \right\}
\end{aligned} \tag{1.46}$$

where *c.c.* means complex conjugate; we may substitute the expression previously derived for $a_k(t)$ and obtain

$$\begin{aligned}\mu_\alpha(t) &= \langle 0|\hat{\mu}_\alpha|0\rangle + \sum_{k\neq 0}\frac{V_{k0}}{\hbar}\langle 0|\hat{\mu}_\alpha|k\rangle\left\{\frac{e^{i\omega t}}{\omega_{k0}+\omega}+\frac{e^{-i\omega t}}{\omega_{k0}-\omega}+c.c.\right\}\\ &= \langle 0|\hat{\mu}_\alpha|0\rangle + F_\beta\cos(\omega t)\sum_{k\neq 0}\frac{\omega_{k0}(\langle 0|\hat{\mu}_\alpha|k\rangle\langle k|\hat{\mu}_\beta|0\rangle+\langle 0|\hat{\mu}_\beta|k\rangle\langle k|\hat{\mu}_\alpha|0\rangle)}{\hbar(\omega_{k0}^2-\omega^2)}\\ &\quad -iF_\beta\sin(\omega t)\sum_{k\neq 0}\frac{\omega(\langle 0|\hat{\mu}_\alpha|k\rangle\langle k|\hat{\mu}_\beta|0\rangle+\langle 0|\hat{\mu}_\beta|k\rangle\langle k|\hat{\mu}_\alpha|0\rangle)}{\hbar(\omega_{k0}^2-\omega^2)}\end{aligned} \tag{1.47}$$

If the molecule is in a non degenerate (real) state, then $\langle 0|\hat{\mu}_\alpha|k\rangle\langle k|\hat{\mu}_\beta|0\rangle$ is real, while the out of phase final term of the previous equation vanishes. So the expectation value of the dipole moment is time dependent and becomes

$$\mu_\alpha(t) = \langle 0|\hat{\mu}_\alpha|0\rangle + \alpha_{\alpha\beta}(\omega)F_\beta\cos(\omega t) \tag{1.48}$$

where we have introduced the frequency dependent polarizability $\alpha_{\alpha\beta}(\omega)$ defined as

$$\alpha_{\alpha\beta}(\omega) = \sum_{k\neq 0}\frac{\omega_{k0}(\langle 0|\hat{\mu}_\alpha|k\rangle\langle k|\hat{\mu}_\beta|0\rangle+\langle 0|\hat{\mu}_\beta|k\rangle\langle k|\hat{\mu}_\alpha|0\rangle)}{\hbar(\omega_{k0}^2-\omega^2)} \tag{1.49}$$

where $\omega_{k0}$is the frequency of the transition between the state 0 and state n ($\hbar\omega_{k0} = E_k - E_0$).

For higher order multipole operators (quadrupole, octupole etc.) one can define a dynamic polarizability in exactly the same way as we did for the dipole operator.

We would like to underline how the frequency dependent polarizability can be considered as a generalization of the static polarizability itself, in fact for the limit $\omega \to 0$ it reduces to the static polarizability, and obviously describes the multipole moment produced on the molecules by the application of an oscillating electric field, and hence the response of the molecule to that field.

It is also important to notice how the dynamic polarizability presents a singularity for $\omega = \omega_{k0}$, so it goes to infinity for a frequency equal to the transition frequency. Some attempts [9] have been made to correct the curve and to describe properly also the absorption emission zone, both via a quantum description of the electromagnetic field or phenomenologically taking into account the spontaneous emission.

In either case the expression for the dynamic polarizability is slightly modified, and takes the form:

$$\alpha_{\alpha\beta}(\omega) = 2\sum_{k\neq 0}\frac{\omega_{k0}\langle 0|\hat{\mu}_\alpha|k\rangle\langle k|\hat{\mu}_\beta|0\rangle}{\hbar[\omega_{k0}^2-(\omega+\frac{1}{2}i\Gamma_k)^2}] \tag{1.50}$$

where Γ_k is a constant describing the probability of transitions from state k. One can see how the singularity at transition frequencies disappears, but the polarizability becomes complex. The real part can be thought as describing the variation of the refractive index with the frequency, while the imaginary part describes the absorption process. Anyway such an analysis is far beyond the scope of this thesis and therefore we will use only the standard definition of dynamic polarizability.

1.4 Electrostatic interactions between molecules

In the previous Section we built a consistent theory of electric properties of molecules; in this and the next section we will use the concept so far derived to describe intermolecular forces (with a particular emphasis on long range interactions) using a multipole expansion of the interaction and the language of perturbation theory. This will allow us to find an efficient way to model and parametrise the intermolecular potential and will also provide us with some tools that can be used in actual *ab initio* computations.

1.4.1 The electric field of a molecule

Suppose we are dealing with a molecule A located at a position $\mathbf{A}$ in some global coordinate system; each particle of this molecule is at a position $\mathbf{a}$ relative to $\mathbf{A}$, i.e. at the global position $\mathbf{a}+\mathbf{A}$. We want to evaluate the potential at a point $\mathbf{B}$ where we will put another molecule B.

In terms of the positions and charges of molecule A particles the potential is

$$V^A(\mathbf{B}) = \sum_a \frac{e^a}{4\pi\varepsilon_0|\mathbf{B}-\mathbf{A}-\mathbf{a}|} = \sum_a \frac{e^a}{4\pi\varepsilon_0|\mathbf{R}-\mathbf{a}|} \tag{1.51}$$

We may now expand this potential in a Taylor series as

$$\begin{aligned}
V^A(\mathbf{B}) &= \sum_a \frac{e^a}{4\pi\varepsilon_0|\mathbf{R}-\mathbf{a}|} \\
&= \sum_a \frac{e^a}{4\pi\varepsilon_0}\left\{\frac{1}{R} + a_\alpha\left(\frac{\partial}{\partial a_\alpha}\frac{1}{|\mathbf{R}-\mathbf{a}|}\right)_{\mathbf{a}=0} + \frac{1}{2}a_\alpha a_\beta\left(\frac{\partial^2}{\partial a_\alpha \partial a_\beta}\frac{1}{|\mathbf{R}-\mathbf{a}|}\right)_{\mathbf{a}=0} + \cdots\right\} \\
&= \sum_a \frac{e^a}{4\pi\varepsilon_0}\left\{\frac{1}{R} - a_\alpha\left(\frac{\partial}{\partial R_\alpha}\frac{1}{|\mathbf{R}-\mathbf{a}|}\right)_{\mathbf{a}=0} + \frac{1}{2}a_\alpha a_\beta\left(\frac{\partial^2}{\partial R_\alpha \partial R_\beta}\frac{1}{|\mathbf{R}-\mathbf{a}|}\right)_{\mathbf{a}=0} + \cdots\right\} \\
&= \sum_a \frac{e^a}{4\pi\varepsilon_0}\left\{\frac{1}{R} - a_\alpha\nabla_\alpha\frac{1}{R} + \frac{1}{2}a_\alpha a_\beta\nabla_\alpha\nabla_\beta\frac{1}{R} + \cdots\right\}
\end{aligned} \tag{1.52}$$

Figure 1.1: Schematic definition of position vectors for two interacting molecules

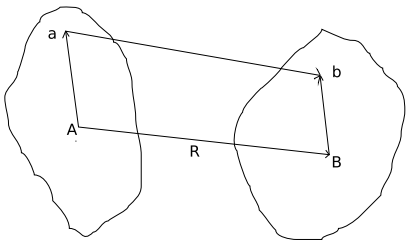

after a minor manipulation we may recognize the dipole operator $\sum_a e^a a_\alpha$, and the second moment operator $\sum_a e^a a_\alpha a_\beta$; moreover as we did before we may easily substitute the second moment operator with the quadrupole one $\hat{\Theta}_{\alpha\beta}$; although not explicitly derived here for the sake of simplicity one could show that even the higher momenta can be treated similarly. When we perform these substitution we get

$$\begin{aligned} V^A(\mathbf{B}) &= \frac{1}{4\pi\varepsilon_0}\left\{q\left(\frac{1}{R}\right) - \hat{\mu}_\alpha\nabla_\alpha\left(\frac{1}{R}\right) + \frac{1}{3}\hat{\Theta}_{\alpha\beta}\nabla_\alpha\nabla_\beta\left(\frac{1}{R}\right) + \cdots\right\} \\ &= Tq - T_\alpha\hat{\mu}_\alpha + \frac{1}{3}T_{\alpha\beta}\hat{\Theta}_{\alpha\beta}\cdots + \frac{(-1)^n}{(2n-1)!!}T^{(n)}_{\alpha\beta\ldots\nu}\xi^{(n)}_{\alpha\beta\ldots\nu} + \cdots \end{aligned} \tag{1.53}$$

where we have defined the $T-$tensors as

$$T = \frac{1}{4\pi\varepsilon_0 R} \tag{1.54}$$

$$T_\alpha = \frac{1}{4\pi\varepsilon_0}\nabla_\alpha\frac{1}{R} = -\frac{R_\alpha}{4\pi\varepsilon_0 R^3} \tag{1.55}$$

$$T_{\alpha\beta} = \frac{1}{4\pi\varepsilon_0}\nabla_\alpha\nabla_\beta\frac{1}{R} = \frac{3R_\alpha R_\beta - R^2\delta_{\alpha\beta}}{4\pi\varepsilon_0 R^5} \tag{1.56}$$

and in general

$$T^{(n)}_{\alpha\beta\ldots\nu} = \frac{1}{4\pi\varepsilon_0}\nabla_\alpha\nabla_\beta\cdots\nabla_\nu\frac{1}{R} \tag{1.57}$$

If we want to avoid ambiguity when dealing with a system of more than two molecules one can label the $T-$tensors with the molecular labels: i.e. T^{AB}, T^{AB}_α; however since this tends to make the notation rather cumbersome in the two molecule case the label are omitted. Notice thought it is important to establish whether we are dealing with T^{AB}or T^{BA}, or in other words if $\mathbf{R} = \mathbf{B} - \mathbf{A}$ or $\mathbf{R} = \mathbf{A} - \mathbf{B}$, in fact the above definition shows that $T^{BA(n)}_{\alpha\beta\ldots\nu} = (-1)^n T^{AB(n)}_{\alpha\beta\ldots\nu}$.

Coming back to the equation 1.53 concerning the potential we may easily see the potential due to a charge is $\frac{q}{4\pi\varepsilon_0 R}$, the potential due to a dipole is $\frac{\mu_\alpha R_\alpha}{4\pi\varepsilon_0 R^3}$ and so on. Moreover having found the potential as a function of the position $\mathbf{R}$, it is now quite easy to find the electric field, field gradient and higher derivatives generated at the position $\mathbf{B}$.

Therefore we get for the electric field

$$\begin{aligned} F^A_\alpha(\mathbf{B}) &= -\nabla_\alpha V^A(\mathbf{B}) \\ &= -T_\alpha q + T_{\alpha\beta}\hat{\mu}_\beta - \frac{1}{3}T_{\alpha\beta\gamma}\hat{\Theta}_{\beta\gamma} + \cdots \\ &\quad -\frac{(-1)^n}{(2n-1)!!}T^{(n+1)}_{\alpha\beta\ldots\nu\sigma}\xi^{(n)}_{\beta\ldots\nu\sigma} + \cdots \end{aligned} \tag{1.58}$$

and for the field gradient

$$\begin{aligned} F^A_{\alpha\beta}(\mathbf{B}) &= -\nabla_\alpha\nabla_\beta V^A(\mathbf{B}) \\ &= -T_{\alpha\beta}q + T_{\alpha\beta\gamma}\hat{\mu}_\gamma - \frac{1}{3}T_{\alpha\beta\gamma\delta}\hat{\Theta}_{\gamma\delta} + \cdots \\ &\quad -\frac{(-1)^n}{(2n-1)!!}T^{(n+2)}_{\alpha\beta\ldots\nu\sigma\tau}\xi^{(n)}_{\gamma\delta\ldots\nu\sigma\tau} \end{aligned} \tag{1.59}$$

Two important general properties belonging to $T-$tensors bearing at least two suffixes are: invariance with respect to interchange of suffixes (i.e. $T_{xy} = T_{yx}$), and tracelsness when at least two suffixes are equal ($T^{(n)}_{\alpha\alpha\gamma\ldots\nu} = 0$); these results follow from the fact that differential operators commute and because $\nabla^2(\frac{1}{R}) = 0$. From these properties one can guess $T^{(n)}_{\alpha\beta\gamma\ldots\nu}$, just like ${\xi^{(n)}}_{\alpha\beta\gamma\ldots\nu}$ has only $2n+1$ independent components.

1.4.2 Electrostatic interactions

We are now able to calculate the interaction between a pair of molecule, we know, in fact, the electrostatic potential exercised by molecule A, centred in $\mathbf{A}$ on the second molecule

B centred in **B**, and we also know how to calculate the energy of a molecule in a given electric potential.

Combining the formulae developed in the previous sections we get the expression for the interaction Hamiltonian as

$$\begin{aligned}
\mathcal{H}' &= q^B V^A + \hat{\mu}^B_\alpha V^A_\alpha + \frac{1}{3}\hat{\Theta}^B_{\alpha\beta} V^A_{\alpha\beta} + \cdots \\
&= q^B \left[T q^A - T_\alpha \hat{\mu}_\alpha + \frac{1}{3} T_{\alpha\beta} \hat{\Theta}^A_{\alpha\beta} + \cdots \right] \\
&+ \hat{\mu}^B_\beta \left[T_\alpha q^A - T_{\alpha\beta} \hat{\mu}_\beta + \frac{1}{3} T_{\alpha\beta\gamma} \hat{\Theta}^A_{\beta\gamma} + \cdots \right] \\
&+ \frac{1}{3}\hat{\Theta}^B_{\alpha\beta} \left[T_{\alpha\beta} q^A - T_{\alpha\beta\gamma} \hat{\mu}_\gamma + \frac{1}{3} T_{\alpha\beta\gamma\delta} \hat{\Theta}^A_{\gamma\delta} + \cdots \right] + \cdots \\
&= T q^A q^B + T_\alpha \left(q^A \hat{\mu}^B_\alpha - \hat{\mu}^A_\alpha q^B \right) \\
&+ T_{\alpha\beta} \frac{1}{3} \left(q^A \hat{\Theta}^B_{\alpha\beta} - \hat{\mu}^A_\alpha \hat{\mu}^B_\beta + \frac{1}{3} \hat{\Theta}^A_{\alpha\beta} q^B \right) + \cdots
\end{aligned} \tag{1.60}$$

notice that some relabeling of the subscripts has been necessary in the derivation of the final equation to avoid clashes, in any case we can see that for ions the leading term is the electrostatic interaction between charges.

Let us now consider neutral molecules in which $q^A = q^B = 0$, in this case the leading term is the dipole-dipole interaction and the equation becomes:

$$\mathcal{H}' = -T_{\alpha\beta} \hat{\mu}^A_\alpha \hat{\mu}^B_\beta - \frac{1}{3} T_{\alpha\beta\gamma} \left(\hat{\mu}^A_\alpha \hat{\Theta}^B_{\beta\gamma} - \hat{\Theta}^A_{\alpha\beta} \hat{\mu}^B_\gamma \right) + \cdots \tag{1.61}$$

Obviously this expression (like the previous ones) is in operator form: if one is interested to get the electrostatic interaction (first order) U_{es} between the two molecules in non degenerate states, it is necessary to replace each involved multipole operator by its expectation value, thus for two neutral molecules we get

$$U_{es} = -T_{\alpha\beta} \mu^A_\alpha \mu^B_\beta - \frac{1}{3} T_{\alpha\beta\gamma} \left(\mu^A_\alpha \Theta^B_{\beta\gamma} - \Theta^A_{\alpha\beta} \mu^B_\gamma \right) + \cdots \tag{1.62}$$

the previous equations have been derived for a pair of molecules isolated from any others. However they are based on the Coulomb interactions between nuclear and electronic charges, which are strictly additive, so we can generalise this result to an assembly of molecules simply by summing over the distinct pairs.

1.4.3 Spherical tensor formulation

For many purposes a spherical tensor formulation of the interaction is much more convenient, anyway it is best obtained by a somewhat different route. In fact the derivation

starts with an expansion of $\frac{1}{r_{ab}}$, as we did for the cartesian formulation, but this time we use the expansion in terms of spherical harmonics which takes the form [8]

$$\frac{1}{|\mathbf{r_1}-\mathbf{r_2}|}=\sum_{lm}\frac{r_<^l}{r_>^{l+1}}(-1)^m C_{l,-m}(\theta_1,\varphi_1)C_{lm}(\theta_2,\varphi_2) \tag{1.63}$$

where $r_<$is the smaller and $r_>$ is the larger of r_1 and r_2. For our purposes we need $\frac{1}{r_{ab}}=\frac{1}{|\mathbf{B}+\mathbf{b}-\mathbf{A}-\mathbf{a}|}$ and so we take $\mathbf{r}_1=\mathbf{B}-\mathbf{A}=\mathbf{R}$ and $\mathbf{r}_2=\mathbf{a}-\mathbf{b}$ and we assume $|\mathbf{a}-\mathbf{b}|<R$ we obtain

$$\frac{1}{|\mathbf{R}+\mathbf{b}-\mathbf{a}|}=\sum_{l=0}^{\infty}\sum_{m=-l}^{l}(-1)^m R_{l,-m}(\mathbf{a}-\mathbf{b})I_{lm}(\mathbf{R}) \tag{1.64}$$

where $R_{l,-m}$ and I_{lm} are the regular and irregular spherical harmonics.
We may now recall the standard addition theorem for spherical harmonics

$$\begin{aligned} R_{LM}(\mathbf{a}+\mathbf{b}) &= \sum_{l_1l_2}\sum_{m_1m_2}\delta_{l_1+l_2,L}(-1)^{L+M}\left[\frac{(2L+1)!}{(2l_1)!(2l_2)!}\right]^{\frac{1}{2}} \\ &\times R_{l_1m_1}(\mathbf{a})R_{l_2m_2}(\mathbf{b})\begin{pmatrix} l_1 & l_2 & L \\ m_1 & m_2 & -M\end{pmatrix} \end{aligned} \tag{1.65}$$

where $\begin{pmatrix} l_1 & l_2 & L \\ m_1 & m_2 & -M\end{pmatrix}$ is a Wigner $3j$ coefficient, when $L=l_1+l_2$ this $3j$ coefficient can be written in explicit formula

$$\begin{aligned} \begin{pmatrix} l_1 & l_2 & L \\ m_1 & m_2 & -M\end{pmatrix} &= (-1)^{l_1-l_2+M}\delta_{m_1+m_2,M}\left[\frac{(2l_1)!(2l_2)!}{(2l_1+2l_2+1)!}\right]^{\frac{1}{2}} \\ &\times \left[\begin{pmatrix} l_1+l_2+m_1+m_2 \\ l_1+m_1\end{pmatrix}\begin{pmatrix} l_1+l_2-m_1-m_2 \\ l_1-m_1\end{pmatrix}\right]^{-\frac{1}{2}} \end{aligned} \tag{1.66}$$

where $\begin{pmatrix} n \\ m\end{pmatrix}$ is the binomial coefficient $\frac{n!}{m!(n-m)!}$.
Using this theorem, and remembering $R_{lm}(-\mathbf{r})=(-1)R_{lm}(\mathbf{r})^l$ we find

$$\begin{aligned} \mathcal{H}' &= \frac{1}{4\pi\varepsilon_0}\sum_{a\in A}\sum_{b\in B}\frac{e^a e^b}{|\mathbf{R}+\mathbf{b}-\mathbf{a}|} \\ &= \frac{1}{4\pi\varepsilon_0}\sum_{l_1l_2}\sum_{m_1m_2m}(-1)^{l_1}\left(\frac{(2l_1+2l_2+1)!}{(2l_1)!(2l_2)!}\right)^{\frac{1}{2}} \end{aligned}$$

$$
\begin{aligned}
&\times \sum_{a\in A} e^a R_{l_1 m_1}(\mathbf{a}) \sum_{b\in B} e^b R_{l_2 m_2}(\mathbf{b}) I_{l_1+l_2,m}(\mathbf{R}) \begin{pmatrix} l_1 & l_2 & l_1+l_2 \\ m_1 & m_2 & m \end{pmatrix} \\
&= \frac{1}{4\pi\varepsilon_0} \sum_{l_1 l_2} \sum_{m_1 m_2 m} (-1)^{l_1} \left(\frac{(2l_1+2l_2+1)!}{(2l_1)!(2l_2)!} \right)^{\frac{1}{2}} \\
&\times \hat{Q}^{A(G)}_{l_1 m_1} \hat{Q}^{B(G)}_{l_2 m_2} I_{l_1+l_2,m}(\mathbf{R}) \begin{pmatrix} l_1 & l_2 & l_1+l_2 \\ m_1 & m_2 & m \end{pmatrix}
\end{aligned} \tag{1.67}
$$

in the last line we introduced the multipole moment operators

$$
\hat{Q}^{A(G)}_{lm} = \sum_{a\in A} e^a R_{lm}(\mathbf{a}) \tag{1.68}
$$

the superscript G is used to remind us the expression is written in the global coordinate system.

As we have seen however it is more convenient to express the interaction in terms of multipole moments defined in the local coordinates system of each molecule. The components in the local system are related to those in the global one by

$$
\hat{Q}^{(L)}_{lk} = \sum_m \hat{Q}^{(G)}_{lm} D^l_{mk}(\Omega) \tag{1.69}
$$

where $\Omega = (\alpha, \beta, \gamma)$ is the rotation that takes the global axes to the local axes, and $D^l_{mk}(\Omega)$ is the Wigner rotation matrix element for this rotation. Equivalently we can write the global components in terms of the local ones

$$
\hat{Q}^{(G)}_{lm} = \sum_k \hat{Q}^{(L)}_{lk} D^l_{km}(\Omega^{-1}) = \sum_k \hat{Q}^{(L)}_{lk} D^l_{km} \left[(\Omega)\right]^* \tag{1.70}
$$

Substituting the previous one in the expression for the interaction Hamiltonian expressed in global coordinate system gives

$$
\begin{aligned}
\mathcal{H}' &= \frac{1}{4\pi\varepsilon_0} \sum_{l_1 l_2} \sum_{k_1 k_2} (-1)^{l_1} \left(\frac{(2l_1+2l_2+1)!}{(2l_1)!(2l_2)!} \right)^{\frac{1}{2}} \hat{Q}^{A(L)}_{l_1 k_1} \hat{Q}^{B(L)}_{l_2 k_2} \\
&\times \sum_{m_1 m_2 m} \left[D^{l_1}_{m_1 k_1}(\Omega_1) \right]^* \left[D^{l_2}_{m_2 k_2}(\Omega_2) \right]^* I_{l_1+l_2,m}(\mathbf{R}) \begin{pmatrix} l_1 & l_2 & l_1+l_2 \\ m_1 & m_2 & m \end{pmatrix}
\end{aligned} \tag{1.71}
$$

The multipole operators are now referred to local molecular axes, and the orientation and distance dependence is all contained in the sum over Wigner functions and irregular spherical harmonics. We may define new functions of the orientation by

$$\begin{aligned}\overline{S}^{k_1k_2}_{l_1l_2j} &= i^{l_1-l_2-j}\left[\begin{pmatrix} l_1 & l_2 & j \\ 0 & 0 & 0 \end{pmatrix}\right]^{-1} \\ &\times \sum_{m_1m_2m}\left[D^{l_1}_{m_1k_1}(\Omega_1)\right]^*\left[D^{l_2}_{m_2k_2}(\Omega_2)\right]^* C_{jm}(\theta,\varphi)\begin{pmatrix} l_1 & l_2 & j \\ m_1 & m_2 & m \end{pmatrix}\end{aligned} \tag{1.72}$$

here θ and φ are the polar angles describing the direction of the intermolecular vector $\mathbf{R}$. In terms of these functions the interaction Hamiltonian becomes:

$$\begin{aligned}\mathcal{H}' &= \frac{1}{4\pi\varepsilon_0}\sum_{l_1l_2}\sum_{k_1k_2}(-1)^{l_1+l_2}\left(\frac{(2l_1+2l_2+1)!}{(2l_1)!(2l_2)!}\right)^{\frac{1}{2}} \\ &\times \hat{Q}^{A(L)}_{l_1k_1}\hat{Q}^{B(L)}_{l_2k_2}R^{-l_1-l_2-1}\begin{pmatrix} l_1 & l_2 & l_1+l_2 \\ 0 & 0 & 0 \end{pmatrix}\overline{S}^{k_1k_2}_{l_1l_2l_1+l_2}\end{aligned} \tag{1.73}$$

now dropping the superscript (L), since we will use local coordinate system from now on and inserting the explicit formula for the $3j-$Wigner symbol we obtain

$$\mathcal{H}' = \frac{1}{4\pi\varepsilon_0}\sum_{l_1l_2}\sum_{k_1k_2}\begin{pmatrix} l_1+l_2 \\ l_1 \end{pmatrix}\hat{Q}^{A}_{l_1k_1}\hat{Q}^{B}_{l_2k_2}\overline{S}^{k_1k_2}_{l_1l_2l_1+l_2}R^{-l_1-l_2-1} \tag{1.74}$$

This formulation explicitly separates each term in the interaction into an operator part, involving multipole operators in local molecular axes, a factor $\overline{S}^{k_1k_2}_{l_1l_2l_1+l_2}$ that describes the orientation dependence, and a distance dependence $R^{-l_1-l_2-1}$. Notice also the orientational part involves a linear combination of product of the Wigner functions and spherical harmonic, with coefficients given by $3j-$Wigner symbols. This fact ensures the result is scalar and invariant under rotation of the entire system, moreover it takes account of the evidence that only five of the eight angular coordinates are independent.

The previous one is a very general and powerful formulation, but a little bit cumbersome for routine use. Moreover it is at the moment expressed in terms of the complex components of the multipole moments, we may transform it to the real components, giving rise to an equivalent expression. We may also obtain a more compact representation by defining analogues to the T tensors of the cartesian formulation:

$$T_{l_1k_1l_2k_2} = \frac{1}{4\pi\varepsilon_0}\begin{pmatrix} l_1+l_2 \\ l_1 \end{pmatrix}\overline{S}^{k_1k_2}_{l_1l_2l_1+l_2}R^{-l_1-l_2-1} \tag{1.75}$$

the interaction just becomes:

$$\mathcal{H}' = \sum_{l_1 l_2} \sum_{k_1 k_2} \hat{Q}^A_{l_1 k_1} \hat{Q}^B_{l_2 k_2} T_{l_1 k_1 l_2 k_2} \tag{1.76}$$

It is useful to underline the T tensors depend only on relative positions of the two molecular axis systems, so they can be evaluated once and for all and be tabulated for further use, some of them can be found for instance in [1].

Of course in order to have the first order value of the interaction (i.e. the electrostatic term) we only have to determine the expectation value of the operator $\hat{Q}_{lk}$ exactly in the same way we did for the cartesian formulation.

1.5 Perturbation Theory of Long Range Intermolecular Forces

Because intermolecular forces are relatively weak it is somehow natural to describe them using perturbation theory. If the molecules are far enough the overlap between their wavefunctions can be ignored, so the theory becomes much simpler. The determination of long range intermolecular forces will be the main issue of this thesis so we will pay some attention in the theoretical development of this kind of interaction.

The reason for the simplification occurring in treating well separated molecules has to do with electron exchange. Suppose we have a wavefunction $\Psi^A(1, 2, \ldots, n_A)$ that describes molecule A and a wavefunctions $\Psi^B(1', 2', \ldots, n'_B)$ for molecule B. Suppose now there is a region of the space associated with Ψ^A such that Ψ^A is non zero only when all its electron are in this region; likewise there will be another region associated with Ψ^B and the two region will not overlap.

The wavefunction for the combined system $A + B$ should be written as an antisymmetrized product $\mathcal{A}\Psi^A\Psi^B$. But this antisymmetrized product contains terms in which electron of molecule A has been exchanged with electron of molecule B the overlap between this and the original product function is

$$\int \Psi^A(1, 2, \ldots, n_A)^* \Psi^B(1', 2', \ldots, n'_B)^* \times \Psi^A(1', 2, \ldots, n_A)^* \Psi^B(1, 2', \ldots, n'_B) d\tau \tag{1.77}$$

when we integrate over the coordinates of electron 1 we get zero because the two wavefunctions are non zero in different regions of the space. This means the terms in which the allocation of electrons between the two molecules is different do not mix with each other at all. Therefore the calculation may be performed without antisymmetrization and the result will be the same.

In practice, however, the overlap is never exactly zero, but the error made by ignoring it decreases exponentially with the distance between the two molecules. Overlap becomes significant when molecules approach each other closely giving rise to the repulsion between the interacting monomers.

The consequence is that, when we are dealing with long range interactions, we can identify a see of n_A electrons as belonging to the molecule A, and therefore define a Hamiltonian $\mathcal{H}^A$ for molecule A in terms of these electrons; similarly the Hamiltonian $\mathcal{H}^B$ for molecule B will be defined in terms of its private set of n_B electrons. The unperturbed Hamiltonian for the combined system is therefore $\mathcal{H}^0 = \mathcal{H}^A + \mathcal{H}^B$ and the perturbation consists of the electrostatic interaction between the particles of molecule A (electrons and nuclei) and those of molecule B

$$\mathcal{H}' = \sum_{a\in A}\sum_{b\in B}\frac{e^A e^B}{4\pi\varepsilon_0 r_{ab}} \tag{1.78}$$

where r_{ab} is the distance between a charged particle on molecule A and another one on molecule B. The previous operator can be expressed in several other useful forms: for examples following Longuet-Higgins [10] we define a charge density operator $\hat{\rho}^A(\mathbf{r})$ for molecule A

$$\hat{\rho}^A(\mathbf{r}) = \sum_{a\in A} e^a \delta(\mathbf{r}-\mathbf{a}) \tag{1.79}$$

and similarly $\hat{\rho}^B(\mathbf{r})$ for molecule B. In the previous we used the Dirac delta distribution $\delta(\mathbf{r}-\mathbf{a})$. In terms of these operators the perturbation becomes

$$\begin{aligned}\mathcal{H}' &= \int \sum_{a\in A}\sum_{b\in B}\frac{e^a\delta(\mathbf{r}-\mathbf{a})\delta(\mathbf{r}'-\mathbf{b})}{4\pi\varepsilon_0|\mathbf{r}-\mathbf{r}'|}d^3\mathbf{r}d^3\mathbf{r}' \\ &= \int \frac{\hat{\rho}^A(\mathbf{r})\hat{\rho}^B(\mathbf{r}')}{4\pi\varepsilon_0|\mathbf{r}-\mathbf{r}'|}d^3\mathbf{r}d^3\mathbf{r}'\end{aligned} \tag{1.80}$$

we may now notice that the potential at $\mathbf{r}$ due to the molecule B is

$$\hat{V}^B(\mathbf{r}) = \int \frac{\hat{\rho}^B(\mathbf{r}')}{4\pi\varepsilon_0|\mathbf{r}-\mathbf{r}'|}d^3\mathbf{r}' \tag{1.81}$$

so we can again write the interaction operator as

$$\mathcal{H}' = \int \hat{V}^B(\mathbf{r})\hat{\rho}^A(\mathbf{r})d^3\mathbf{r} \tag{1.82}$$

or equivalently

$$\mathcal{H}' = \int \hat{V}^A(\mathbf{r}')\hat{\rho}^B(\mathbf{r}')d^3\mathbf{r}' \tag{1.83}$$

(Notice, incidentally, the variable that appears in these integration is a dummy, so it does not matter whether it is $\mathbf{r}$ or $\mathbf{r}'$; the choice of variable is made simply to retain connection with the earlier formulae.)

Now if we switch our attention to the unperturbed states we may notice they are simple product functions $\Psi_m^A \Psi_n^B$, which we abbreviate as $|mn\rangle$, and they are eigenfunctions of the unperturbed Hamiltonian $\mathcal{H}^0$

$$\begin{aligned} \mathcal{H}^0|mn\rangle &= (\mathcal{H}^A + \mathcal{H}^B)|mn\rangle \\ &= (E_m^A + E_n^B)|mn\rangle \\ &= E_{mn}^0|mn\rangle \end{aligned} \tag{1.84}$$

For closed shell molecules, ordinary non degenerate Rayleigh Schrödinger perturbation theory gives the energy to the first and second order of the ground [2] state of the system ($m = n = 0$). So the energy may be expressed as:

$$E_{00} = E_{00}^0 + E_{00}' + E_{00}'' \tag{1.85}$$

where

$$E_{00}^0 = E_0^A + E_0^B \tag{1.86}$$

$$E_{00}' = \langle 00|\mathcal{H}'|00\rangle \tag{1.87}$$

$$E_{00}'' = -\sum_{m=n\neq 0} \frac{\langle 00|\mathcal{H}'|mn\rangle\langle mn|\mathcal{H}'|00\rangle}{E_{mn}^0 - E_{00}^0} \tag{1.88}$$

This gives rise to the long range approximation to the interaction energy (sometimes called the 'polarization approximation' [11]). As the first order energy is concerned, this is just the the ground state expectation value of the interaction Hamiltonian, and gives rise to the electrostatic contribution we already discussed in the previous Section. Note however if we write the perturbation using the charge density operator we can express the interaction as

$$E_{00}' = \int \frac{\rho^A(\mathbf{r})\rho^B(\mathbf{r}')}{4\pi\varepsilon_0|\mathbf{r} - \mathbf{r}'|} d^3\mathbf{r} d^3\mathbf{r}' \tag{1.89}$$

since the integration over the coordinates of the particles in molecule A just replaces the operator $\hat{\rho}^A(\mathbf{r})$ by it expectation value $\rho^A(\mathbf{r})$ and the same holds for B; but the previous formula is just the exact classical interaction energy of the two molecular charge distribution in a forme that does not depend on the multipole expansion.

[2] In fact this need not to be the ground state; it may be a state in which one or both molecules are excited. However it may not be a degenerate state of the combined system. This excludes all the excited states in the case where the molecule are identical

The second order energy describes the induction and dispersion contributions. To better analyse it we first separate it in three parts. Noting that the only term excluded in the sum over states is the one in which both molecules are in the ground state, we consider separately the term in the sum for which the molecule A is excited but molecule B is in its ground state, the term for which molecule B is excited while molecule A is in ground state, and the terms where both molecules are excited. This gives:

$$E'' = U^A_{ind} + U^B_{ind} + U_{disp} \tag{1.90}$$

$$U^A_{ind} = -\sum_{m\neq 0} \frac{\langle 00|\mathcal{H}'|m0\rangle\langle m0|\mathcal{H}'|00\rangle}{E^A_m - E^A_0} \tag{1.91}$$

$$U^B_{ind} = -\sum_{n\neq 0} \frac{\langle 00|\mathcal{H}'|0n\rangle\langle 0n|\mathcal{H}'|00\rangle}{E^B_n - E^B_0} \tag{1.92}$$

$$U_{disp} = -\sum_{\substack{m\neq 0\\ n\neq 0}} \frac{\langle 00|\mathcal{H}'|mn\rangle\langle mn|\mathcal{H}'|00\rangle}{E^A_m + E^B_n - E^A_0 - E^B_0} \tag{1.93}$$

these describes respectively the induction energy of molecule A, the induction energy of molecule B, and the dispersion energy.

1.5.1 The induction energy

As in the case of the first order energy we may write the perturbation in term of the charge density operator, this would lead to the 'non expanded' expression for the induction energy, that do not depend on the validity of the multipole expansion, and so can be used at short range where it does not converge [10] . However, when long range approximation is valid the multipole expansion proves to be the most simply and useful model to treat this kind of interactions, we will, therefore, derive expressions for the induction energy expanding the interaction operator $\mathcal{H}'$ in multipoles

$$\mathcal{H}' = Tq^Aq^B + T_\alpha(q^A\hat{\mu}^B_\alpha - \hat{\mu}^A_\alpha q^B) - T_{\alpha\beta}\hat{\mu}^A_\alpha\hat{\mu}^B_\beta + \cdots \tag{1.94}$$

in the previous equation we dropped the term involving quadrupole, at least for the moment, substituting this Hamiltonian in the equation for the induction energy of molecule B we get

$$U^B_{ind} = -\sum_{n\neq 0}\langle 00|Tq^Aq^B + T_\alpha(q^A\hat{\mu}^B_\alpha - \hat{\mu}^A_\alpha q^B) - T_{\alpha\beta}\hat{\mu}^A_\alpha\hat{\mu}^B_\beta + \cdots|0n\rangle$$

$$\begin{aligned} &\times \quad \langle 0n|Tq^Aq^B + T_{\alpha'}(q^A\hat{\mu}^B_{\alpha'} - \hat{\mu}^A_{\alpha'}q^B) - T_{\alpha'\beta'}\hat{\mu}^A_{\alpha'}\hat{\mu}^B_{\beta'} + \cdots|00\rangle \\ &\times \quad (E^B_n - E^0_n)^{-1} \end{aligned} \tag{1.95}$$

We may rearrange the previous equation noting that the matrix elements of q^B vanish because the excited states are orthogonal to the ground state and the charge is just a constant, moreover we may perform the implied integration over the coordinates of A obtaining the expectation values of the multipole operators

$$\begin{aligned} U^B_{ind} &= -\sum_{n\neq 0} \frac{\langle 0|T_\alpha q^A\hat{\mu}^B_\alpha - T_{\alpha\beta}\mu^A_\alpha\hat{\mu}^B_\beta + \cdots|n\rangle\langle n|T_{\alpha'}q^A\hat{\mu}^B_{\alpha'} - T_{\alpha'\beta'}\mu^A_{\alpha'}\hat{\mu}^B_{\beta'} + \cdots|0\rangle}{E^B_n - E^0_n} \\ &= -(q^AT_\alpha - \mu^A_\beta T_{\alpha\beta} + \cdots)\sum_{n\neq 0}\frac{\langle 0|\hat{\mu}^B_\alpha|n\rangle\langle n|\hat{\mu}^B_{\alpha'}|0\rangle}{E^B_n - E^0_n}(q^AT_{\alpha'} - \mu^A_{\beta'}T_{\alpha'\beta'} + \cdots) \end{aligned} \tag{1.96}$$

we can recognize here the sum over states expression for the polarizability $\alpha_{\alpha\alpha'}$ so the induction energy may be expressed as

$$U^B_{ind} = -\frac{1}{2}(q^AT_\alpha - \mu^A_\beta T_{\alpha\beta} + \cdots)\alpha^B_{\alpha\alpha'}(q^AT_{\alpha'} - \mu^A_{\beta'}T_{\alpha'\beta'} + \cdots) \tag{1.97}$$

If we recognize that the term $(q^AT_\alpha - \mu^A_\beta T_{\alpha\beta} + \cdots)$ is nothing but the inverse of the electric field at B due to the molecule A ($F^A_\alpha(\mathbf{B})$), we found the induction energy can be expressed as $-\frac{1}{2}F^A_\alpha(\mathbf{B})F^A_{\alpha'}(\mathbf{B})\alpha^B_{\alpha\alpha'}$, exactly the same result we would have expected from a straightforward classical treatment of the field. (The only role played by quantum mechanics is in fact to provide the formula for the polarizability).

In this derivation so far we ignored all the term of the multipolar expansion other than dipole operator for molecule B. It is however clear, by analogy with the previous formulae or by explicit calculation, that we shall have other terms in the induction energy, involving dipole-quadrupole polarizability, quadrupole-quadrupole polarizability and so on; in this case the induction energy takes the form

$$\begin{aligned} U^B_{ind} &= -\frac{1}{2}F^A_\alpha(\mathbf{B})F^A_{\alpha'}(\mathbf{B})\alpha^B_{\alpha\alpha'} - \frac{1}{3}F^A_\alpha(\mathbf{B})F^A_{\alpha'\beta'}(\mathbf{B})A_{\alpha,\alpha'\beta'} \\ &\quad -\frac{1}{6}F^A_{\alpha\beta}(\mathbf{B})F^A_{\alpha'\beta'}(\mathbf{B})C_{\alpha\beta,\alpha'\beta'} \end{aligned} \tag{1.98}$$

notice by the way the induction energy is always negative.

1.5.1.1 Non Additivity of the Induction Energy

A very important feature arises when we consider the case of a molecule surrounded by several others. We can still express the induction energy as $-\frac{1}{2}F^A_\alpha(\mathbf{B})F^A_{\alpha'}(\mathbf{B})\alpha^B_{\alpha\alpha'}$, but

the field is now the total field due to the other molecules. Consider now two contrasting situations. In the first one molecule B is surrounded by one polar neighbor, so that $F(\mathbf{B}) = \frac{2\mu}{4\pi\varepsilon_0 R^3}$ and the induction energy is

$$U_{ind}^{B} = -\frac{2\alpha\mu^2}{(4\pi\varepsilon_0)^2 R^6} \tag{1.99}$$

Let us consider molecule B as surrounded by two polar neighbors, aligned in such a way their fields are placed in the same direction at B; in this case the total field is just twice the preceding one $F(\mathbf{B}) = \frac{4\mu}{4\pi\varepsilon_0 R^3}$ and the induction energy becomes:

$$U_{ind}^{B} = -\frac{8\alpha\mu^2}{(4\pi\varepsilon_0)^2 R^6} \tag{1.100}$$

four times bigger than the original one. If now we consider the situation in which the two neighbors have fields that are in opposite directions we will have a null field at B so the induction energy will be zero.

With this very simple example we have illustrated very clearly the severe non additivity of induction energy.

Apart for these relatively simple effect we have a much more subtle source of non additivity for the induction energy: consider, for instance, two spherical atoms with polarizabilities α^A and α^B placed at a distance R and experiencing an external electric field F. The field polarises both atoms inducing a dipole moment in both of them, but the induced dipole of each atom produces an additional field at the other, and this must be added to the applied field. Because the effective field experienced by each atom is actually enhanced, the induction energy will be enhanced as well. We have used, for the sake of simplicity, an undefined external electric field, to carry on our example, but the same would have applied to the field produced by a polar molecule. It follows that in general we can not expect to add together the fields due to the static moments of the other molecules in order to calculate the induction energy, altought this is often a reasonable, and even quite good, approximation expecially when dealing with not very polar or polarizable systems.

1.5.2 The Dispersion Energy

Unlike the preceding components, which can be compared with classical analogues, dispersion interaction is a wholly quantic phenomen and can not be treated in any way without the help of quantum mechanical formalism. It may however be physically interpreted as the coupling of oscillations in the charge density (polarizability) of the two molecules giving rise to attractive interactions.

Let us go back to the dispersion energy expressed using the general perturbation theory as we derived previously (for the moment we are concerned only with the dipole-dipole contribution)

$$U_{disp} = - \sum_{\substack{m \neq 0 \\ n \neq 0}} \frac{\langle 00|\mathcal{H}|mn\rangle\langle mn|\mathcal{H}'|00\rangle}{E^A_{m0} + E^B_{n0}} \tag{1.101}$$

where we have used the simplified notation $E^A_{m0} = E^A_m - E^A_0$ and $E^B_{n0} = E^B_n - E^B_0$, we may now manipulate a little bit the preceding expression

$$\begin{aligned} U_{disp} &= - \sum_{\substack{m_A \neq 0 \\ n_B \neq 0}} \frac{\langle 0_A 0_B|\hat{\mu}^A_\alpha T_{\alpha\beta}\hat{\mu}^B_\beta|m_A n_B\rangle\langle m_A n_B|\hat{\mu}^A_\gamma T_{\gamma\delta}\hat{\mu}^B_\delta|0_A 0_B\rangle}{E^A_{m0} + E^B_{n0}} \\ &= -T_{\alpha\beta}T_{\gamma\delta} \sum_{\substack{m_A \neq 0 \\ n_B \neq 0}} \left(\frac{1}{E^A_{m0} + E^B_{n0}} \right. \\ &\times \left. \langle 0_A|\hat{\mu}^A_\alpha|m_A\rangle\langle m_A|\hat{\mu}^A_\gamma|0_A\rangle\langle 0_B|\hat{\mu}^B_\beta|n_B\rangle\langle n_B|\hat{\mu}^B_\delta|0_B\rangle \right) \end{aligned} \tag{1.102}$$

Altought we have factorized the matrix elements in terms referring to A and terms referring to B we were not able to do same for the denominator, so the previous expression is quite uneasy to deal with.

There are mainly two commonly used approaches to handle it: the first one due to London [12] and the second one due to Casimir Polder [13], we will anyway, show the two approaches are absolutely equivalent. Usually, for practical applications the London formula may be treated by the so called *Unsöld* or *average-energy* approximation [14], in this case it will be equivalent to the Casimir Polder one only when the same approximation it applied to the both of them.
We may write the dispersion interaction as

$$\begin{aligned} U_{disp} &= -T_{\alpha\beta}T_{\gamma\delta} \sum_{\substack{m \neq 0 \\ n \neq 0}} \frac{E^A_{m0} \cdot E^B_{n0}}{E^A_{m0} + E^B_{n0}} \\ &\times \frac{\langle 0_A|\hat{\mu}^A_\alpha|m_A\rangle\langle m_A|\hat{\mu}^A_\gamma|0_A\rangle}{E^A_{m0}} \frac{\langle 0_B|\hat{\mu}^B_\beta|n_B\rangle\langle n_B|\hat{\mu}^B_\delta|0_B\rangle}{E^B_{n0}} \end{aligned} \tag{1.103}$$

In the second part of the previous equation we can easily recognize the sum over state expression for the polarizabilities $\alpha^A_{\alpha\beta}$ and $\alpha^B_{\gamma\delta}$, the only problem arising from the factor $\frac{E^A_{m0}\cdot E^B_{n0}}{E^A_{m0}+E^B_{n0}}$. We may however approximate this factor using average energies ε_A and ε_B. We express this term in the form

$$\frac{E^A_{m0}\cdot E^B_{n0}}{E^A_{m0}+E^B_{n0}} = \frac{\varepsilon_A\cdot\varepsilon_B}{\varepsilon_A+\varepsilon_B}(1+\Delta_{mn}) \tag{1.104}$$

where

$$\Delta_{mn} = \frac{\frac{1}{\varepsilon_A}-\frac{1}{E^A_{m0}}+\frac{1}{\varepsilon_B}-\frac{1}{E^B_{n0}}}{\frac{1}{E^A_{m0}}+\frac{1}{E^B_{n0}}} \tag{1.105}$$

with the latter being an identity for each particular value of m and n. We may anyway choose ε_A and ε_B so that Δ_{mn}becomes negligible for all m and n; the latter actually requires that all the states $|m_A\rangle$ that make important contributions have excitation energies close to the average value ε_A, and likewise for $|n_B\rangle$. With these developments the dispersion energy becomes

$$\begin{aligned} U_{disp} &= -\frac{\varepsilon_A\varepsilon_B}{4(\varepsilon_A+\varepsilon_B)}T_{\alpha\beta}T_{\gamma\delta} \\ &\times \sum_{\substack{m_A\neq 0\\ n_B\neq 0}} \frac{\langle 0_A|\hat{\mu}^A_\alpha|m_A\rangle\langle m_A|\hat{\mu}^A_\gamma|0_A\rangle}{E^A_{m0}}\frac{\langle 0_B|\hat{\mu}^B_\beta|n_B\rangle\langle n_B|\hat{\mu}^B_\delta|0_B\rangle}{E^B_{n0}} \\ &= -\frac{\varepsilon_A\varepsilon_B}{4(\varepsilon_A+\varepsilon_B)}T_{\alpha\beta}T_{\gamma\delta}\alpha_{\alpha\beta}\alpha_{\gamma\delta} \end{aligned} \tag{1.106}$$

The latter is the well known London Formula [12], based on the static polarizabilities of the two interacting monomers. Although sometimes used in practically computation the London formula suffer from the impossibility of an a priori strict determination of $\varepsilon_A$and ε_B, sometimes the two quantity are set equal to the lowest ionization energies of A and B respectively to get an upper bound of the magnitude of the dispersion energy.

The Casimir Polder approach [13] led an alternatively formula that proved to be much more useful; it is based on the identity

$$\frac{1}{A+B} = \frac{1}{\pi}\int_0^\infty \frac{AB}{(A^2+\nu^2)(B^2+\nu^2)}d\nu \tag{1.107}$$

applying this formula to the energy denominator of the dispersion energy expressed as $\hbar(\omega^m_A+\omega^n_B)$ one gets

$$U_{disp} = -\frac{2\hbar}{\pi}T_{\alpha\beta}T_{\gamma\delta}$$

$$\times \int_0^\infty \sum_{m\neq 0} \frac{\langle 0_A|\hat{\mu}_\alpha^A|m_A\rangle\langle m_A|\hat{\mu}_\gamma^A|0_A\rangle}{\hbar(\omega_m^A)^2+\nu^2)} \sum_{n\neq 0} \frac{\langle 0_B|\hat{\mu}_\beta^B|n_B\rangle\langle n_B|\hat{\mu}_\delta^B|0_B\rangle}{\hbar(\omega_n^B)^2+\nu^2)}$$

If we recall now the expression, developed using time dependent perturbation theory, for the response to an oscillating electric field $F_\beta e^{-i\omega t}$ with frequency ω, and in particular the expression for frequency dependent polarizability

$$\alpha_{\alpha\beta}(\omega) = \sum_{m\neq 0} \frac{\omega_m \langle 0|\hat{\mu}_\alpha|m\rangle\langle m|\hat{\mu}_\beta|0\rangle}{\hbar(\omega_m^2-\omega^2)} \tag{1.108}$$

we see that the dispersion energy can now be expressed in terms of the polarizability at the imaginary frequency $i\nu$

$$U_{disp} = -\frac{\hbar}{2\pi} T_{\alpha\beta} T_{\gamma\delta} \int_0^\infty \alpha_{\alpha\gamma}^A(i\nu)\alpha_{\beta\delta}^B(i\nu)d\nu \tag{1.109}$$

the latter is the well known and widely used Casimir Polder formula where

$$\alpha_{\alpha\gamma}^A(i\nu) = \sum_{m\neq 0} \frac{\omega_m^A \langle 0_A|\hat{\mu}_\alpha^A|m_A\rangle\langle m_A|\hat{\mu}_\gamma^A|0_A\rangle}{\hbar((\omega_m^A)^2+\nu^2)} \tag{1.110}$$

The concept of polarizability at imaginary frequencies may appear as physically very bizarre. It could be thought of as describing the response to an exponentially increasingly electric field, but this is stretching physical interpretation to perhaps unreasonable limits, and it is better to view it merely as a mathematical formalism. Anyway its mathematical properties are much more regular than those of polarizability at real frequencies, because the denominator has no zero point and increases monotonically with ν. Accordingly $\alpha_{\alpha\gamma}^A(i\nu)$ decreases monotonically from the static polarizability ($\nu = 0$) to zero ($\nu \to \infty$). This means it can be determined quite accurately as a function of ν, either by *ab initio* calculations or from experimental data. In the case of *ab initio* calculations the value of polarizabilities are computed at some value of imaginary frequencies and then Casimir Polder is solved using a numerical quadrature for the integral. Due to the mathematical regularity of the imaginary frequency polarizabilities usually good results can be achivied with a relative small number of computed polarizabilities.

The previous formulae have been obtained using the cartesian formalism and the dipole operator, but exactly the same derivation can be performed with higher rank multipole operators or in the spherical tensor formalism, and one may still get London or Casimir Polder formula providing the dipole polarizability has been substituted with the proper polarizability component depending on the specific multipole operator in use.

1.6 Long Range Molecular Coefficients

As a consequence of the particular form assumed by the interaction potential at large distances, and in particular as a consequence of the dependence on R^{-n} of the T tensor, each component of the interaction (electrostatic, induction, dispersion) can be expressed as $-C_n R^{-n}$ the factors $C_n$being the long range intermolecular coefficients.

In particular, assuming the spherical tensor formalism we have

$$U_{es} = \sum_{l_a l_b} C_n^{l_a l_b} R^{-n} \tag{1.111}$$

$$U_{ind/disp} = \sum_{l_a l_b} \sum_{l'_a l'_b} C_{n+n'}^{l_a l_b, l'_a l'_b} R^{-n-n'} \tag{1.112}$$

where $n = l_a + l_b + 1$, $n' = l'_a + l'_b + 1$, and the parameters l_a, l_b describes the order of the involved multipole.

Long range molecular coefficients are useful not only because they can be used to describe the long range behavior of the interaction, but also because they are very interesting by themselves: in fact they embody all dependence on the electric properties which characterize the charge distributions of the individual molecules and their relative orientation in the dimer.

Assuming point multipoles located at the center of mass of each molecule and neglecting translation of the reference frame we obtain the general formulae [15]

$$C_n^{l_a l_b}(es) = (-1)^{l_b}(l_a + l_b)! \sum_{q_a q_b} P_{q_a q_b}^{l_a l_b} \mu_{l_a q_a}^A \mu_{l_b q_b}^B \tag{1.113}$$

$$\begin{aligned} C_{n+n'}^{l_a l_b, l'_a l'_b}(ind, A) &= \frac{1}{2}(-1)^{l_b + l'_b}(l_a + l_b)!(l'_a + l'_b)! \\ &\times \sum_{q_a q_b} \sum_{q'_a q'_b} P_{q_a q_b}^{l_a l_b} P_{q'_a q'_b}^{l'_a l'_b} \alpha_{l_a q_a, l'_a q'_a}^A \mu_{l_b q_b}^B \mu_{l'_b q'_b}^B \end{aligned} \tag{1.114}$$

$$\begin{aligned} C_{n+n'}^{l_a l_b, l'_a l'_b}(ind, B) &= \frac{1}{2}(-1)^{l_b + l'_b}(l_a + l_b)!(l'_a + l'_b)! \\ &\times \sum_{q_a q_b} \sum_{q'_a q'_b} P_{q_a q_b}^{l_a l_b} P_{q'_a q'_b}^{l'_a l'_b} \mu_{l_a q_a}^A \alpha_{l_b q_b, l'_b q'_b}^B \mu_{l'_b q'_b}^A \end{aligned} \tag{1.115}$$

$$\begin{aligned} C_{n+n'}^{l_a l_b, l'_a l'_b}(disp) &= (-1)^{l_b + l'_b}(l_a + l_b)!(l'_a + l'_b)! \\ &\times \sum_{q_a q_b} \sum_{q'_a q'_b} P_{q_a q_b}^{l_a l_b} P_{q'_a q'_b}^{l'_a l'_b} \sum_{l_a l_b, l'_a l'_b} D_{n+n'}^{l_a l_b, l'_a l'_b} \end{aligned} \tag{1.116}$$

where we have ignored the factors that are unity in atomic units coordinates (like $\hbar$) and we have defined the dispersion constants $D_{n+n'}^{l_a l_b, l'_a l'_b}$ as

$$\begin{aligned} D_{n+n'}^{l_a l_b, l'_a l'_b} &= \frac{1}{4} \sum_a \sum_b \frac{\varepsilon_a \varepsilon_b}{\varepsilon_a + \varepsilon_b} \alpha^A_{l_a q_a, l'_a q'_a} \alpha^B_{l_b q_b, l'_b q'_b} \\ &= \frac{1}{2\pi} \int_0^\infty \alpha^A_{l_a q_a, l'_a q'_a}(i\omega) \alpha^B_{l_b q_b, l'_b q'_b}(i\omega) d\omega \end{aligned} \tag{1.117}$$

In the proceeding of this thesis we will focus mainly on the dispersion energy and coefficients so let us spend a little more time on the latter expressions.

We may see how we were able to factorise, in the dispersion coefficients expression, the components depending on electric properties, i.e. the dispersion constants, and the factors depending also on geometrical (mutual orientation) parameters, i.e. the P factors. It is clear the quantum chemical effort will be focused on the determination of $D_{n+n'}$ for the symmetry allowed components, and then one will get dispersion coefficients $C_{n+n'}$ by a simple algebraical combination, once the P factors have been explicitated.

Probably the best way to find out working expression for the factors P is to make explicit the dependence on the Euler angles (Ω_A, Ω_B) [2] and, obviously, to consider all the consistent simplification arising from the local symmetry of the interacting monomer. We will present explicit cases for two very simple systems of particular interest in this work

- Two atoms in $S-$states. In this case all Euler angle are zero and the only non vanishing dispersion constants will be the ones for which

$$n = n' \, l'_a = l_a \, l'_b = l_b \tag{1.118}$$

furthermore we will have

$$[(l_a + l_b)!]^2 (P^{l_a l_b}_{q_a q_b})^2 = \begin{pmatrix} 2l_a + 2l_b \\ 2l_a \end{pmatrix} \tag{1.119}$$

in this case we have

$$C^{l_a l_b}_{2n} = \begin{pmatrix} 2l_a + 2l_b \\ 2l_a \end{pmatrix} D^{l_a l_b}_{2n} \tag{1.120}$$

if we consider some particular situations we will have:
dipole-dipole interaction: $l_a = l_b = 1$, $2n = 6$

$$C_6^{1,1} = 6 D_6^{1,1} \tag{1.121}$$

Table 1.2: D_6 Constants for linear molecules

$\mathbf{D_6}$	
A	$(\alpha_{\parallel\parallel\parallel})^A, (\alpha_{\parallel\parallel\parallel})^B$
B = C	$(\alpha_{\parallel\parallel\parallel})^A, (\alpha_{\perp\perp})^B$
D	$(\alpha_{\perp\perp})^A (\alpha_{\perp\perp})^B$

dipole-quadrupole interaction: $l_a = 1$, $l_b = 2$, $2n = 8$

$$C_8^{1,2} = 15 D_8^{1,2} \tag{1.122}$$

- Two linear molecules in $S-$states. In this cases the situation becomes a little bit more complicated, so let us only present the final results.
  As concerns the case where $l_a = l_b = l'_a = l'_b = 1$ we are treating an interaction in which only the dipole operator is involved and we get $n + n' = 6$. In Table 1.2 and 1.3 we show the actual values of D_6 constants and C_6 coefficients respectively in terms of cartesian polarizability ($\alpha_{\parallel\parallel}$ means a dipole polarizability parallel to the bond axis, while $\alpha_{\perp\perp}$ perpendicular to the same bond axis).
  When we are dealing with the case $l_a = 2\, l_b = l'_a = l'_b = 1$ we are treating an interaction in which the dipole and quadrupole operator are involved on the first molecule, while only the dipole is acting on the second one, we get therefore $n+n' = 7$. In Table 1.4 and 1.5 we show the result for dispersion constants and coefficients respectively. (Again $A_{\parallel\parallel,\parallel}$ means a dipole-quadrupole polarizability in which the quadrupole moment operator has the two components along the bond axis, as well as the dipole operator, for the other components the interpretation follows accordingly.)

Table 1.3: C_6 Coefficients for linear molecules

$\mathbf{L}_A$	$\mathbf{L}_B$	$\mathbf{M}$	$\mathbf{C}_6^{L_A L_B M}$
0	0	0	$\frac{2}{3}(A + 2B + 2C + 4D)$
0	2	0	$\frac{2}{3}(A - B + 2C - 2D)$
2	0	0	$\frac{2}{3}(A + 2B - C - 2D)$
2	2	0	$2(A - B - C + D)$
2	2	1	$-\frac{4}{9}(A - B - C + D)$
2	2	2	$\frac{1}{18}(A - B - C + D)$

Table 1.4: D_7 Constants for linear molecules

$\mathbf{D}_7$	
A	$(A_{\parallel\parallel,\parallel})^A(\alpha_{\parallel,\parallel})^B$
B	$\frac{2}{\sqrt{3}}(A_{\parallel\perp,\perp})^A(\alpha_{\parallel\parallel})^B$
C	$(A_{\parallel\parallel,\parallel})^A(\alpha_{\perp\perp})^B$
D	$\frac{2}{\sqrt{3}}(A_{\parallel\perp,\perp})^A(\alpha_{\perp\perp})$

Table 1.5: C_7Coefficients for linear molecules

$\mathbf{L}_A$	$\mathbf{L}_B$	$\mathbf{M}$	$\mathbf{C}_7^{L_A L_B M}$
0	1	0	$-\frac{12}{5}(A + \sqrt{3}B + 2C + 2\sqrt{3}D)$
0	3	0	$-\frac{8}{15}(3A - \sqrt{3}B + 6C - 4\sqrt{3}D)$
2	1	0	$-\frac{12}{5}(A + \sqrt{3}B - C - \sqrt{3}D)$
2	1	1	$\frac{2}{5}(A + \sqrt{3}B - C - \sqrt{3}D)$
2	3	0	$-\frac{28}{15}(3A - 2\sqrt{3}B - 3C + 2\sqrt{3}D)$
2	3	1	$\frac{14}{45}(3A - 2\sqrt{3}B - 3C + 2\sqrt{3}D)$
2	3	2	$-\frac{1}{45}(3A - 2\sqrt{3}B - 3C + 2\sqrt{3}D)$

Chapter 2

The Computation of Intermolecular Forces

In this Chapter we will present the most common, and classical, methods developed and applied to compute Intermolecular Forces at *ab initio* level. In particular we will focus our attention on the Supramolecular Approach, spending some time analysing, in a preliminary way, the problem of the Basis Set Superposition Error, and in the application of the Long Range Perturbation Theory (LRPT methods), considering in particular the approaches based on London and Casimir Polder formulae. At the end some time will be dedicated to the Symmetry Adapted Perturbation Theory (SAPT).

2.1 Supramolecular Approach

The Supramolecular Method's philosophy is, actually, the most simple and straightforward. Let us, in fact, consider a molecular systems composed of two interacting fragments A and B. The interaction energy can be expressed simply as the difference of the energy of the complex AB and the energy of the isolated fragments A and B. Even if this may seem a very simple and crude treatment it is, still nowaday, by far the most common procedure for the quantitative determination of the interaction.

The first problem connected with this approach is the interaction energy is some order of magnitude lower than the energy of the isolated monomers, so very accurate computation are needed in order to get valuable result.

Moreover the Supramolecular Approach gives, in the field of the Born Oppenheimer approximation, an interaction (hyper-)surface representing the combination of all the contributions to the interaction. For this reason, in contrast with LRPT methods, is quite

hard to get out the various contributes (electrostatic, induction, dispersion, exchange) giving rise to the total interaction potential. These contributes as we saw in the previous Chapter, have a well defined physical meaning, and is therefore, sometimes, important to separate them. The latter is also quite important to define some model potential which can be used, for instance, in Molecular Dynamics fields, since usually these potentials have the form

$$U(R) = \beta e^{-\alpha R} - \sum_n C_n R^{-n} \tag{2.1}$$

2.1.1 The Basis Set Superposition Error

There is however a more subtle and fundamental problem arising with this approach, a problem that has, by the way, given rise to a tremendous amount of work in order to find the most suitable solution, this is the *Basis Set Superposition Error.*

Again the interpretation of this problem is very simple, if one considers the description of the fragment A **within** the complex it is easy to see it can be improved by the basis functions of the fragment B and vice versa, whereas such an effect is not possible in the calculation of the isolated monomers. This unbalance provokes that the overall description of the complex AB is improved with respect to the description of the monomers. Hence the interaction energy, expressed as the difference between the energies of the dimers and its constituent is biased by the fact that the basis set where the corresponding wave functions are expanded are different. Moreover the variational principle implies that the computed energy difference is artificially increased, as the complex is expanded in a larger basis set compared with the ones in which the fragments are expanded.

This effect was firstly pointed out by Jansen and Ros in 1969, even if the terminology BSSE was first used by Liu and Mc Lean in 1973.

Since this problem was first evidenced a number of methods and strategies have been developed to eliminate or, at least, minimise it. Obviously the most natural way of eliminating BSSE, avoid the truncation of the basis so obtaining the exact wave functions is practically unfeasible from a computation point of view, since it would imply the use of infinite basis sets. It is however useful to improve the basis sets of the monomers such as the presence of the functions from the other fragment would not improve their description.

Another rather unexplored solution would be the use of a set of functions centred at some given points in the space to compute the energy of the complex and its constituents, the three dimensional space might be saturated of basis functions whose positions and parameters should be kept constant for each calculations. However the so obtained

wavefunctions will be neither translationally nor rotationally invariant, moreover linear dependencies might easily appear if the space is too much saturated with basis functions. A more promising tool, mostly applied in DFT methods with the local spin density, may be the use of plane waves. This has been extensively used in Car-Parrinello molecular dynamic but is scarcely used in electronic structure computations. Nowadays most recently efforts are going toward the combination of plane waves and nuclear centred functions, in this case the BSSE problem in intermolecular calculation will still remain.

2.1.1.1 The Counterpoise Correction

The by far most used way to treat BSSE is still the so called Counterpoise Correction, originating from a work by Boys and Bernardi [16] (1970).

The authors proposed the use of a Counterpoise Correction (CP) to calculate the energy of the AB system in such a way that the separate energies of the fragments A and B are computed using the full basis set used for the complex. For each fragment calculations, the electrons belonging to the other monomers are omitted, the nuclear charge of the latter is set to zero but the basis set functions are maintained, the difference between the (CP) computed energies of the monomers and the usually computed ones represents the Counterpoise correction.

The overall procedure may be schematized as follows

- Compute the energy of the complex AB (at the geometry R) using basis set $A+B$ $E_{AB}^{A+B}(R)$
- Compute the energy of the monomer A using basis set A E_A^A and the energy of the monomer B using basis B E_B^B
- Compute the energy of the monomer A and B using basis set $A+B$ (ghost orbitals of the other monomer are present) E_A^{A+B} and $E_B^{A+B}(R)$ respectively
- Calculate CP Correction as

$$CP(R) = E_A^A + E_B^B - E_A^{A+B} - E_B^{A+B} \tag{2.2}$$

- Calculate the BSSE corrected intermolecular energy as

$$E_{AB}^{CP}(R) = E_{AB}^{A+B}(R) + CP(R) \tag{2.3}$$

The Counterpoise corrected curve $E_{AB}^{CP}(R)$ lies above the uncorrected results, and the position of the minimum, as well as the general shape of the potential surface is similarly

affected. The CP corrected curves have, always, minima at larger distances than the uncorrected ones, although the effect on the minimum is of slightly smaller magnitude than the one on the value of the energy itself.

After the Counterpoise Correction was introduced, and it proved efficient, there was a widespread debate over the fact whether the BSSE was overestimated with this simple and straightforward procedure. Some alternative Counterpoise schemes were proposed, for instance it was suggested to calculate CP using only the virtual ghost orbital instead of the complete set. However the BSSE being a completely unphysical effect it is rather difficult to explain it with physical consideration like the Pauli exclusion principle. It has been subsequently shown that the original CP scheme is the one better reproducing inherent BSSE free values for small systems like Helium dimer.

One more subtle complication arises when one considers polyatomic interacting molecules, in this case one should deal, in order to correctly design interaction potentials, with the relaxation of the intermolecular coordinates due to the interaction. Unfortunately this fact was not taken into account in the original formulation, because only interacting atoms were considered.

The total CP corrected energy is, therefore, usually calculated as the sum of the counterpoise corrected interaction energy at the supermolecular geometries and the fragment relaxation energy, however while the CP corrected energy is calculated using the total basis set $A + B$ the relaxation is calculated used only the monomer basis adding therefore another rather crude approximation.

The interplay within the intermolecular relaxation and BSSE is anyway all but a trivial task: the conventionally CP scheme cannot, in fact, be applied in an unambiguous way when geometries of the fragments become different from the ones of the monomers because the position of the ghost orbitals becomes not defined. When dealing with such a problem one should, therefore, differentiate between the interaction energy and the stabilization energy. The former stands for the difference between the complex energy and the ones of their monomers at the supramolecular geometries. The latter represents the total stabilization energy resulting from bringing the monomers from infinite separation to the equilibrium distance.

2.1.1.2 Aprioristic correction

Some quite different approaches to the treatment of the BSSE are the aprioristic correction methodologies. In these cases rather than recalculate the energy in the fragments, one tries to eliminate the BSSE sources in the calculation of the complex itself. The most common among these approaches is the Chemical Hamiltonian (CHA) firstly pro-

posed by Mayer [17]. Briefly speaking starting from the SCF level one can, using second quantization formalism, split the Hamiltonian in the sum of all the intramonomer contributes and the pure intermolecular operator. The BSSE is eliminated projecting all the intramonomer into the subspace spanned by the basis functions of the corresponding fragment, the final result is therefore a description of the dimer where the BSSE has been eliminated with no *a posteriori* treatment. So far this methodology has been applied at HF, DFT, MP2 and CI level and the results converge well towards the CP corrected ones. Despite of this finding the non hermitian nature of the resulting Hamiltonian and the fact that the energy has to be computed using a different Hamiltonian resulted in a not widespread success of the CHA methods. Some other methods, partly based on the localization of molecular orbitals, have been proposed but almost all proved to be unable to correctly reproduce CP and experimental results, their most important problem being a systematic overestimation of the interaction energy (or correspondingly a systematic overestimate of the BSSE). Some preliminary study were performed by us using a localization technique and a topological selection of excitation in order to eliminate intermolecular excitations in the CI Hamiltonian but results are still far from being acceptable.

2.1.2 Current trends

Nowadays CP correction is still the most widely used tool to eliminate the BSSE and many authors used it in intermolecular calculations. In some very particular cases however, there is a strong tendency to use the largest possibly basis set in order to have BSSE tending to zero and therefore simply neglecting its effects. Among the *a priori* methodologies only the CHA proves to be an efficient and practical computational methodology, even if its use is still much less common than the CP correction. The success of the Supramolecular Approach in the computation of intermolecular forces is due mainly to its efficiency and to its conceptual and practical simplicity. In fact, it implies nothing more than the simple calculation of molecular energies (at least using the very common feature of ghost orbitals) and therefore, it can be performed without consistent effort using almost any code capable of solving the Schrödinger equation for the energy at any desired level of theory.

2.2 Perturbation Theory

The use of Perturbation theory in the computation of intermolecular interactions is conceptually quite different from the supramolecular approach. While the latter is based

on the direct calculation of energy differences between the complex and the fragments, Perturbation Theory methods make direct use of the formalism derived in the previous Chapter, hence they decompose the energy terms in the sum of electrostatic, inductive, dispersive (and for the short range exchange) contributions. They are usually aimed at the determination of the Intermolecular coefficients C_n appearing in the expansion formula (E^{LR} stands for energy at long range)

$$E^{LR} = -\sum_n C_n R^{-n} \tag{2.4}$$

As the name implies they make a consistent use of the Rayleigh Schrödinger Perturbation Theory and are capable of determining intermolecular coefficients from the electric properties of a single monomer, moreover they usually give, the values of these properties as byproducts.We may refer these methods as one-body, in contrast with the Supramolecular two-body approaches in which it is always necessary to explicitly calculate the energy of the dimer.

We will here briefly talk about long range perturbation theory (LRPT) where one may get rid of the antisymmetry requirements and use the standard tools of perturbation theory and at the end about the Symmetry Adapted Perturbation Theory.

2.2.1 Electrostatic and Inductive Terms

The determinations of electrostatic and inductive interaction terms is actually a very simple task in the framework of LRPT, due to the very simple and straightforward form assumed by the interaction.

Electrostatic contribution in fact requires only the knowledge of first order perturbation quantity (multipole operators)

$$C_n \propto Q^A_{lq} Q^B_{l'q'} \tag{2.5}$$

where Q are general multipole moments of monomer A and B respectively. They may be very easily determined by a large variety of quantum chemistry codes, both analytically solving the zero order perturbation theory (this task requires the knowledge of the unperturbed wave function only)

$$Q_{lq} = \langle \Psi_0 | \hat{Q}_{lq} | \Psi_0 \rangle \tag{2.6}$$

and numerically using the so called Finite Field technique. The latter makes explicitly use of the definition of the multipole moment as minus the first derivative of the energy

against an electric field (field gradient, and so on)

$$Q_{lq} = -\frac{\partial \langle \Psi_0 | \mathcal{H} | \Psi_0 \rangle}{\partial F_{lq}} \tag{2.7}$$

hence it requires only the determination of the monomer energy for various values of electric field and subsequently a numerical derivation. This is a very common task easily performed by almost all quantum chemistry codes, the only supplementary complication being the capability to compute energies in the presence of an electric field.

As far as the induction energy is concerned the expression involved are only slightly more complicated involving also the second order property: the polarizabilities. We remind in fact the expression for the induction coefficients is

$$C_n \propto Q^A_{lq} \alpha^B_{lq,l'q'} Q^B_{l'q'} \tag{2.8}$$

the only difficulty may lie on the determination of the static polarizability. This can be performed analytically solving the first order perturbation equation

$$\alpha = 2 \langle \Psi_0 (E_1 - \hat{Q}_{lq}) | (\mathcal{H} - E_0)^{-1} | (E'_1 - \hat{Q}_{l'q'}) \Psi_0 \rangle \tag{2.9}$$

where we defined $E_1 = \langle \Psi_0 | \hat{Q}_{lq} | \Psi_0 \rangle$ $E'_1 = \langle \Psi_0 | \hat{Q}_{l'q'} | \Psi_0 \rangle$ $E_0 = \langle \Psi_0 | \mathcal{H}_0 | \Psi_0 \rangle$ (let us underline the previous one is nothing but the general expression of first order perturbation theory and its solution can be expressed via the sum over state we used in the definition of polarizability in the previous chapter). Obviously the solution of this equation is a little bit more complicated than the zero order one but can still be performed by a large number of codes, some more complication may arise for method like Coupled Cluster in which the Hamiltonian looses its hermicity. Anyway the static polarizability can still be computed using the finite field methodology since it is defined like minus the second derivative of the energy with respect to the electric field (or field gradient .....)

$$\alpha_{lq,l'q'} = -\frac{\partial^2 E}{\partial F_{lq} \partial F_{l'q'}} \tag{2.10}$$

this computation is performed exactly the same way like the multipole one, via the computation of the energy for various values of field strength and numerical derivation to the second order.

2.2.2 Dispersion Terms

If the calculation of electrostatic and inductive terms is very easily performed in the framework of perturbation theory (requiring only very standard technique if used with

finite field machinery) the same can not be said for the dispersion terms. The working equation for the calculation of dispersion coefficients (and constants) using LRPT are the Casimir-Polder and London formulae, we derived earlier. Among the two the Casimir-Polder one is certainly, up to now, the most widely used in this context, as it is easy to understand from the formula itself

$$D_n = \frac{1}{2\pi}\int_0^\infty \alpha^A_{l_a q_a, l'_a q'_a}(i\omega)\alpha^B_{l_b q_b, l'_b q'_b}(i\omega)d\omega \tag{2.11}$$

it implies the computation of imaginary frequency polarizabilities for each molecule and subsequently a numerical integration to get the value of the constants.

The frequency dependent polarizability is obtained solving the first order perturbation equation

$$\begin{aligned} L^{\pm}_{\omega} &= \langle \Psi_0(E_1 - \hat{Q}_{lq})|(\mathcal{H} \pm \omega - E_0)^{-1}|(E'_1 - \hat{Q}_{l'q'})\Psi_0\rangle \\ \alpha(i\omega) &= L^+ + L^- \end{aligned} \tag{2.12}$$

the latter can not be considered a trivial task to be performed, requiring an iterative process in a complex space but can nonetheless be done by some commercial or free codes like for instance ADF [18] or DALTON [19]. It is also possible to obtain imaginary frequency polarizabilities using method which do not involve the iteration in complex space, for instance one approximation we will talk about in the proceeding is the Pade' Approximation which allows to obtain lower and upper bound to the polarizability from the Cauchy Moments. In any case once the polarizability has been determined for a reasonable number of imaginary frequencies it is necessary to perform a numerical quadrature. Usually this task is performed with the Gauss Legendre method

$$\int_{-1}^{+1} f(x)dx = \sum_{i=-1}^{+1} f(x_i)\gamma_i \tag{2.13}$$

where $f(x_i)$ states for the value of the integration function at the point x_i and γ_i is the weight at the point x_i, if we consider the Casimir Polder formula we may see the integration limits are not -1 and $+1$ so it is necessary to perform a variable substitution: following Amos scheme [20] we set

$$y = \xi\frac{1+x}{1-x} \tag{2.14}$$

where ξ is an arbitrary variable, in that case we will have

$$\begin{aligned} \lim_{x\to 1^+} y &= 0 \\ \lim_{x\to 1^-} y &= +\infty \end{aligned} \tag{2.15}$$

which falls in the Gauss Legendre integration interval, upon substitution we have (remembering $\frac{dy}{dx} = \frac{2\xi}{(1-x)^2}$)

$$\begin{aligned}\int_0^\infty \alpha(i\omega)\alpha'(i\omega)d\omega &= 2\xi \int_{-1}^{+1} \alpha(\frac{1+i\omega}{1-i\omega})\alpha'(\frac{1+i\omega}{1-i\omega})\frac{1}{(1-i\omega)^2}d(\frac{1+i\omega}{1-i\omega}) \\ &= 2\xi \sum_{-1}^{+1} \alpha(x_i)\alpha'(x_i)\frac{\gamma_i}{(1-x_i)^2} \end{aligned} \tag{2.16}$$

which led to the numerical quadrature considering $\frac{\gamma_i}{(1-x_i)^2}$ as modified weights and x_i the modified values of frequence at which polarizability has to be calculated.

In practical calculations it is often necessary to work with a number of integration points of eight or sixteen frequencies in order to get reasonable results, while the ξ parameter is usually kept at 0.2 or 0.3; the best results are probably the ones in which the number of frequencies is kept to 32, even if the latter would imply a very high computational cost, in the case one is directly computing dynamic polarizabilities with perturbation theory and is not relying on approximate methods like Pade' approximation.

Anyway, although the method is intrinsically not variationally bounded implying a numerical quadrature, and in some instance it is not computationally economic. Casimir Polder it is often considered as the standard *de facto* in LRPT dispersion calculation, as far as the number of chosen point is kept reasonably high, and new approaches are often tested against it. In fact a quite high number of dispersion constants has been calculated using this approach (with dynamic polarizability determined at various levels of theory) for a large variety of molecular and atomic systems.

Some other approaches exploit the London formula instead, and although less common than Casimir Polder based ones are worth to be mentioned here. In all these approaches the computational effort relies on the determination of the pseudospectral decomposition (i.e. the determination of the transition moments between ground and excited states at the London formula's numerator and the energy dimension terms at the denominator), once the pseudospectra are obtained a straightforward application of the London formula yields the values of the Dispersion Constants see for example the work of Magnasco and coworkers [21].

2.2.3 Symmetry Adapted perturbation Theory (SAPT)

A very interesting and promising method which allows the inclusion of short range repulsion on the perturbation theory framework is the Symmetry Adapted Perturbation theory [22].

Consider, for instance, two interacting molecule A and B we will have: $\mathcal{H} = \mathcal{H}_A + \mathcal{H}_\mathcal{B} + V = \mathcal{H}_0 + V$ and at the first order $(\mathcal{H}_0 + V)\Psi = (E + E_{int})\Psi$. But the standard Rayleigh Schrödinger perturbation theory, does not take into account the antisymmetry property of the wavefunction in the resulting space $\mathcal{H}_A \otimes \mathcal{H}_B$, the wavefunction being, in fact, antisymmetric upon the permutation of two electrons. With SAPT on the other hand the solution is forced to respect the correct perturbative symmetry with the use of opportune antysimetrizers in the $n-$order perturbative equation

$$(E_{int})_n = \langle \Psi_0 | V\mathcal{G} | \Psi_{n-1} \rangle \tag{2.17}$$

in this case the $n - order$ eigenfunction becomes

$$\Psi_n = \Psi_0 + R_0[\langle \Psi_0 | V\mathcal{G}' | \Psi_{n-1} \rangle - V]\mathcal{F}\Psi_{n-1} \tag{2.18}$$

where R_0 represent the resolutor and $\mathcal{G}\,\mathcal{G}'\,\mathcal{F}$ are opportune symmetrized projectors. Different kind of SAPT solutions can be obtained depending on the use of different symmetrized projectors, for instance in the case $\mathcal{F} = \mathcal{G}' = 1$ we have the simplest solution (the feeblest antysimmetrization) called Symmetrized Rayleigh Schrödinger. We will not proceed in an exhaustive treatment of the SAPT method but we would like to remind how this method can be used at many level of theory and has been capable of yeld very accurate values of intermolecular energies (expecially when used at Coupled Cluster level), both for the attractive and repulsive part of the potential.

2.2.4 Final Considerations

As previously stated Perturbation Theory based methods allow for the separate determination of all the components of interaction energy which have a proper definite physical meaning and it relates them to the electrical properties of the monomers. Supramolecular Approach, on the other hand, only gives the interaction potential curve. For these reasons the previous have to be preferred if one is interested in finding out the individual contribution of the interaction in order to better investigate its nature. It is also worth to be mentioned how these methods giving (mainly) the values of the intermolecular coefficients allows for a very easy parametrization of the potential, helping in building accurate intermolecular parameters to be used subsequently.

Moreover being One Body methods they are inherently BSSE free and usually they are computationally cheaper than corresponding Two Body methods. The computational demanding quantities depend only on the electric properties of one single monomer, so they are computed in the space defined by that particular monomer. This is particularly

important if one is interested in building tables of intermolecular coefficients involving homo and hetero dimers.

On the contrary theoretical formulation and code needed are in general much more complicated than the Supramolecular machinery, thus leading to a greater complexity and difficulty in the use of these formulations.

Chapter 3

The Computational Machinery

During this thesis we, mostly, performed computations at FCI and Coupled Cluster (expecially $R_{12}-$Coupled Cluster) level, moreover some innovative applications developed at the previously cited levels of theory will be presented. For these reasons we will introduce here the basic theory of these two methods, and some of their most common features used in this work.

3.1 The Full Configuration Interaction Method

The problem we are addressing by the Full Configuration Interaction (FCI) [23] method is to find an approximate but highly accurate (actually the most accurate possible solution with a given basis set) of the molecular $n-$electron Schrödinger equation. We may even say the FCI solution represent the exact solution to the wavefunction equation in the subspace spanned by a given orbital expansion set.

Let us define the Schrödinger equation (using atomic units) as:

$$\mathcal{H}\Psi = \sum_{k=1}^{n} h_k + \sum_{k<l}^{n} \frac{1}{r_{kl}}\Psi = E\Psi \tag{3.1}$$

Here the one electron operator h_k includes kinetic energy and Coulomb attractions by all the nuclei in the molecule, while the two electron terms $\frac{1}{r_{kl}}$ represent the electron electron repulsion. We also remind the physical solution of the Schrödinger equation must obey the Fermi-Dirac statistic, i.e. to be antisymmetric under electron exchange, and should also be eigenfunctions to the total spin operators S^2 and S_z.

Usually, since the very early days of quantum mechanics [24], the many body problem we are talking about is solved building the $n-$electrons wavefunction from an orthonormal set of spin-orbitals χ_k. These spin orbital are composed by a spacial part or orbital

that is nothing but a function φ of the space coordinates x, y, z of the electron and a spin part, α, β taken such as to be an eigenfunction of the spin operators S^2, S_z. So that we will have $\chi = \alpha\varphi$, $\beta\varphi$.

The most famous, and maybe the simplest, example of an antisymmetric function, useful to express the solution of such an equation, is the Slater determinant, in fact the latter offered a very simple alternative to the more esoteric theoretical group methods [25], providing the conceptual framework to computational quantum chemistry.

In this framework the FCI method can be very simply defined by expanding the wavefunction Ψ as a linear combination of **all** the Slater determinants one can obtain from a given set of spin orbitals $\{\varphi_k\}$. The expansion coefficients are then obtained by the Rayleigh-Ritz variational method: solving the eigenvalue problem of an Hamiltonian matrix **H**. This is the reason why given a spin orbital basis set (and therefore an orbital basis set) FCI represent the best variational solution one can obtain. At this point one could surely enlarge the orbital basis and improve the approximation, moving towards converge to the exact physical solution to the problem (some convergence theorems have also been given [26]), however there is a serious drawback: the exceedingly rapid increase of the dimension of the matrix **H** with the number of the electrons and spinorbitals. In fact the numbers of Slater determinants grows combinatorially for n_α, n_β electrons in N orbitals

$$N_{det} = \begin{pmatrix} N \\ n_\alpha \end{pmatrix} \begin{pmatrix} N \\ n_\beta \end{pmatrix} \tag{3.2}$$

the combinatorial explosion of dimensions is the key problem of FCI, severely limiting its applicability, for this reasons many methods to reduce the CI space have been introduced giving rise to various CI truncating schemes (which have to be considered like approximations to the FCI), the latter are nowadays commonly used much more than the FCI itself. It has to be recalled however that the previous expression can be reduced if one takes full advantages of the symmetry property of the molecular system. If we consider, for instance, a molecule belonging to a point group with order h we will show later how the number of determinants becomes

$$N_{det} \simeq \frac{1}{h} \begin{pmatrix} N \\ n_\alpha \end{pmatrix} \begin{pmatrix} N \\ n_\beta \end{pmatrix} \tag{3.3}$$

therefore the dimensions are reduced up to a factor eight if one is working with a high symmetric system in the framework of Abelian symmetry groups.

A major step in the CI (and FCI) technique was, anyway, the one taken by Roos with the introduction of the direct method [27], avoiding the explicit construction of the Hamiltonian matrix **H**, with the use of iterative algorithms for computing eigenvectors

like Lanczos or Davidson methods. In this context one starts from a vector guess $\mathbf{x}_0$ and improves it at each cycle by various operation, all of them involving the same fundamental operation (FO)

$$\mathbf{y} = \mathbf{H}\mathbf{x} \tag{3.4}$$

the multiplication of the Hamiltonian matrix $\mathbf{H}$ by a vector $\mathbf{x}$ to give a new vector $\mathbf{y}$ in the FCI space. It was, as we said, pointed out by Roos that this multiplication can be performed without computing and storing the matrix $\mathbf{H}$ but directly from the one and two electron integrals list. The latter is much shorter than the vector $\mathbf{x}$, being of the order N^4/h, therefore the only quantities one needs to store are the two vectors $\mathbf{x}$ and $\mathbf{y}$, and the integrals. CI vectors can be stored as two dimensional arrays, in this case the FO is performed running along the columns.

The first FCI algorithm allowing for large scale computation is due to Handy and coworkers [28, 29] and implemented Siegbahn's idea of the resolution of the identity in FCI space to break down the two electron part of the Hamiltonian in a sum over intermediate excited states. It was followed later by the method proposed by Olsen et Al. [33] who used a resolution of the identity in string rather than in determinants space. Here we will present the fundamental of the implementation of the code for direct FCI expanded in Slater determinants developed and commonly used in our laboratory [34].

It is however important to underline that FCI is not only a computational challenge, it is indeed a very useful tool to obtain benchmarks and to asses the reliability of the approximate methods, like, for instance, truncated CI, MCSCF, Coupled Cluster etc...

3.1.1 Representation of the CI vectors

Let us assume the system belongs to a spacial Abelian symmetry group $\mathcal{G}$ of order h. All the orbitals are taken to be symmetry adapted, and we will denote by S_i the symmetry species of the orbital i. The Slater determinants are represented by couples of strings $|\theta_\alpha\theta_\beta\rangle$. Each string θ is an ordered sequence of occupation numbers like, for instance, 1, 0, 0, 1, where a one in a position k means that orbital k is occupied (notice however this convention implies the orbital are arranged in a definite order in the Slater determinants). The association of strings to give a Slater determinants is, in fact, an antisymmetrized tensor product

$$|\theta_\alpha\theta_\beta\rangle = |\theta_\alpha\rangle \wedge |\theta_\beta\rangle \tag{3.5}$$

$$|\sum_i c_i\theta_\alpha \sum_j c_j\theta_\beta\rangle = \sum_{ij} c_i c_j |\theta_\alpha\theta_\beta\rangle \tag{3.6}$$

We may now define the string symmetry $S(\theta)$ as the products of the symmetries of its occupied orbitals, $S(\theta) = S_i * S_j$ (where $*$ is the group multiplication). We have to point out all the strings are sequentially ordered in some way, therefore we may define $I(\theta)$ as the address or ordinal number of θ, in such a way that any Slater determinant $|\theta_\alpha \theta_\beta\rangle$ corresponds to the couple $I(\theta_\alpha), I(\theta_\beta)$. Moreover the strings are separately ordered symmetry by symmetry; that means the function $I(\theta)$ lists first strings of symmetry 1, then strings of symmetry 2 and so on. Because the FCI eigenvector has a definite symmetry too S_v, we will be able to combine only those strings that respect the relation:

$$S_v = S(\theta_\alpha) * S(\theta_\beta) \tag{3.7}$$

denoting by $\Theta(S)$ the set of strings of symmetry S, a general vector V in the FCI space can be therefore written as

$$V = \sum_S \sum_{\theta_\alpha \in \Theta(S)} \sum_{\theta_\beta \in \Theta(S_v * S^{-1})} \mathbf{x}_S[I(\theta_\alpha), I(\theta_\beta)]|\theta_\alpha \theta_\beta\rangle \tag{3.8}$$

The components of the vector V are arranged as a sequence of two dimensional arrays or blocks $\mathbf{x}_S$ with $S = 1, 2, \ldots, h$. Only one block at a time needs to be kept in core memory, the others being stored on the disk. It is important to stress the key feature of this way of addressing the vector: string addresses are precomputed and stored in lists implementing the mapping generated by the Hamiltonian. The number of strings grows only as the square root of the number of Slater determinants, and when $n_\alpha = n_\beta$ a further reduction by a factor 2 is achieved taking into account the spin reversal symmetry of the Hamiltonian [33, 34].

3.1.2 The FCI Hamiltonian

We are now facing the problem of expressing the general Hamiltonian in a FCI space of n electrons generated by a finite spin orbital basis set $\mathcal{B}$ composed of N orbitals of either spin. If we are using the second quantization formalism we may write this operator as

$$\mathcal{H} = \sum_{i,j,\sigma} h_{i,j} a^\dagger_{i\sigma} a_{j\sigma} + \frac{1}{2} \sum_{i,j,k,l,\sigma,\tau} \langle ij|kl\rangle a^\dagger_{i\sigma} a^\dagger_{j\tau} a_{l\tau} a_{k\sigma} \tag{3.9}$$

where we used Latin indeces (i, j, k, l) to label orbitals and Greek indices (σ, τ) to label spins, $h_{i,j}$ represent the one electron integrals while $\langle ij|kl\rangle$ represent the two electron ones in physical (Dirac) notation. Because of $\mathbf{H}$ being total symmetric all the matrix elements (integrals) will vanish unless $S_i = S_j^{-1}$ or $S_i * S_j = S_k * S_l$; moreover the number N_{int} of two electrons integrals is also decreased by a factor h.

The Hamiltonian can be seen as being decomposed in a linear combination of elementary one and two electrons operators $a^\dagger_{i\sigma}a_{j\sigma}$ and $a^\dagger_{i\sigma}a^\dagger_{j\tau}a_{l\tau}a_{k\sigma}$. Any of these operators when acting on a Slater determinant $|\theta_\alpha\theta_\beta\rangle$ may only produce an other determinant $\pm|\theta_{\alpha'}\theta_{\beta'}\rangle$ or annihilate the determinant itself. In order to implement the action of the Hamiltonian operator we may consider two approaches: integral driven or string driven approach. Let us first consider the easiest one electron part and analyse both of them.

Integral driven For each orbital couple (i,j) we may construct a set of NVO_{ij} string couples such as $\theta^{iK} = a^\dagger_i a_j \theta^{jK}$ for $K = 1, 2, \ldots, NVO_{ij}$. Actually what we will work with will be the list of addresses plus the sign factor s_K, we will, therefore, have to deal with $I(\theta^{iK})$, $I(\theta^{jK})$ and s_K.

String driven . In this case for each string θ we construct a list grouping together the couples (i,j) and the string $\xi_k = a^\dagger_i a_j \theta$ (as usual we will work with the strings addresses) building the Hamiltonian from them.

The overall length of the one electron list will be the same in both cases, and therefore, at this level the two choices are equivalent. The two electron part of the Hamiltonian represents the most difficult but most important part to treat, we may, first of all, notice the operator can be split in two types:

$$\mathcal{H}_{\sigma\sigma} = \frac{1}{2}\sum_{i,j,k,l,\sigma} \langle ij|kl\rangle a^\dagger_{i\sigma}a^\dagger_{j\sigma}a_{l\sigma}a_{k\sigma} \tag{3.10}$$

$$\mathcal{H}_{\sigma\tau} = \frac{1}{2}\sum_{i,j,k,l,\sigma,\tau} \langle ij|kl\rangle a^\dagger_{i\sigma}a^\dagger_{j\tau}a_{l\sigma}a_{k\tau} \tag{3.11}$$

obviously the two represent the same spin ($\alpha\alpha$ or $\beta\beta$) and the opposite spin ($\alpha\beta$) contribution. Let us start with the same spin (consider for instance the $\beta\beta$ part) we still have two possibility:

Integral driven . We treat the operator $E_{ijkl} = a^\dagger_{i\beta}a^\dagger_{j\beta}a_{l\beta}a_{k\beta}$ exactly in the same way we did for the one electron case. Obviously the main difference will be the length of the two electron lists, the latter being approximately

$$\frac{1}{h}\begin{pmatrix} n \\ 2 \end{pmatrix}\begin{pmatrix} N \\ n \end{pmatrix}\left[\begin{pmatrix} N-n \\ n \end{pmatrix} + 2(N-n) + 1\right] \tag{3.12}$$

and therefore grows slowlier than the FCI space and it is computationally efficient and simple.

String driven . In this case the two electron operator is split as the product of two one electron steps consisting of single excitation [33]

$$E_{ijkl} = a^{\dagger}_{i\beta} a_{k\beta} a^{\dagger}_{j\beta} a_{l\beta} - \delta_{jk} a^{\dagger}_{i\beta} a_{l\beta} \tag{3.13}$$

In this case for each columns of $\mathbf{y}_S$ we must compute contributions coming from several columns of $\mathbf{x}_S$, a temporary linear array of length one column $\mathbf{x}_S$ is needed.

The overall operation count for this step is the same in the two cases and it is roughly given by

$$\frac{N_{det}(N - n_\beta)^2 n^2_{beta}}{4} \tag{3.14}$$

Obviously the $\alpha\alpha$ part is implemented in exact the same way providing one interchanges rows and columns in both $\mathbf{x}_S$ and $\mathbf{y}_S$ The most time consuming part of the entire operation is indeed the $\mathcal{H}_{\alpha\beta}$; in this case we have

$$\mathcal{H}_{\alpha\beta}|\theta_\alpha\theta_\beta\rangle = \frac{1}{2}\sum_{i,k}(a^{\dagger}_{i\alpha} a_{k\alpha}|\theta_\alpha\rangle) \wedge \sum_{j,l}(a^{\dagger}_{j\beta} a_{l\beta}|\theta_\beta\rangle) \tag{3.15}$$

the full operator core has been decomposed in products of α factor affecting only rows and β factor affecting only columns of the vectors $\mathbf{x}_S$ and $\mathbf{y}_S$, which has to be implemented as two nested one-electron operations. The external loop is performed using the integral driven lists, the internal is performed with the string driven or integral driven lists either. In our laboratory code this task is achieved using temporary arrays where all the rows of $\mathbf{x}_S$ and $\mathbf{y}_S$ affected a given $a^{\dagger}_{i\alpha} a_{k\alpha}$ are gathered. Then all the operation corresponding to the β part are performed using BLAS vector routines (DAXPY); the entire $\alpha\beta$ process can therefore be schematized as

1. gathering the needed rows and columns
2. a series of DAXPY over columns corresponding to to the β one electron loop
3. a scatter from the temporary arrays to $\mathbf{x}_S$ and $\mathbf{y}_S$

It has to be noted however the one electron operators do not separately conserve spacial symmetry, the requirement is, indeed, $S(i) * S(k) = S(j) * S(l)$, therefore all the one electron lists are needed, regardless of their symmetries. The overall length of the one electron lists becomes approximately

$$n \left(\begin{array}{c} N \\ n \end{array} \right) (N - n + 1) \tag{3.16}$$

which has to be compared with the length for the same spin component, the computational cost for this part becomes

$$\frac{N_{det}[n_\beta(N-n_\alpha+1][n_\alpha(N-n_\alpha+1]}{h} \tag{3.17}$$

The vector performance, is strongly influenced by the length of the innermost loop, i.e. by the average length of one electron lists for couple (i,j)

3.1.3 Davidson algorithm in CI method

One of the most used algorithm to solve iteratively the (F)CI problem is without any doubt the Davidson one [35]. This particular algorithm, strongly related to the Krylov type algorithms, proved to be very efficient in the case of large sparse matrices like the CI Hamiltonian matrix $\mathcal{H}$. It is, therefore, still widely used in many QC codes, although it dates back to the seventies. Its main features are schematically presented here:

1. set $i = 0$
2. set a trial function (vector) $\mathbf{x}_i$
3. compute using the FO $\mathbf{y}_{i+1} = \mathcal{H}\mathbf{x}_i$ and $\varepsilon_{i+1} = \frac{\langle \mathbf{x}_i \mathbf{y}_{i+1} \rangle}{\langle \mathbf{x}_i \mathbf{x}_i \rangle}$
4. compute the residual as $r_{i+1} = \mathbf{y}_{i+1} - \mathbf{x}_i$, if $r_{i+1} \leq THR$ (THR being the chosen convergence threshold) stop
5. precondition the vector r_{i+1}, you get $p_{i+1} = (Diag_{\mathcal{H}} - \varepsilon_{i+1})^{-1} r_{i+1}$
6. orthogonalize the p vector to all the preceding
7. compute $\mathbf{x}_{i+1} = \sum_{j=0}^{i+1} p_j^{ort}$
8. apply FO to compute $\mathbf{y}_{i+2}$ and the reduced matrix $\mathbf{H_R}$

$$H_R(i,j) = \mathbf{x}_i \mathbf{y}_j \tag{3.18}$$

9. diagonalize the reduced Hamiltonian matrix and compute the energies (eigenvalues) and set $i = i + 1$
10. go back to point 4

The Davidson method efficiency is due to the particular form of the preconditioner, and to the diagonal dominance character of the CI Hamiltonian matrices.

3.1.4 Second order perturbative solutions

The problem we address is the computation of second (and eventually higher) order properties at the (F)CI level. This implies the solution of the perturbation theory equation which we may write as

$$(\mathcal{H} - E_0 \pm \hbar\omega)\psi_\pm = (\langle\psi_0|\hat{V}|\psi_0\rangle - \hat{V})\psi_0 \tag{3.19}$$

here ψ_0 is an eigenstate of the $\mathcal{H}$ operator with energy (eigenvalue) E_0 and $\hat{V}$ represents a perturbation operator. The previous equation is nothing but the perturbative equation we found out in the treatment of molecules in an oscillating electric field we performed previously.
The solution of this equation can be approximated by expanding both ψ_0 and $\psi_\pm$ in a linear space $\mathcal{L}$. In the first case this lead to the familiar eigenvalue problem for the matrix $\mathbf{H}$ of the Hamiltonian in the chosen basis set,

$$\mathbf{H}\mathbf{v}_0 = E_0\mathbf{v}_0 \tag{3.20}$$

while the latter becomes a system of linear equations

$$(\mathbf{H} - E_0 \pm \hbar\omega)\mathbf{v}_1 = E_1\mathbf{v_0} - \mathbf{w}_0 \tag{3.21}$$

where $\mathbf{v_0}$, $\mathbf{v}_1$ and $\mathbf{w}_0$ represent, respectively, the vectors of the components of the unperturbed eigenvector ψ_0, of the first order function $\psi_\pm$, and of the function $\hat{V}\psi_0$. If we choose $\mathcal{L}$ to be the FCI space we have, as we know, a factorial growth of $\mathcal{L}$ dimensions with the number of electrons and atomic orbital; in this case our problem will be how to deal with so large dimensions. System of linear equations can be solved using methods which are similar to the ones used for the FCI eigenvalue problem, i.e. iterative methods combining the idea of the Krylov space with the direct techniques, allowing therefore the use of the FCI FO operation $\mathbf{y} = \mathbf{Hx}$. The analytic perturbative solution has many advantages compared to the numeric finite field type, expecially:

- full exploitation of the symmetry of the molecule, avoiding computations with non totally symmetric Hamiltonians including external fields
- allow access to frequency dependent polarizabilities

3.1.4.1 The computational algorithm

Let us take a deeper look at the actual way to solve the perturbative equation which has been implemented in our laboratory FCI code [36].

The right hand side of the perturbative equation in matrix form, $\mathbf{b} = E_1\mathbf{v_0} - \mathbf{w}_0$ is easily computed from the eigenvector $\mathbf{v}_0$ obtained from a FCI computation. The perturbation operator $\hat{V}$ being, in this context, a general multipole operator which acts like a one electron operator

$$\hat{V} = \sum_{ij} V_{ij} a_i^\dagger a_j \tag{3.22}$$

so its application to $\mathbf{v}_0$ can be accomplished using the standard FCI techniques. The only feature to be pointed out concerns the fact $\hat{V}$ will be, in general, non totally symmetric, therefore $\hat{V}\psi_0$ and $\psi_\pm$ may belong to different symmetry classes. We may now rewrite the equation as

$$\mathbf{A}(\eta)\mathbf{x} = \mathbf{b} \tag{3.23}$$

where $\mathbf{A}(\eta) = \mathbf{H} - (E_0 + \eta)\mathbf{I}$ and $\eta = \pm\hbar\omega$. We notice, by the way, the matrix $\mathbf{A}(0)$ is real symmetric with eigenvalues $E_k - E_0$ corresponding to the excitation energy from state $\mathbf{v}_0$ and that it also has a null eigenvector $\mathbf{v}_0$, we will moreover assume it is non degenerate. The perturbative equation admits solutions only if at least one of the two following conditions is fullfilled

- $\det \mathbf{A} \neq 0$
- $\mathbf{b}$ is orthogonal to the null space of $\mathbf{A}(\eta)$

The first condition is fullfilled when η is different from an excitation energy $E_k - E_0$ and from zero. This fact impose to restrict η to $\pm$ the distance of the closest eigenvalue from E_0, anyway this limitation is the same one imposed by perturbation theory itself. Moreover since the right hand side $\mathbf{b}$ is orthogonal to $\mathbf{v}_0$ by construction so the solution $\mathbf{x}$ will be. For this reason where $\eta = 0$ we fullfill the second validity condition and the equation allows a linear manifold of solutions. In this manifold we choose the solution of minimal norm, i.e. the one orthogonal to $\mathbf{v}_0$. In order to ensure a compact notation to represent the solution and other quantities it can be useful to recall the reduced resolvent [37] of the Hamiltonian $\mathbf{R}(\eta)$, which we may define as

$$\mathbf{R}(\eta) = (\mathbf{H} - E_0 - \eta)^{-1}\mathbf{P}_0 \tag{3.24}$$

$$\mathbf{x} = \mathbf{R}(\eta)\mathbf{b} \tag{3.25}$$

where $\mathbf{P}_0$ is the projection on the eigenvector $\mathbf{v}_0$. With the help of the general variational principle we may now give a unified presentation of the numerical method used to practically achieve the solution. The solution of the perturbative equation, in fact, corresponds to a stationary point of the quadratic forms

1. $\mathcal{Q}_1(x) = \frac{1}{2}\mathbf{x}^\dagger\mathbf{A}(\eta)\mathbf{x} - \mathbf{b}^\dagger\mathbf{x}$ This relation represent the Hylleras variational principle in the linear space $\mathcal{L}$, $\mathcal{Q}_1$ may also be defined Hylleras functional.

2. $\mathcal{Q}_2(x) = \|\mathbf{b} - \mathbf{A}(\eta)\mathbf{x}\|^2$

The vector $\mathbf{r} = \mathbf{b} - \mathbf{A}(\eta)\mathbf{x}$ is usually known as the residual norm associated to $\mathbf{x}$, and the latter can be accepted as a solution when $\mathbf{r}$ is small, i.e. when its norm is less than a given threshold, moreover $-\mathbf{r} = \nabla\mathcal{Q}_1$. The stationary point will always be a minimum for $\mathcal{Q}_2$, while for $\mathcal{Q}_1$ this condition is verified only when the matrix $\mathbf{A}(\eta)$ is real and positive definite. The latter conditions define also the range of applicability of the minimization of the Hylleras functional $\mathcal{Q}_1$, in the other cases the solution shall be obtained with the minimization of the residual norm.

The conjugate gradient The condition for which one can use the minimization of the Hylleras functional are fullfilled when $-(E_0 \pm \hbar\omega)$ is greater or equal to the minimum eigenvalue of $\mathcal{H}$ in the symmetry subspace defined by $\hat{V}\psi_0$. In that case, the solution will be achieved minimizing the $\mathcal{Q}_1$ functional, i.e. finding the solution to

$$\nabla\mathcal{Q}_1 = \mathbf{A}(\eta)\mathbf{x} - \mathbf{b} = 0 \tag{3.26}$$

the latter relation is solved iteratively using the so called conjugate gradient method. The algorithm may be structured in the following way

1. compute the vector $\mathbf{b}$

2. set $i = 0$

3. set a guess vector $\mathbf{x}_0$ and compute the residual $\mathbf{r}_0 = \mathbf{b} - \mathbf{A}\mathbf{x}$ (usually $\mathbf{x}$ is chosen to be null, in this case $\mathbf{r} = \mathbf{b}$)

4. set $i = i + 1$

5. apply the preconditioner $\mathbf{p}_{i-1} = (Diag\mathbf{A})^{-1}\mathbf{r}_{i-1}$

6. compute $\rho_{i-1} = \mathbf{r}_{i-1}^\dagger\mathbf{p}_{i-1}$

7. A-orthonormalize $\mathbf{p}_{i-1}$ to all the previous vectors[1]

8. compute $\mathbf{p}_i = \mathbf{r}_{i-1} + \frac{\rho_{i-1}}{\rho_{i-2}}\mathbf{p}_{i-2}$

[1]For A-orthonormalization it is intended an orthonormalization of the $\mathbf{p}$ vectors, performed using the matrix $\mathbf{A}$ as the metric.

9. compute $\mathbf{Ap}_i$
10. compute $\beta_i = \sum_k \frac{\mathbf{Ap}_k^\dagger \mathbf{b}}{\mathbf{Ap}_k^\dagger \mathbf{Ap}}$
11. update the residual $\mathbf{r}_i = \mathbf{r}_{i-1} - \beta_i \mathbf{Ap}_i$
12. compute $\|\mathbf{r}_i\|$ if it is less than a threshold stop
13. go back to point 4

The algorithm is based on the idea a good direction to find the minimum is found moving along the residual, and even better along the direction fixed by the preconditioned residual. The preconditioner is still based on the diagonal due to the nature of diagonal dominance of the Hamiltonian matrix, the β is chosen so that to minimise $\mathcal{Q}_1$ in the direction defined by $\mathbf{p}$. As always the time consuming operation is the multiplication $\mathbf{Ap}$ which can be assimilated to the FO of the FCI.
We may see the minimum of the Hylleras functional has a value which is equal to

$$\mathcal{Q}_{min} = -\frac{1}{2}\mathbf{b}^\dagger \mathbf{A}^{-1}\mathbf{b} \tag{3.27}$$

In the case $\omega = 0$ (static polarizability) we will therefore have $\alpha = -2\mathcal{Q}_{min}$, when $\omega \neq 0$ we will have $\alpha(\omega) = -\mathcal{Q}^+_{min} - \mathcal{Q}^-_{min}$ where $\mathcal{Q}^+_{min}$ is the solution obtained with $\eta = \hbar\omega$ and $\mathcal{Q}^-_{min}$ with $\eta = -\hbar\omega$.

The Residual Norm Minimization In the case when $\mathbf{A}(\eta)$ is not positive definite, as is commono for excited states, or when the frequence ω is an imaginary or complex quantity, one can not rely on the Hylleras Functional to get a solution to the perturbation equation. As already stated in this case we have to deal with the residual norm $\|\mathbf{r}(x)\| = \|\mathbf{b} - \mathbf{A}(\eta)\mathbf{x}\|^2$ and minimise it.
In this case we may express, following again Krylov and Davidson ideas, the solution as a linear combination of vectors $\mathbf{h}$

$$\mathbf{x}_n = \sum_{i=1}^{n} \beta_i \mathbf{h}_i \tag{3.28}$$

where the vectors are chosen such as they respect the condition $\mathbf{h}_i = Diag(\mathbf{A}^{-1}\mathbf{r}_{i-1})$.
The main computational steps to be performed are summarized here:

1. set $i = 0$
2. compute the vector $\mathbf{b}$

3. choose a guess vector $\mathbf{x}_0$ and compute $\mathbf{r}_0 = \mathbf{b} - \mathbf{A}\mathbf{x}_0$ if the guess is chosen to be the null vector than $\mathbf{r}_0 = \mathbf{b}$

4. set $i = i + 1$

5. compute $\mathbf{h}_i = Diag(\mathbf{A})^{-1}\mathbf{r}_{i-1}$ and write it on disk

6. compute $\mathbf{A}\mathbf{h}_i$

7. compute all the scalar products $\gamma_{ji} = \mathbf{p}_j\mathbf{A}^\dagger\mathbf{A}\mathbf{h}_i$

8. othonormalize the vector $\mathbf{A}\mathbf{h}_i$ to all the previous vectors $\mathbf{A}\mathbf{p}_j$, and write on the disk the orthonormal vector $\mathbf{A}\mathbf{p}_i$

9. compute $\|\mathbf{A}\mathbf{p}_i\|$

10. compute the coefficients $\beta = \sum_i \frac{\mathbf{A}\mathbf{p}_i^\dagger\mathbf{b}}{\mathbf{A}\mathbf{p}_i^\dagger\mathbf{A}\mathbf{p}_i}$

11. update the residual according to the equation

$$\mathbf{r}_i = \mathbf{r}_{i-1} + \beta_i\mathbf{A}\mathbf{p}_i \tag{3.29}$$

12. check convergence, if not converged go back to point 4

13. compute the expansion coefficients of the solution in the base $\mathbf{h}_i$ by inverting the triangular matrix γ_{ji}

14. compute solution by linear combination with coefficients β_i of the vectors $\mathbf{h}_i$

15. Schmidt orthogonalize the solution to $\mathbf{v}_0$ if needed and exit

Even if this algorithms uses tools whose computational cost is substantially equivalent to the ones used by conjugate gradient, the convergence toward the soution is significantly slower in the residual norm method, resulting in an overall increase in the required computational time. Nevertheless it is applicable in cases in which the conjugate gradient would have failed. In a case of a complex $\mathbf{A}$ matrix, the scheme is essentially unaltered from the mathematical point of view. However the implementation is complicated by the fact that all the vectors (with the exception of $\mathbf{b}$) are complex and require therefore twice as much disk space. Moreover the implementation is usually organized such as to separate real and imaginary parts of the vector, therefore the computational cost per iteration is, in complex cases, also doubled.

3.2 The Coupled Cluster Method

Currently Coupled Cluster (CC) methods play undoubtedly one of the leading roles in high precision *ab initio* calculations, and they are implemented in several high performance packages. In particular this is true for the non degenerate single reference variant, while multi reference CC (MRCC) is still far from being so universally accepted and used. For this reason CC can be seen as a very useful method to determine non degenerate ground states of many molecular systems, where its accuracy is often comparable to the FCI one, but with a much lesser computational effort; in return, however, one has to pay the prize of the loss of variational protection, which is not ensured by truncated Coupled Cluster. Moreover with single reference CC it is practical impossible to treat, with an high level of accuracy, degenerate systems, in which a single reference determinant is not sufficient to get a correct description of the WF; this fact limits CC applicability, preventing its use for several problems involving excited states, or magnetic systems, where the truncated CI (in particular multi reference CI) is still preferable.

3.2.1 The Coupled Cluster Ansatz

Consider, as usual, the problem defined by the Scrödinger equation

$$\mathcal{H}\Psi = E\Psi \tag{3.30}$$

the key idea was to expand the WF Ψ by the use of an exponential Ansatz

$$|\Psi\rangle = e^{T}|\Phi\rangle \tag{3.31}$$

$$\langle\Psi| = \langle\Phi|e^{T^{\dagger}} \tag{3.32}$$

This idea was firstly introduced in the classical statistical mechanic field [38] and subsequently translated to the field of Nuclear Physics [39] and finally to quantum chemistry by the pioneristic work of Čížek [40]. In the previous equation Φ is a Slater determinant, often referred to as the reference determinant while T is an excitation operator acting on the Slater determinant, which can be expressed as follows:

$$T = T_1 + T_2 + T_3 + \cdots + T_n \tag{3.33}$$

in this context T_1 represents the operator for single excitations, T_2 the operator for double excitations and so on. The latter may be expressed in second quantization as:

$$T_1 = \sum_i \sum_a t_i^a a_i a_a^{\dagger} \tag{3.34}$$

$$T_2 = \sum_{ij} \sum_{ab} t_{ij}^{ab} a_i a_j a_a^\dagger a_b^\dagger \tag{3.35}$$

or in general

$$T_n = (n!)^{-2} \sum_{ab\ldots n} \sum_{ij\ldots n} t_{ij\ldots n}^{ab\ldots n} a_i a_j \ldots a_n a^\dagger a_b^\dagger \ldots a_n^\dagger \tag{3.36}$$

where the indices i, j represents occupied orbitals, the indeces a, b virtual orbitals a and $a^\dagger$ are normal ordered [2] creation and anhillation operators respectively, and t are the coupled clusters amplitudes. Solving for the unknown amplitudes is the necessary passage to get the CC approximate solution to the WF.
Before briefly recall the CC working equations let us just clarify one of the key features of Coupled Cluster methods: size consistency. Consider a non interacting system $A + B$ whose Hamiltonian is $\mathcal{H} = \mathcal{H}_A + \mathcal{H}_B$, assuming a truncation on T to $n-$excitations, and using the fact excitations operators commute, we may write

$$\Psi_n^{AB} = e^{T_A} e^{T_B} \Phi^A \Phi^B = e^{T_A + T_B} \Phi^A \Phi^B \tag{3.37}$$

the energy will be

$$\begin{aligned} E_n^{AB} &= \frac{\langle e^{T_A} e^{T_B} \Phi^A \Phi^B | \mathcal{H} | e^{T_A} e^{T_B} \Phi^A \Phi^B \rangle}{\langle e^{T_A} e^{T_B} \Phi^A \Phi^B | e^{T_A} e^{T_B} \Phi^A \Phi^B \rangle} \\ &= \frac{\langle e^{T_A} \Phi^A | \mathcal{H}_A | e^{T_A} \Phi^A \rangle \langle e^{T_B} \Phi^B | e^{T_B} \Phi^B \rangle}{\langle e^{T_A} \Phi^A | e^{T_A} \Phi^A \rangle \langle e^{T_B} \Phi^B | e^{T_B} \Phi^B \rangle} \\ &+ \frac{\langle e^{T_B} \Phi^B | \mathcal{H}_B | e^{T_B} \Phi^B \rangle \langle e^{T_A} \Phi^A | e^{T_A} \Phi^A \rangle}{\langle e^{T_A} \Phi^A | e^{T_A} \Phi^A \rangle \langle e^{T_B} \Phi^B | e^{T_B} \Phi^B \rangle} = E^A + E^B \end{aligned} \tag{3.38}$$

therefore the energy for non interacting system will scale linearly with the number of particles, like it is required by the definition of size consistency.
Let us assume, up to now, intermediate normalization, which follows directly providing one considers the orthogonality of the basis

$$\langle \Phi | \Psi \rangle = 1 \tag{3.39}$$

and let us expand e^T in a Taylor series

$$\begin{aligned} e^T &= 1 + T + \frac{1}{2} T^2 + \frac{1}{3!} T^3 + \cdots \\ &= 1 + T_1 + T_2 + \frac{1}{2} T_1^2 + T_1 T_2 + \frac{1}{2} T_2^2 + \cdots \end{aligned} \tag{3.40}$$

[2] Normal ordered are defined those operators in which all the annihilation operators have been moved to the right, and all the creation operators to the left, by the action of a commutator operator.

This series is finite in practice because the number of molecular orbitals is finite, as is the number of excitations. In order to simplify the task for finding the coefficients, the expansion of T into individual excitation operators is terminated at the second or slightly higher level of excitation (rarely exceeding four). This approach is warranted by the fact that even if the system admits more than four excitations, the contribution of T_5, T_6 etc. to the operator T is small. Furthermore, if the highest excitation level in the T operator is n

$$T = 1 + T_1 + ... + T_n \tag{3.41}$$

then Slater determinants excited more than n times do still contribute to the wave function $|\Psi\rangle$ because of the non-linear nature of the exponential Ansatz. Therefore, coupled cluster terminated at T_n usually recovers more correlation energy than configuration interaction with maximum n excitations.
Consider, in fact,

$$\begin{aligned} C_0 &= 1 && (3.42)\\ C_1 &= T_1 && (3.43)\\ C_2 &= T_2 + \frac{1}{2}T_1^2 && (3.44)\\ C_3 &= T_3 + T_1T_2 + \frac{1}{3!}T_1^3 && (3.45)\\ &\vdots && \\ & && (3.46) \end{aligned}$$

it is possible to write the WF as

$$|\Psi\rangle = e^T|\Phi\rangle = (1 + C_1 + C_2 + C_3 + \ldots)|\Phi\rangle = C|\Phi\rangle \tag{3.47}$$

therefore if all possible excitation from a given reference state have been taken into account CI and CC prove to be fully equivalent, as soon as no approximations are introduced.

3.2.2 Coupled Cluster Equations

The exponential Ansatz described above is essential to coupled cluster theory, but we do not yet have a recipe for determining the cluster amplitudes (t_i^a, t_{ij}^{ab}, etc.) which parametrise the Coupled Cluster Schrödinger wave equation

$$\mathcal{H}e^T|\Phi_0\rangle = E_{CC}|\Phi_0\rangle \tag{3.48}$$

one may left project the previous equation onto the reference state $\langle\Phi_0|$ to get the the energy

$$E_{CC} = \langle\Phi_0|\mathcal{H}e^T|\Phi_0\rangle \tag{3.49}$$

and left project the same equation onto the space define by the excited determinants $\langle\Phi_{ij\ldots}^{ab\cdots}|$ produced by the action of the cluster operator, T, on the reference state

$$\langle\Phi_{ij\ldots}^{ab\cdots}|\mathcal{H}e^T|\Phi_0\rangle = 0 \tag{3.50}$$

the latter projection will give raise to an equation for each specific amplitude $t_{ij\ldots}^{ab\cdots}$ (coupled to other amplitudes). These equations are non-linear (due to the presence of e^T) and energy dependent. Furthermore, they are formally exact; if the cluster operator, T, is not truncated. This projective technique represent a particularly convenient way of obtaining the amplitudes which define the coupled cluster wavefunction, $e^T\Phi_0$. However, the asymmetric energy formula shown does not conform to any variational conditions when the energy is determined from an expectation value equation. As a result, the computed energy will not be an upper bound to the exact energy in the very common event that the cluster operator, T, is truncated

Although these energy and amplitudes expressions are useful for gaining a formal understanding of the coupled cluster method, they are not amenable to practical computer implementation [41]. One must first rewrite these expressions in terms of the one- and two-electron integrals arising from the electronic Hamiltonian as well as the cluster amplitudes, which, apart from the energy itself, are the only unknown quantities. To that end, it is convenient to exercise mathematical foresight and multiply the Schrödinger equation by the inverse of the exponential operator, e^{-T}, obtaining the so called similarity transformed Hamiltonian $e^{-T}\mathcal{H}e^T$. Upon subsequent left-projection by the reference, Φ_0, and the excited determinants, $\Phi_{ij\ldots}^{ab\cdots}$, one obtains modified energy and amplitude equations,

$$E_{CC} = \langle\Phi_0|e^{-T}\mathcal{H}e^T|\Phi_0\rangle \tag{3.51}$$

$$\langle\Phi_{ij\ldots}^{ab\cdots}|e^{-T}\mathcal{H}e^T|\Phi_0\rangle = 0 \tag{3.52}$$

It may be shown [42] that these equation are fully equivalent to the previous ones but present two many advantages. First, the amplitude equations are now decoupled from the energy equation. Second, a simplification via the so-called Campbell-Baker-Hausdorff formula [43] of $e^{-T}\mathcal{H}e^T$ leads to a linear combination of nested commutators of $\mathcal{H}$ with the cluster operator, T,

$$e^{-T}\mathcal{H}e^T = \mathcal{H} + [\mathcal{H},T] + +\frac{1}{2!}[[\mathcal{H},T],T] + \frac{1}{3!}[[[\mathcal{H},T],T],T]$$

$$+ \quad \frac{1}{4!}\left[\left[\left[\left[\mathcal{H},T\right],T\right],T\right],T\right]+\cdots \tag{3.53}$$

$$\tag{3.54}$$

This expression is usually referred to simply as the Hausdorff expansion, and although it may not immediately appear to be a simplification of the coupled cluster equations, the infinite series truncates naturally in a manner somewhat analogous to that described earlier for the operator, He^T.

Let us now take a deeper look at how the nested commutators operate. Let us firstly express the CC Hamiltonian in second quantization formalism as

$$\mathcal{H}=\sum_{pq}h_{pq}a_p^\dagger a_q+\frac{1}{4}\sum_{pqrs}\langle pq|rs\rangle a_p^\dagger a_q^\dagger a_s a_r \tag{3.55}$$

as usual in the previous equation h_{pq} represents a one-electron matrix component of the Hamiltonian while $\langle pq|rs\rangle$ (physical notation) represents the two-electron part. The Hamiltonian equation contains general annihilation and creation operators (e.g., $a_p^\dagger$ or a_q) which may act on orbitals in either the occupied or virtual subspaces. The cluster operators T_n, on the other hand, contain terms that are restricted to act in only one of these spaces (e.g., $a_b^\dagger$ which may act only on the virtual orbitals). As pointed out earlier, the cluster operators therefore commute with one another, but not with the Hamiltonian, $\mathcal{H}$. For example, consider the commutator of the pair of general second-quantized operators from the one-electron component of the Hamiltonian with the single-excitation pair found in the cluster operator, T_1:

$$\left[a_p^\dagger a_q,a_a^\dagger a_i\right]=a_p^\dagger a_q a_a^\dagger a_i-a_a^\dagger a_i a_p^\dagger a_q \tag{3.56}$$

the anticommutator relations of annihilation and creation operators may be applied to the two terms on the right-hand side of this expression to give

$$\left[a_p^\dagger a_q,a_a^\dagger a_i\right]=a_p^\dagger \delta_{qa} a_i-a_a^\dagger \delta_{ip} a_q \tag{3.57}$$

The important point here is that the commutator has reduced the number of general-index second-quantized operators by one. Therefore, each nested commutator from the Hausdorff expansion of $\mathcal{H}$ and T serves to eliminate one of the electronic Hamiltonian's general-index annihilation or creation operators in favor of a simple delta function. Since $\mathcal{H}$ contains at most four such operators (in its two-electron component), all creation or annihilation operators arising from $\mathcal{H}$ will be eliminated beginning with the quadruply nested commutator in the Hausdorff expansion. All higher-order terms will contain commutators of only the cluster operators, T, and are therefore zero. Hence, the equation

for the Hamiltonian truncates itself naturally after the first five terms. This convenient property it is a general feature resulting entirely from the two-electron property of the Hamiltonian and the fact that the cluster operators commute; it is not dependent on the number of electrons in the system, the level of substitution included in T, or any consideration of the types of determinants upon which the operators act. Using the truncated Hausdorff expansion, we may obtain analytic expressions for the commutators and insert these into the coupled cluster energy and amplitude equations.

3.2.2.1 Coupled Cluster Working Equation

We will now briefly construct working equations for the coupled cluster singles and doubles (CCSD) method. Beginning from the approximation $T = T_1 + T_2$, we use algebraic techniques to sketch programmable equations for the cluster amplitudes, t_i^a and t_{ij}^{ab}, in terms of the one- and two-electron integrals of the electronic Hamiltonian. As a first step we must introduce a few important tools of second quantization such as normal ordering and Wick's theorem to make the mathematical analysis much less complicated. The approach described here may easily be extended to higher-order cluster approximations (e.g., CCSDT and CCSDTQ, where the latter includes quadruple excitations), as well as many-body perturbation theory expressions. The general quantum chemistry community has been slow to accept diagrammatic analyses of many-body perturbation theory and coupled cluster methods, but today this may be considered the standard formalism to be used in this context. An extensive analysis of a similar diagrammatic technique may be found in the text by Harris, Monkhorst, and Freeman [44].
Using the anticommutation relations an arbitrary string of annihilation and creation operators can be written as a linear combination of normal-ordered strings (most of which contain reduced numbers of operators) multiplied by Kronecker delta functions. These reduced terms may be viewed as arising from so-called contractions between operator pairs. A contraction between two arbitrary annihilation/creation operators, A and B, is defined as

$$\overline{AB} = AB - \{AB\}_v \tag{3.58}$$

where $\{AB\}_v$ indicates the normal ordered form of the pair. That is, the contraction between the operators is simply the original ordering of the pair minus the normal-ordered pair. For example, if both operators are annihilation or creation operators, the contraction is zero because such pairs are already normal ordered:

$$\overline{a_p a_q} = a_p a_q - \{a_p a_q\}_v = a_p a_q - a_p a_q = 0 \tag{3.59}$$

$$\overline{a_p^\dagger a_q^\dagger} = a_p^\dagger a_q^\dagger - \{a_p^\dagger a_q^\dagger\}_v = a_p^\dagger a_q^\dagger - a_p^\dagger a_q^\dagger = 0 \tag{3.60}$$

In addition, a third combination where A is a creation operator and B is an annihilation operator is also zero, since the string is again already normal ordered:

$$\overline{a_p^\dagger a_q} = a_p^\dagger a_q - \{a_p^\dagger a_q\}_v = a_p \dagger a_q - a_p^\dagger a_q = 0 \tag{3.61}$$

The final combination where A is an annihilation operator and B is a creation operator is not zero, however, due to the anticommutation relations

$$\overline{a_p a_q^\dagger} = a_p a_q^\dagger - \{a_p a_q^\dagger\}_v = a_p a_q^\dagger + a_q^\dagger a_p = \delta_{pq} \tag{3.62}$$

Wick's theorem [45] provides a recipe by which an arbitrary string of annihilation and creation operators, $ABC\ldots XYZ$, may be written as a linear combination of normal-ordered strings. Schematically, Wick's theorem is

$$\begin{aligned} ABC\ldots XYZ &= \{ABC\ldots XYZ\}_v \\ &+ \sum_{single} \{\overline{AB}\ldots XYZ\}_v \\ &+ \sum_{double} \{\overline{AB}\ldots X\overline{YZ}\}_v + \cdots \end{aligned} \tag{3.63}$$

If we apply the previous Wick theorem, to an operator $A = a_p a_q^\dagger a_r a_s^\dagger$ we obtain

$$A = a_q^\dagger a_s^\dagger a_p a_r - \delta_{pq} a_s^\dagger a_r + \delta_{ps} a_q^\dagger a_r - \delta_{rs} a_q^\dagger a_p + \delta_{pq}\delta_{rs} \tag{3.64}$$

This result is identical to that obtained using the anticommutation relations, the use of the Wick's theorem, however, greatly simplifies the derivation of the coupled cluster equation. The composite string of annihilation and creation operators may then be rewritten using Wick's theorem as an expansion of normal-ordered strings. However, the only terms that need to be retained in this expansion are those that are fully contracted'. All other terms will give a zero result, by construction. Moreover, in many-electron theories such as configuration interaction or coupled cluster theory, it is more convenient to deal with the n-electron reference determinant, $|\Phi_0\rangle$, rather than the true vacuum state, $|\ \rangle$. We will therefore alter the definition of normal ordering from the one relative to the true vacuum to the one relative to the reference state $|\Phi_0\rangle$ (which is sometimes called the Fermi vacuum). The one-electron states occupied in $|\Phi_0\rangle$ are referred to as hole states, and those unoccupied in $|\Phi_0\rangle$ are referred to as particle states. This nomenclature is based upon the determinant produced when annihilation-creation operator strings act on the Fermi vacuum. That is, a hole is created when an originally occupied state is acted upon by an annihilation operator such as a_i, whereas a particle is created when an originally unoccupied state is acted upon by a creation operator such as $a_a^\dagger$. Therefore,

we will refer to operators that create or destroy holes and particles as quasiparticle (or just q-particle) construction operators. That is, q-annihilation operators are those which annihilate holes and particles (e.g., $a_i^\dagger$ and a_a) and q-creation operators are those which create holes and particles (e.g., a_i and $a_a^\dagger$). Therefore, a string of second-quantized operators is normal ordered relative to the Fermi vacuum if all q-annihilation operators lie to the right of all q-creation operators. This new definition of normal ordering changes our analysis of the Wick's theorem contractions only slightly. Whereas before, the only nonzero pairwise contraction required the annihilation operator to be to the left of the creation operator, now the only nonzero contractions place the q-particle annihilation operator to the left of the q-particle creation operator.
The second quantized form of the electronic Hamiltonian

$$\mathcal{H} = \sum_{pq} \langle p|h|q\rangle a_p^\dagger a_q + \frac{1}{4}\langle pq|rs\rangle a_p^\dagger a_q^\dagger a_r a_s \tag{3.65}$$

may be cast into normal-ordered form using Wick's theorem and assume the expression (if we skip all the details of the evaluation)

$$\begin{aligned} \mathcal{H} &= \sum_{pq} \langle p|h|q\rangle \{a_p^\dagger a_q\} + \frac{1}{4}\langle pq|rs\rangle \{a_p^\dagger a_q^\dagger a_r a_s\} \\ &+ \sum_i \langle i|h|i\rangle + \sum_{ij} \frac{1}{2}\langle ij|ij\rangle \end{aligned} \tag{3.66}$$

where i and j represents occupied orbitals and $\{\}$ indicates a normal ordered operator with respect to the Fermi level. The last two terms of the previous equation are not but the Hartree Fock Energy obtained from a particular Slater determinant Φ_0 (or in other words the Fermi vacuum expectation value of the Hamiltonian). The notation for the Hamiltonian can be slightly simplified as

$$\mathcal{H} = \mathcal{F}_N + \mathcal{V}_N + \langle \Phi_0|\mathcal{H}|\Phi_0\rangle \tag{3.67}$$

where the subscript N indicates normal ordering of all the component operators strings. From these expression one may get a very general relation:

$$\mathcal{H}_N = \mathcal{H} - \langle \Phi_0|\mathcal{H}|\Phi_0\rangle \tag{3.68}$$

the normal-ordered form of an operator is simply the operator itself minus its reference expectation value. For the example given above, the normal-ordered Hamiltonian is just the Hamiltonian minus the SCF energy (i.e., $\mathcal{H}_N$ may be considered to be a correlation operator).

Up to this point to get working equation one should take the normal ordered similarity transformed Hamiltonian $\overline{H} = e^{-T}\mathcal{H}e^{T}$ and perform the Hausdorff expansion, remembering an usefull corollary comes from the Wick's theorem: the only nonzero terms in the Hausdorff expansion are those in which the Hamiltonian, $\overline{H}$, has at least one contraction with every cluster operator, T_n, on its right. This fact drastically diminishes the number of matrix elements to be computed. Accordingly the Coupled Cluster equation will be

$$E_{CC} - E_{SCF} = \langle \Phi_0 | \overline{H} | \Phi_0 \rangle \tag{3.69}$$

for the energy

$$0 = \langle \Phi_i^a | \overline{H} | \Phi_0 \rangle \tag{3.70}$$

for the single amplitudes and

$$0 = \langle \Phi_{ij}^{ab} | \overline{H} | \Phi_0 \rangle \tag{3.71}$$

for the doubles amplitudes. The latter can be solved using any algorithm for the numerical solution of non linear equations, with the computational cost relying essentially on the calculations of the normal ordered similarity transformed Hamiltonian components.

3.2.3 Linear R_{12} terms in Coupled Cluster

Highly accurate molecular electronic energies and properties can be obtained computationally when the molecular electronic trial function depends explicitly on the inter-electronic distances $r_{ij} = |\mathbf{r}_i - \mathbf{r}_j|$ in the system. This has been known since the early days [46, 47] of quantum mechanics, but it proved very difficult to develop generally applicable computational methods on the basis of explicitly correlated wave functions. For small molecules truly impressive results have been obtained with Gaussian geminals or exponentially correlated gaussian (ECG), but it appears difficult to extend such calculations to systems larger than very small molecules (like H_2, H_3^+, He_2). Even if some attempts have been made to adapt the theory of Gaussian geminals to larger systems the evaluation of the many electron integrals poses a bottle neck which is very hard to overcome. It is only in the late 1980's and early 1990's [49, 50] that affordable computational methods have been developed for molecules having more than four electrons. This development has been possible through the numerical techniques that were applied to avoid the many electrons integrals giving rise to the so called R_{12} methods. In particular an approximate resolution of the identity (closure relation) was inserted into those integrals. We will here briefly recall an overview of the R_{12} methods at Coupled Cluster level (CCSD(T)-R_{12}) in the proceeding of this thesis some application of this technique to the determination of electric properties will be presented.

3.2.3.1 The R_{12} approach

The essence of the R_{12} approach can be summarized as follows: in order to satisfy the electron-electron cusp condition, and thus to enhance the convergence of the calculated energy with respect to increasing the basis set by functions with higher angular momenta, it is sufficient to extend the usual wave function expansion by augmenting the reference determinant by a singly linear term r_{12}. In other words pair functions resulting from multiplication of a product of two occupied orbitals with the inter-electronic coordinates are introduced into the final wave function expansion. These idea can be formulated in general as

$$|\Psi\rangle = \frac{1}{2}\hat{r}_N|\Phi\rangle + \hat{\Omega}|\Phi\rangle \tag{3.72}$$

where $|\Psi\rangle$ is the desired $r_{12}-$dependent final wave function, and $\hat{\Omega}$ is an arbitrary wave operator. The factor $\frac{1}{2}$ was chosen to ensure the proper value of the wave function derivative for $r_{12} \to 0$ (Kato Condition [48]). As it stand the previous Ansatz would not give rise to practical algorithms for many electron system due to the appearance of three and four electron integrals in the final working equations. Moreover there is a substantial overlap between the conventional and the R_{12} term. Hence it is at first desirable to outproject all the contributions that overlap with the conventional configuration space. In the proceeding we will use the following notation: we will use, in our mathematical treatment, a formal infinite and complete spin orbital basis $\{\varphi_\kappa\}$ and a finite and incomplete spin orbital basis set (the actual basis set in which we expand the conventional problem) $\{\varphi_p\}$. The spin orbital occurring in the following formulation will respect this convention: $i, j, \ldots$ belong to the space of occupied orbitals, $a, b, \ldots$ belong to the space of virtual orbitals, while $\alpha, \beta, \ldots$ belong to the space of the complementary orbitals (i.e. they are orbitals of the formal infinite complementary basis), obviously in the final equation terms referring to complementary orbitals shall vanish.
Let us now examine what happens when the $\hat{r}_N$ operators acts on the reference determinant

$$\hat{r}_N|\Phi\rangle = \left(\frac{1}{4}r_{ab}^{ij}\tilde{a}_{ij}^{ab} + \frac{1}{4}r_{\alpha\beta}^{ij}\tilde{a}_{ij}^{\alpha\beta} + \frac{1}{2}r_{a\beta}^{ij}\tilde{a}_{ij}^{a\beta} + r_{aj}^{ij}\tilde{a}_{i}^{a} + r_{\alpha j}^{ij}\tilde{a}_{i}^{\alpha}\right) \tag{3.73}$$

where $r_{\mu\nu}^{\kappa\lambda} = \langle\mu\nu|r_{12}|\kappa\lambda\rangle$ represents the anti symmetrized inter-electronics integrals while $\tilde{a}_{\kappa\lambda}^{\mu\nu}$ are normal ordered $N-$body combination of creation and annihilation operators referred to the Fermi level vacuum. In the previous equation we have used the fact that only terms with excitation operators survive; thus the subscript of any $\tilde{a}$ must refer to occupied spin orbitals and the superscript to virtuals. Let us now assume our conventional configurational space includes all single and double excitations, the projector onto

this space, therefore, will be

$$\hat{\mathcal{M}} = |\Phi\rangle\langle\Phi| + \tilde{a}_i^a|\Phi\rangle\langle\Phi|\tilde{a}_a^i + \tilde{a}_{ij}^{ab}|\Phi\rangle\langle\Phi|\tilde{a}_{ab}^{ij} + \ldots \tag{3.74}$$

Consequently since r_N is a two particle operator and since the expectation value with $|\Phi\rangle$ is zero for any normal ordered operator the outprojector will become

$$(1-\hat{\mathcal{M}})r_N|\Phi\rangle = \left(\frac{1}{4}r_{\alpha\beta}^{ij}\tilde{a}_{ij}^{\alpha\beta} + \frac{1}{2}r_{a\beta}^{ij}\tilde{a}_{ij}^{a\beta} + r_{\alpha j}^{ij}\tilde{a}_i^{\alpha}\right)|\Phi\rangle \tag{3.75}$$

From these equations one recognizes that the finite number of configuration space functions created using the actual "computational" one-electron basis would now be supplemented by single and double excitations created using the complementary subspace $\{\varphi_\alpha\}$. One can argue here that it is possible to have a basis set saturated such that the last two terms vanish. Consequently, we can consider an Ansatz in which $r_{\alpha\beta}^{ij}\tilde{a}_{ij}^{\alpha\beta}|\Phi\rangle$ are the only supplementary excitations

$$|\Psi\rangle = \frac{1}{4}r_{\alpha\beta}^{ij}\tilde{a}_{ij}^{\alpha\beta}|\Phi\rangle + \hat{\Omega}|\Phi\rangle \tag{3.76}$$

we denote the supplementary excitations as R_{12} double excitations. The sum over α and β in the previous Ansatz can be understood by rewriting it as

$$|\varphi_\alpha\rangle\langle\varphi_\alpha| = |\varphi_\kappa\rangle\langle\varphi_\kappa| - |\varphi_p\rangle\langle\varphi_p| = 1 - |\varphi_p\rangle\langle\varphi_p| = 1 - \hat{P} = \hat{Q} \tag{3.77}$$

where $\hat{P}$ is the projector onto the finite spin orbital basis and $\hat{Q}$ the projector onto the complementary spin orbital subspace. To illustrate the R_{12} double excitations, we can operate with $r_{\alpha\beta}^{ij}\tilde{a}_{ij}^{\alpha\beta}$ onto the two-electron determinant $|ij\rangle$ to obtain

$$\begin{aligned}
\frac{1}{2}\bar{r}_{\alpha\beta}^{ij}\tilde{a}_{ij}^{\alpha\beta}|ij\rangle &= \frac{1}{2}|\alpha\beta\rangle\langle\alpha\beta|r_{12}|ij\rangle \\
&= \frac{1}{4}|\varphi_\alpha\varphi_\beta - \varphi_\beta\varphi_\alpha\rangle\langle\varphi_\alpha\varphi_\beta - \varphi_\beta\varphi_\alpha|r_{12}|ij\rangle \\
&= \frac{1}{2}|\varphi_\alpha\varphi_\beta\rangle\langle\varphi_\alpha\varphi_\beta|r_{12}|ij\rangle - \frac{1}{2}|\varphi_\alpha\varphi_\beta\rangle\langle\varphi_\beta\varphi_\alpha|r_{12}|ij\rangle \\
&= |\varphi_\alpha\varphi_\beta\rangle\langle\varphi_\alpha\varphi_\beta|r_{12}|ij\rangle \;=\; \hat{Q}_{12}r_{12}|ij\rangle
\end{aligned} \tag{3.78}$$

where we have introduced the notation

$$\hat{Q}_{12} = |\varphi_\alpha\varphi_\beta\rangle\langle\varphi_\alpha\varphi_\beta| = \hat{Q}_1\hat{Q}_2 = (1-\hat{P}_1)(1-\hat{P}_2) \tag{3.79}$$

We can now extend the Ansatz by introducing the pseudo excitation operator

$$\hat{\mathcal{R}}_{ij}^{kl} = \frac{1}{2}r_{\alpha\beta}^{kl}\tilde{a}_{ij}^{\alpha\beta} \tag{3.80}$$

in that case we get

$$\hat{\mathcal{R}}_{ij}^{kl}|ij\rangle = \hat{Q}_{12}r_{12}|kl\rangle \tag{3.81}$$

Thus a pair function $|ij\rangle$ is substituted with the function $\hat{Q}_{12}r_{12}|kl\rangle$ by the action of the pseudo excitation operator $\hat{\mathcal{R}}_{ij}^{kl}$. This extension of the R_{12} double excitation space gives more flexibility and leads to a method that is invariant with respect to rotation upon the occupied orbitals [51]

3.2.3.2 R_{12} Coupled Cluster Theory

Coupled Cluster is characterized by an exponential Ansatz for the wave operator $\hat{\Omega}$

$$|\Psi\rangle = \hat{\Omega}|\Phi\rangle = e^{\hat{S}}|\Phi\rangle \tag{3.82}$$

where in the conventional sense the operator $\hat{S}$ is identical with the global cluster excitation operator $\hat{T}$. Similarly we may associate an amplitude to the R_{12} double excitation operator. We define the operator

$$\hat{R} \equiv \hat{R}_2 = \frac{1}{4}c_{kl}^{ij}\hat{\mathcal{R}}_{ij}^{kl} \tag{3.83}$$

therefore the wave equation will be

$$|\Psi\rangle = \hat{R}|\Phi\rangle + e^{\hat{T}}|\Phi\rangle \tag{3.84}$$

The operator $\hat{R}$ commutes with the conventional excitation operator

$$\left[\hat{R}, \hat{T}\right] = 0 \tag{3.85}$$

and one may add it to the exponential to give

$$\hat{S} = \hat{R} + \hat{T} \tag{3.86}$$

The Ansatz $\hat{S}$ defines the so called Coupled Cluster R_{12} theory (CC-R_{12}) having

$$|\Psi\rangle_{CC-R12} = e^{(\hat{R}+\hat{T})}|\Phi\rangle = e^{\hat{R}}e^{\hat{T}}|\Phi\rangle \tag{3.87}$$

It is interesting to notice that, when $e^{\hat{R}}$ is expanded in a Taylor series one can recognize a similar formal structure as found in Hylleras type wave functions

$$|\Psi\rangle_{CC-R12} = \sum_{m=0}^{\infty}\frac{1}{m!}\hat{R}^m|\Psi^{(m)}\rangle \tag{3.88}$$

using $\hat{R}$ instead of the original $\hat{r} = \sum_{i>j} r_{ij}$ operators. With the similarity transformed Hamiltonian defined one can obtain the equation for the correlation energy and the cluster amplitudes projecting the Schrödinger equation in the space of the reference determinant and of the conventional excited determinants respectively, but in this case it is also necessary to project the equation in the space of the R_{12} double excitation. The Coupled Cluster equations will therefore become

$$\begin{aligned} \Delta E &= \langle \Phi | e^{-\hat{S}} \mathcal{H}_N e^{\hat{S}} | \Phi \rangle && (3.89) \\ 0 &= \langle \Phi | \tilde{a}^{ij\cdots}_{ab\cdots} e^{-\hat{S}} \mathcal{H}_N e^{\hat{S}} | \Phi \rangle && (3.90) \\ 0 &= \langle \Phi | (\hat{\mathcal{R}}^{kl}_{ij})^{\dagger} e^{-\hat{S}} \mathcal{H}_N e^{\hat{S}} | \Phi \rangle && (3.91) \end{aligned}$$

3.2.3.3 The Resolution of the Identity

One of the key point in practical use of the CC-R_{12} method is concerned with the insertion of the resolution of the identity [52] into many electron integrals. The equation derived in the previous treatment, in fact, would imply the use of three and four electron integrals whose evaluation and use would be very cumbersome, and would limit the applicability of the present method to very small systems. It is therefore very important to introduce an approximation which is capable of overcome this problem, allowing to discard these many electron integrals, without a significant loss in accuracy.
Let us consider an othonormal spin orbital basis set $\{\varphi_{p'}\}$ in which we assume

$$|\varphi_{p'}\rangle\langle\varphi_{p'}| = 1 \tag{3.92}$$

the previous equation is an approximation of the resolution of the identity (RI) in the finite basis $\{\varphi_{p'}\}$ which is used to replace the exact RI

$$|\varphi_{\kappa}\rangle\langle\varphi_{\kappa}| = 1 \tag{3.93}$$

in the infinite basis set. As an example let us see how the invocation of this approximation will simplify the matrix elements involved. Consider for instance the element $\mathbf{X}$

$$\begin{aligned} \bar{X}^{kl}_{mn} &= \langle mn | r_{12} \hat{Q}_{12} r_{12} | kl \rangle = \frac{1}{2} r^{\alpha\beta}_{mn} r^{kl}_{\alpha\beta} \\ &= \frac{1}{2} r^{\mu\nu}_{mn} r^{kl}_{\mu\nu} - \frac{1}{2} r^{\mu q}_{mn} r^{kl}_{\mu q} - \frac{1}{2} r^{p\nu}_{mn} r^{kl}_{p\nu} + \frac{1}{2} r^{pq}_{mn} r^{kl}_{pq} \\ &= \langle mn | r^2_{12} | kl \rangle - \frac{1}{2} r^{\mu q}_{mn} r^{kl}_{\mu q} - \frac{1}{2} r^{p\nu}_{mn} r^{kl}_{p\nu} + \frac{1}{2} r^{pq}_{mn} r^{kl}_{pq} \end{aligned} \tag{3.94}$$

The RI approximation consists of replacing the sums over μ and ν in the three-electron integrals $r^{\mu q}_{mn} r^{kl}_{\mu q}$ and $r^{p\nu}_{mn} r^{kl}_{p\nu}$ by sums over p' and q'

$$\bar{X}^{kl}_{mn} = \langle mn | r^2_{12} | kl \rangle - \frac{1}{2} r^{p'q}_{mn} r^{kl}_{p'q} - \frac{1}{2} r^{pq'}_{mn} r^{kl}_{pq'} + \frac{1}{2} r^{pq}_{mn} \bar{r}^{kl}_{pq} \tag{3.95}$$

therefore three electrons integrals are avoided and are replaced by sums over products of two electron integrals. On the other matrix elements the RI acts accordingly, these situations will not be presented here for the sake of simplicity.
Obviously, a large spin orbital basis $\{\varphi_{p'}\}$ is needed to make a good RI approximation, but this basis need not to be as large as the one that would be required in conventional coupled-cluster calculations in an attempt to match the highly accurate correlation energies of the R_{12} approach. Furthermore, the basis $\{\varphi_{p'}\}$ need not be nearly complete in all symmetries. For atoms, for example, the required highest angular symmetry ℓ' is given by $\ell' = \ell + 2\ell_{occ}$, where ℓ is the highest angular symmetry of the basis $\{\varphi_p\}$ and ℓ_{occ} the highest occupied angular symmetry; for molecules the relation is $\ell' = 3\ell_{occ}$.

Part II

Intermolecular Forces and Electric Properties: Applications

Chapter 4

Interpolative Computation of Dispersion Interactions

The evaluation of Dispersion Constants via a numerical quadrature of the Casimir Polder formula is a very common task,

$$D_{ab} = \frac{1}{2\pi} \int_0^\infty \alpha_a^A(i\omega)\alpha_b^B(i\omega)d\omega \tag{4.1}$$

however the number of frequencies for which the polarizability has to be determined is in general quite high (up to eight or sixteen at least) and moreover no explicit expression for the dependence of the polarizabilities on the frequency is provided. An approach allowing the overcoming of these limitations was proposed by Magnasco et Al. [53] recently. In this procedure any available set of data, including values obtained for a given polarizability together with the corresponding imaginary frequencies can be used to build a simple interpolative expression providing an explicit continuous dependence on the frequency. The adjustable parameters occurring in the interpolative formula are optimized by imposing that some values of the polarizability, belonging to the initial set, ought to be exactly intercepted. This representation is suggested as a useful and simple tool to generate further values of polarizabilities from points which have been previously calculated only at some frequencies and, owing to its intrinsic easy integrability, to perform fast direct evaluations of dispersion constants, thus removing any need of undertaking numerical quadratures.

4.1 The Interpolative Formula

The sum over state expression of the polarizability which represents this quantity in terms of a finite number of parameters stating for effective oscillator strengths and transition energies can be be used as the starting point in the interpolative procedure. Any imaginary frequency-dependent polarizability (FDP) can hence be represented through a summation collecting n contributions from exact or approximate excited states of the concerned atomic or molecular system

$$\alpha_{lm,l'm'}(i\omega) = 2\sum_{j=1}^{n} \frac{\varepsilon_j \mu_j^{lm} \mu_j^{l'm'}}{\varepsilon_j^2 + \omega^2} \tag{4.2}$$

An efficient rational interpolative formula for FDPs should hence have the following structure

$$\alpha_{lm,l'm'}(i\omega) = \sum_{j=1}^{n} \frac{\sigma_j}{\tau_j + \omega^2} \tag{4.3}$$

where optimization of the interpolation procedure follows from imposing a fully exact reproduction for $2n$ available numerical values of the concerned FDP (α_1; α_2; ... ; α_{2n}) provided by evaluations performed at known imaginary frequencies ($i\omega_1$; $i\omega_2$; ...; $i\omega_{2n}$):

$$\begin{aligned}
\sum_{j=1}^{n} \frac{\sigma_j}{\tau_j + \omega_1^2} &= \alpha_1 \\
\sum_{j=1}^{n} \frac{\sigma_j}{\tau_j + \omega_2^2} &= \alpha_2 \\
&\cdots \\
\sum_{j=1}^{n} \frac{\sigma_j}{\tau_j + \omega_{2n}^2} &= \alpha_{2n}
\end{aligned} \tag{4.4}$$

Since the previous algebraic system contains $2n$ equations, it is adequate to accomplish the univocal determination of the $2n$ parameters σ and τ. The optimized values of the non linear τ are exactly coincident with the n positive roots of a n^{th} degree polynomial equation, whose expression involves n nested summations

$$\sum_{p(1)=1}^{n+1} \sum_{p(2)=p(1)+1}^{n+2} \cdots \sum_{p(n)=p(n-1)+1}^{2n} (-1)^{p(1)+p(2)+\ldots+p(n)} \tag{4.5}$$

$$\begin{aligned}
&\times w_{p(1)} w_{p(2)} \ldots w_{p(n)} \\
&\times w_{q(1)} w_{q(2)} \ldots w_{q(n)} \alpha_{p(1)} \alpha_{p(2)} \ldots \alpha_{p(n)} \\
&\times \left[\tau + \omega_{p(1)}^2\right] \left[\tau + \omega_{p(2)}^2\right] \cdots \left[\tau + \omega_{p(n)}^2\right] = 0
\end{aligned} \tag{4.6}$$

where $q(1), q(2), \ldots, q(n)$ symbolize the n integers that are residual in the set $1, 2, \ldots, 2n$ after deleting the n integers $p(1), p(2), \ldots, p(n)$ with $q(1) < q(2) < \ldots < q(n)$, the $2n$ terms $w_{p(1)}, w_{p(2)}, \ldots, w_{p(n)}, w_{q(1)}, w_{q(2)}, \ldots, w_{q(n)}$ are products collecting differences between squared values of the frequencies

$$\begin{aligned} w_{p(s)} &= d_{p(s),p(s)} d_{p(s),p(s+1)} \ldots d_{p(s),p(n)} \\ w_{q(s)} &= d_{q(s),q(s)} d_{q(s),q(s+1)} \ldots d_{q(s),q(n)} \\ s &= 1, 2, \ldots, n \end{aligned} \tag{4.7}$$

and

$$d_{\kappa,\lambda} = \begin{cases} \omega_\kappa^2 - \omega_\lambda^2 & (\kappa < \lambda) \\ 1 & (\kappa = \lambda) \\ \omega_\lambda^2 - \omega_\kappa^2 & (\kappa > \lambda) \end{cases} \tag{4.8}$$

Once the non-linear parameters τ have been determined, mathematical manipulations give the following general formula for the optimized values of the linear parameters σ

$$\begin{aligned} \sigma_j &= (-1)^j \frac{\prod_{q=1}^n (\tau_j + \omega_q^2}{\prod_{q=1}^n t_{j,q}} \sum_{p=1}^n (-1)^p \frac{\alpha_p}{\tau_j + \omega_p^2} \\ &\times \frac{\prod_{q=1}^n (\tau_q + \omega_p^2}{\prod_{q=1}^n d_{p,q}} \quad (j = 1, 2, \ldots, n) \end{aligned} \tag{4.9}$$

where

$$t_{\kappa,\lambda} = \begin{cases} \tau_\kappa - \tau_\lambda & (\kappa < \lambda) \\ 1 & (\kappa = \lambda) \\ \tau_\lambda - \tau_\kappa & (\lambda < \kappa) \end{cases} \tag{4.10}$$

The interpolative expressions become therefore a tool (i) to get further values of the concerned multipole polarizabilities, thus enlarging the initial sets required for evaluating the interpolative parameters, and (ii) to estimate dispersion constants, since the Casimir-Polder integral can now be treated in the well-known analytical way

$$\begin{aligned} D_{ab} &= \frac{1}{2\pi} \int_0^\infty \alpha_a^A(i\omega) \alpha_b^B(i\omega) d\omega \\ &= \frac{1}{2\pi} \sum_{j=1}^{n_A} \sum_{k=1}^{n_B} \int_0^\infty \frac{\sigma_j^A \sigma_k^B}{(\tau_j^A + \omega^2)(\tau_k^B + \omega^2)} \\ &= \frac{1}{4} \sum_{j=1}^{n_A} \sum_{k=1}^{n_B} \frac{\sigma_j^A \sigma_k^B}{\sqrt{\tau_j^A \tau_k^B} \left(\sqrt{\tau_j^A} + \sqrt{\tau_j^A} \right)} \end{aligned} \tag{4.11}$$

It is apparent that, at least in principle, this interpolative approach can be used to deal with any available set comprising frequencies and corresponding evaluations of a given multipole polarizability. Also the number n of terms included in the calculation is, still in principle, fully free from constraints, its upper limit being fixed by the size of the foregoing set. High values of n, however, give rise to mathematical steps which become quite tedious, especially because the evaluation of the non-linear parameters τ involves the roots of a n^{th} degree polynomial equation. While for $n \leq 4$ their search is supported by well-known analytical formulae [54, 55], the approach must be approximate and iterative when n becomes larger, but in this case inaccuracies due to numerical instabilities and usually yielding some unphysical negative τ_j have been observed. The required frequencies may, in principle, be chosen freely, but some care should be taken since the interpolated polarizabilities (and consequently dispersion constants) may be strongly dependent on this choice; in some particularly case one can even obtain some unphysical negative τ_j using a small number n of frequencies. It seems, in fact, important and even crucial a dominant inclusion of contributions coming from the region of low frequencies. A simple empirical formula was derived by us [56] for perform an efficient choice of the frequencies

$$\omega_p = \frac{p-1}{2N-(p-1)} \quad (p = 1, 2, 3, \ldots, N) \tag{4.12}$$

The previous formula mixes some intermediate and large values of the frequencies to the low ones, whose prevalence is suitably kept, so that a detailed scansion of the overall trend displayed by the polarizability is obtained in a balanced way.

4.2 C_7 Calculation for LiH homodimer

Previous studies performed in our laboratory involved the determination of LiH C_6 Dispersion Coefficients starting from Full-CI evaluations of frequency-dependent dipole and dipole quadrupole polarizabilities for ground state LiH in the imaginary frequency range $0. - 56. a.u.$, using both a limited set of 58 Gaussian type orbitals (GTOs) (about 700.000 Slater determinantsin each symmetry-adapted subspace) and 16-point Gaussian quadrature of the Casimir-Polder formula and an enlarged basis of 109 GTOs [58] (10^7 symmetry adapted determinants) with a 32 point quadrature of the Casimir Polder integral. We decided, therefore, to apply the interpolative scheme previously described at the determination of C_7 LiH coefficients. Hence we limited the calculations to the first four frequencies of the previous 32 point Gauss Legendre quadrature (plus the static values). In this way, we avoid the need of enlarging too much the range of frequencies to account

Table 4.1: FCI calculated values of frequency dependent dipole and dipole quadrupole polarizabilities (atomic units) at few selected imaginary frequencies for ground state LiH at $R = 3.015a_0$ (109 GTOs)

ω	α_{110}	α_{111}	α_{210}	α_{211}
0	26.15424	29.69799	-109.19560	-85.79136
0.02736	25.50401	29.08920	-106.96836	-84.46604
0.14388	16.61677	19.29949	-74.28072	-61.57549
0.35238	7.59846	8.01669	-34.89639	-29.10402
0.65094	3.45799	3.40626	-15.15589	-12.66231

Table 4.2: 2-term interpolation parameters σ and τ (atomic units) for the c.o.m. FDPs reported in the previous table

	α_{110}	α_{111}	α_{210}	α_{211}
σ	0.023566	0.032088	0.026041	0.037611
	0.224820	0.299789	0.158118	0.196396
τ	0.448479	0.828835	-1.763250	-2.318699
	1.592386	1.147266	- 6.537275	-4.735371

for the tails of higher polarizabilities, reducing, at the same time, the computation to the frequency region relevant to the interpolation method. Since higher polarizabilities are origin-dependent so are dispersion constants and dispersion coefficients. To facilitate comparison with Literature results, we have chosen to present all results in the center-of-mass origin. The AO basis set employed in the present work is the 14s9p4d3f/14s9p1d1f GTOs on Li and 11s6p3d/11s6p1d on H and is near to the saturation for the LiH molecule, the systems is kept at a nuclear distance of $3.015a_0$. In Table 4.1 and 4.2 we report the values of frequency dependent polarizabilities (in spherical tensor phormalism) and of the interpolation parameters σ and τ respectively.

Finally, the values of the four dipole-quadrupole dispersion constants A, B, C, D resulting from FCI calculation of c.o.m. polarizabilities for ground state LiH have been collected at the top of Table 4.3, where also the $C_7^{L_A L_B M}$ dispersion coefficients for the LiH-LiH homodimer are given in the $L_A L_B M$ scheme. Lastly, we want to stress here that calculations of cross-polarizabilities are not protected by any variational principle. As far as possible, their calculation should hence rest on use of largely extended basis sets, which must include the appropriate polarization functions, a goal that may be reasonably

Table 4.3: Dipole Quadrupole Dispersion Coefficients and Constant for the LiH homodimer. Dispersion Constants: $A = -77.398$, $B = C = -87.362$, $D = -71.099$

L_A	L_B	M	$C_7^{L_A L_B M}$
0	1	0	1458.15
0	3	0	82.47
2	1	0	-57.51
2	1	1	9.585
2	3	0	3.538
2	3	1	0.5896
2	3	2	-0.0421

reached if we can restrict calculations to few frequencies as we have done in the present calculation.

4.3 BeH_2 C_6 Dispersion Coefficients

The structure of the $^1\Sigma_g^+$ ground state of the centrosymmetric linear BeH_2 molecule has only recently been obtained from the analysis of IR emission spectra [63, 64], giving a Be-H distance of $R = 2.506a0$. Following our previous work on LiH [57], frozen core FCI calculations of frequency dependent dipole polarizabilities (FDPs) of ground state BeH_2 at this distance have been performed using an extended set of 208 contracted GTO functions ([9s9p5d3f] on Be [59] and [9s8p6d] on H [60]) involving about $58 \cdot 10^6$ symmetry adapted Slater determinants at eight optimized imaginary frequencies. In such a way, the analytic evaluation of the Casimir Polder integral over these optimized frequencies allows for the evaluation of the three dipole dispersion constants for the BeH_2-BeH_2 homodimer, from which isotropic C_6 and anisotropy γ_6 coefficients are derived for the first time. (In particular the latter is defined as $\gamma_6 = \frac{C_6^{L_A L_B M}}{C_6^{000}}$).

4.3.1 Basis set Choice and numerical results

After preliminary FCI calculations using a small Sadlej basis set [61] containing 42 GTO functions, attention was focused, as we already stated, on an extended set of 208 contracted GTOs. Since a full electron FCI with such a large basis set (about $27 \cdot 10^{10}$ determinants) is, to our knowledge, hardly possible today, the feasibility of frozen core

versus full electron approximation was tested by computing the Cauchy moments at the CCSD level and studying the convergence of $[n, n-1]$ Pade' approximants to the polarizability [62]. In Table 4.4 we report the values of the approximants, as one can guess substantial stability was obtained for the $[6, 5]$ term, showing that frozen-core results are within 0.6% of the full-electron results for $\alpha_{\|}$ while a somewhat larger error holds for $\alpha_{\perp}$.

The calculated CCSD molecular energy at $R = 2.506a0$ was $E = 15.89012E_h$ with static dipole polarizabilities (in atomic units) $\alpha_{\|} = 19.9920$, $\alpha_{\perp} = 19.7256$ and a quadrupole moment $\Theta = 1.9852$ for the full-electron case. The corresponding CCSD frozen core results are, respectively, $E = 15.85074E_h$, $\alpha_{\|} = 19.8762$, $\alpha_{\perp} = 19.7572$, $\Theta = 2.0017$. An even larger basis set involving 1 more g functions on Be and two more f functions on H was found, as expected, to have minor effects on the properties, improving the energy by only $0.16 \cdot 10^3 E_h$, and was therefore discarded. FCI calculations in the frozen core approximation were then performed at the 8 optimized imaginary frequencies provided by the selecting formula equation [57] and subsequently treated according to the interpolation method for the FDPs. Polarisabilities results are collected in Table 4.5, while Table 4.6 presents the values of the interpolative parameters σ and τ for $N = 2$ and $N = 4$, with frequencies for the $N = 2$ case being simply a subset of the $N = 4$ case. Finally in Table 4.7 the N-term dispersion constants for the BeH_2 homodimer are given, while in table 4.8 we present the value of the $C_6^{L_A L_B M}$ dispersion coefficients computed at $N = 4$ level. It can be seen that $N = 2$ gives values which are only slightly larger (from 0.04% to 0.13%) than the $N = 4$ results. The results show that, the BeH_2-BeH_2 dispersion interaction in long range has a sensibly spherical leading term with very small anisotropy coefficients γ_6.

4.3.2 Concluding remarks

A frozen core FCI calculation of the static and frequency-dependent dipole polarizabilities of the ground state of the centrosymmetric linear BeH_2 molecule at the experimental Be-H distance of $R = 2.506$ has been performed using an extended set of 208 contracted GTO functions. The feasibility of frozen core versus full electron approximation was tested in detail by computing the Cauchy moments at the CCSD level and studying the convergence of $[n, n-1]$ Pade' approximants to the polarizability. The calculations were limited to a set of eight frequencies selected according to a simple formula developed by us using N-term rational interpolation technique. The C_6 dispersion coefficients of the homodimer BeH_2-BeH_2 were then computed in the $N = 4$ approximation, showing that the BeH_2-BeH_2 dispersion interaction in long range is sensibly spherical in its leading term. A theoretical study of the static dipole polarizability of the polymeric beryllium

hydride chain was recently done by Abdurahman [65] using large basis sets on either Be and H. Even if a direct comparison is not possible because the bond length of the single molecule is not reported in [65], the values of $\alpha_{\parallel}$ and $\alpha_{\perp}$ for the monomer BeH_2 calculated there using CCSD(T) techniques seem to be in reasonable agreement with our results.

Table 4.4: Convergence of $[n, n-1]$ Pade' approximants to frequency dependent dipole polarizabilities of BeH_2 at $R = 2.506a0$ in (i) full-electron and (ii) frozen-core calculations using the [Be9s9p5d3f/H9s8p6d] 208 GTO basis set as a function of frequence $i\omega$

$i\omega$	0.14286	0.33333	0.60000	1.00000	1.66667	3.00000	7.00000
(i) Full Electron $\alpha_{\parallel}$							
$[1,0]$	17.69470	11.71273	6.07615	2.71565	1.07072	0.34317	0.06393
$[2,1]$	17.71996	11.96271	6.51379	3.06106	1.24729	0.40652	0.07625
$[3,2]$	17.72000	11.96880	6.55645	3.13052	1.29840	0.42822	0.08076
$[4,3]$	17.72000	11.96899	6.56148	3.14783	1.31753	0.43814	0.08300
$[5,4]$	17.72000	11.96899	6.56227	3.15402	1.32879	0.44583	0.08495
$[6,5]$	17.72000	11.96899	6.56236	3.15601	1.33571	0.45297	0.08719
(i) Full Electron $\alpha_{\perp}$							
$[1,0]$	17.01258	10.55861	5.17331	2.23805	0.86878	0.27656	0.05139
$[2,1]$	17.06328	10.99025	5.83884	2.72745	1.11067	0.36207	0.06792
$[3,2]$	17.06335	11.00084	5.90689	2.83512	1.18965	0.39567	0.07492
$[4,3]$	17.06335	11.00109	5.91382	2.86097	1.22057	0.41260	0.07883
$[5,4]$	17.06335	11.00109	5.91399	2.86212	1.22249	0.41384	0.07914
$[6,5]$	17.06335	11.00109	5.91397	2.86201	1.22230	0.41372	0.07911
(ii) Frozen Core $\alpha_{\parallel}$							
$[1,0]$	17.58433	11.62616	6.02465	2.69088	1.06061	0.33989	0.06331
$[2,1]$	17.60885	11.86724	6.44314	3.01889	1.22758	0.39967	0.07493
$[3,2]$	17.60889	11.87282	6.48109	3.07906	1.27103	0.41792	0.07870
$[4,3]$	17.60889	11.87297	6.48498	3.09153	1.28405	0.42445	0.08015
$[5,4]$	17.60889	11.87297	6.48548	3.09490	1.28937	0.42773	0.08095
$[6,5]$	17.60889	11.87297	6.48553	3.09569	1.29145	0.42942	0.08141
(ii) Frozen Core $\alpha_{\perp}$							
$[1,0]$	17.04499	10.58609	5.18978	2.24589	0.87195	0.27759	0.05158
$[2,1]$	17.09394	11.00270	5.83052	2.71565	1.10367	0.35941	0.06739
$[3,2]$	17.09400	11.01231	5.89117	2.80967	1.17151	0.38801	0.07332
$[4,3]$	17.09400	11.01251	5.89666	2.82894	1.19331	0.39950	0.07593
$[5,4]$	17.09400	11.01251	5.89675	2.82941	1.19403	0.39994	0.07604
$[6,5]$	17.09400	11.01251	5.89672	2.82925	1.19376	0.39977	0.07600

Table 4.5: Frozen core FCI calculated values of frequency dependent dipole polarizabilities (atomic units) at 8 selected imaginary frequencies for ground state BeH2 at $R = 2.506$ (208 GTOs)

$i\omega$	$\alpha_{\parallel}$	$\alpha_{\perp}$
0.000000	19.94072	19.67005
0.142857	17.65902	17.02216
0.333333	11.89590	10.97265
0.600000	6.493246	5.878688
1.000000	3.098275	2.826123
1.666667	1.293614	1.203108
3.000000	$4.320870 \cdot 10^{-1}$	$4.105680 \cdot 10^{-1}$
7.000000	$8.273100 \cdot 10^{-2}$	$7.986400 \cdot 10^{-2}$

Table 4.6: N-term interpolation parameters τ and σ

$\tau_{\parallel}$	$\sigma_{\parallel}$	$\tau_{\perp}$	$\sigma_{\perp}$
$N = 2$			
$1.474240417 \cdot 10^{-1}$	2.687187852	$1.216995978 \cdot 10^{-1}$	2.166374414
$7.905210630 \cdot 10^{-1}$	1.354249989	$9.184312289 \cdot 10^{-1}$	1.716594851
$N = 4$			
$1.318886010 \cdot 10^{-1}$	1.940393032	$1.044900679 \cdot 10^{-1}$	1.489460843
$2.888086521 \cdot 10^{-1}$	1.292161534	$2.859865552 \cdot 10^{-1}$	1.306055224
$9.979251902 \cdot 10^{-1}$	$7.417767521 \cdot 10^{-1}$	1.134818275	$9.294001376 \cdot 10^{-1}$
12.24689544	$1.338347707 \cdot 10^{-1}$	8.752124445	$2.593369001 \cdot 10^{-1}$

Table 4.7: N-term BeH_2 dispersion constants D

N	$A = D_{\parallel,\parallel}$	$B = C = D_{\parallel,\perp}$	$D = D_{\perp,\perp}$
2	20.45895	19.44097	18.49104
4	20.45078	19.42488	18.46691

Table 4.8: Angle-dependent $C_6^{L_A L_B}$ dispersion coefficients $\gamma_6^{L_A L_B M}$ anisotropy coefficients in the BeH_2-BeH_2 from frozen core FCI calculations for BeH_2 at $R = 2.506$ (208 GTOs)

L_A	L_B	M	$C_6^{L_A L_B M}$	$\gamma_6^{L_A L_B M}$
0	0	0	114.679	1
0	2	0	1.96124	0.0171
2	0	0	1.96124	0.0171
2	2	0	0.13584	0.00118
2	2	1	-0.03019	-0.000263
2	2	2	0.003773	0.000033

Chapter 5

LSDK: A Davidson computation for the Dispersion Coefficients

We want in this Chapter to describe an alternative technique [66] we have implemented in our FCI code and present high level results for Be (C_6, C_8) and LiH (C_6, C_7). We recall, anyway, that in order to compute good quality values large AO basis sets including many polarization functions are needed, and, in a FCI context, this is feasible only for small systems.

5.1 Introduction

We are, in this context, dealing with a perturbative problem in the (tensor) product space $FCI_A \otimes FCI_B$ [59] where the zeroth order Hamiltonian is given by the sum of the FCI Hamiltonians of the the separated molecules A and B

$$\mathcal{H} = \mathcal{H}_A + \mathcal{H}_B \tag{5.1}$$
$$\mathcal{H}_A|\Phi_A\rangle = E_A|\Phi_A\rangle \tag{5.2}$$
$$\mathcal{H}_B|\Phi_B\rangle = E_B|\Phi_B\rangle \tag{5.3}$$
$$\tag{5.4}$$

As usual the perturbation operator $\hat{V}_{AB}$ is given by the Coulombic interactions between all charged particles of molecule A and those of molecule B and can be expanded in an (asymptotic) power series in the inverse of the intermolecular separation. The series coefficients can be resolved into sums of products of multipoles centred on the interacting molecules and angular factors accounting for their reciprocal spacial orientation. Due to the linearity of perturbative equations, one can treat separately each product of multipole

operators $\hat{Q}A\ \hat{Q}_B$ and write down for it a 1^{st} order equations in the space $FCI_A \otimes FCI_B$ for dispersion interactions:

$$(\mathcal{H}_A - E_A^0 + \mathcal{H}_B - E_B^0)|\Phi_{AB}\rangle = -(E_A^1 - \hat{Q}_A)|\Phi_A\rangle(E_B^1 - \hat{Q}_B)|\Phi_B\rangle \tag{5.5}$$

where E_1^A and E_B^1 represent the first order correction to the energy $\langle\Phi|\hat{Q}|\Phi\rangle$ for molecule A and B respectively. The Dispersion Coefficients may therefore be computed from the dispersion constants having the general form

$$\langle\hat{Q}'_A\hat{Q}'_B|\hat{Q}_A\hat{Q}_B\rangle_\otimes = \langle\Phi_A\varphi_B|(E_1^A - \hat{Q}_A)(E_1^B - \hat{Q}_B)|\Phi_{AB}\rangle_\otimes \tag{5.6}$$

using the general formulae we gave in the previous chapters. Here we used the subscript $\otimes$ to stress the dispersion constants belong to the space of the two interacting monomers $FCI_A \otimes FCI_B$. Notice, moreover, that in general the multipole operators present in the previous formula may be different: in particular in the case where $\hat{Q}'_A = \hat{Q}_A$ and $\hat{Q}'_B = \hat{Q}_B$ the dispersion constant will be called diagonal, otherwise non-diagonal, and computational methods will, in general, be different in the two cases. One common method used to compute dispersion coefficients is the London formula [12] which uses the eigenvectors of $\mathcal{H}_A$ and $\mathcal{H}_B$ and which we may expressed as

$$\langle\hat{Q}'_A\hat{Q}'_B|\hat{Q}_A\hat{Q}_B\rangle_\otimes = \sum_{i_A>0,j_B>0} \frac{\langle 0_A|\hat{Q}'_A|i_A\rangle\langle i_A|\hat{Q}_A|0_A\rangle\langle 0_B|\hat{Q}'_B|j_B\rangle\langle j_B|\hat{Q}_B|0_B\rangle}{E_i^A - E_0^A + E_j^B - E_0^B} \tag{5.7}$$

where $\langle i_A|\hat{Q}_A|0_A\rangle$ is the overlap of the vector $-(E_A^1 - \hat{Q}_A)|\Phi_A\rangle$ with the excited eigenvector $|i_A\rangle$ and similarly for B. This equation is not directly translated into a practical computational procedure even if all involved quantities are in principle available in FCI. In fact given the large dimensions of the FCI spaces ($10^6 - 10^9$ determinants), the sum over the eigenvectors has to be truncated, and, more important, the computational cost of obtaining several excited eigenvectors is exceedingly high. In [59] the previous was computed by expanding the London formula in a Ritz Lanczos basis. The Lanczos recursion is a way to generate an orthonormal basis of the Krylov subspace $\{\mathcal{H}^i\mathbf{b}_0, i = 1, 2, \ldots, k\}$ of FCI space which moreover brings the Hamiltonian in a tridiagonal; here $\mathcal{H}$ is the FCI Hamiltonian and $\mathbf{b}_0$ is an arbitrary starting vector.
Suppose we start a Lanczos recursion for molecule A from the vector $\mathbf{b}_0^A = -(E_A^1 - \hat{Q}_A)|\Phi_A\rangle$, and another recursion for molecule B from $\mathbf{b}_0^B = -(E_B^1 - \hat{Q}_B)|\Phi_B\rangle$. After n_A and n_B steps we will have two sets of Lanczos vectors spanning iterative subspaces IS_A and IS_B of dimensions $n_A + 1$ and $n_B + 1$, respectively. If we diagonalize each Hamiltonian in its subspace spanned by the Lanczos vectors we can use the eigenvectors

(Ritz vectors) $i_A^R\rangle$, $j_B^R\rangle$ as pseudostates and therefore we get the following approximation of the London formula equation for the diagonal matrix element $\langle \hat{Q}'_A \hat{Q}'_B | \hat{Q}_A \hat{Q}_B \rangle$

$$S_{n_A,n_B} = \sum_{i=0}^{n_A} \sum_{j=0}^{n_B} \frac{R_{Ai}^2 R_{Bj}^2}{\varepsilon_i^A - E_0^A + \varepsilon_j^B - E_0^B} \tag{5.8}$$

where $R_{Ai} = \langle (E_A^1 - \hat{Q}_A)\Phi_A | i_A \rangle$ is a transition multipole between the ground state Φ_A and the ith pseudostate $|i_A^R\rangle$, and ε_i^A is the eigenvalue corresponding to the ith eigenvector (i.e. the pseudostate excitation energy). Loosely speaking, the idea in [59] is to improve the approximation by enlarging the Lanczos subspaces and iterate until convergence on the value of S_{n_A,n_B} is (hopefully) reached. As n_A, n_B increase the approximation improves; the process may be continued until a stable value of S_{n_A,n_B} is reached. This does not guarantee rigorous convergence to the exact value, but it is nonetheless a stopping criterion. Notice that the Ritz eigenvectors and eigenvalues change at each step, because the Lanczos space is enlarged. The procedure proved successful in a number of cases, but in many other situations it failed, an example being the Beryllium atom with the B_3 basis of Papadopulos et Al. [67]. As it was pointed out in [59] a reason for this failure is probably the following. The Lanczos procedure is known to converge first to the extreme eigenvalues of the matrix [68]. On the other hand, by inspection of London formula, the states most contributing to the dispersion constants have:

- low excitation energies
- large multipole transition moments with the ground state.

Usually these states are found in the lower and medium portion of the spectrum of the FCI molecular Hamiltonian. The Lanczos vectors, on the other hand, are too rich in highly excited states with small transition multipoles: all the computational effort is wasted in bringing in the wrong portion of the spectrum. Such situations arise with uncontracted AO bases, especially those containing many s orbitals with high exponents, like Papadopoulos B_3 basis. An estimate (lower bound) of the highest eigenvalue is obtained by the Lanczos procedure itself and is 700,000 hartree. The size of the FCI space seems to be not as important. An example of small Full CI basis where the Lanczos expansion failed was constructed by uncontracting the (small) basis of Sadlej and Urban [61] for beryllium: this provided a Full CI space of only 170,000 determinants, but we could not achieve convergence after 100 Lanczos iterations (the highest eigenvalue is 12,000 hartree).

5.2 Preconditioned Expansion of the London Formula

The idea is to avoid generating vectors spanning the high energy portion of the spectrum of $\mathcal{H}^{FCI}$ by a Davidson like preconditioner based on the diagonal. We modify the previously described procedure in such a way that the iterative subspace IS_n spans the lower energy part of the spectrum, then, at each step, we project the FCI Hamiltonian in IS_n and use its eigenvalues and eigenvectors in the London formula. Let us consider first the computation of a fully diagonal matrix element $\langle \hat{Q}'\hat{Q}'\hat{Q}\hat{Q}\rangle$ where we have only one iterative subspace IS_n spanned by the vectors $\mathbf{b}_0, \mathbf{b}_1, \ldots, \mathbf{b}_n$ recursively generated. The projection of the FCI Hamiltonian in this iterative subspace is the reduced Hamiltonian matrix $\mathbf{H}^n$ of elements $\mathbf{b}_i^\dagger \mathcal{H} \mathbf{b}_k$, the staring vector is $\mathbf{b}_0 = -(E^1 - \hat{Q})|\Phi\rangle$ as in the Lanczos expansion. The next step is to define a prescription to enlarge the iterative subspace. A first prescription to generate a vector $\mathbf{r}$ not lying in IS_n is

$$\mathbf{r} = (\mathcal{H}^{FCI} - \alpha \mathbf{b}_k) \tag{5.9}$$

where α is a parameter at our disposal, in this case we take into account only the last basis vector $\mathbf{b}_k$; we label this first possibility as a). Another possibility is the residual of the equation

$$(\mathcal{H}^{FCI} - \alpha)\mathbf{x} = \mathbf{b}_0 \tag{5.10}$$

where $\mathbf{x}$ is the solution of the same equation projected in the iterative subspace, we label this possibility as b).

As Concerns α the Lanczos choice is $\alpha = \mathbf{b}_k \dagger \mathcal{H}^{FCI} \mathbf{b}_k$: in this case the previous equation gives the projection of the gradient of the energy functional $\langle \varphi | \mathcal{H} | \varphi \rangle$ in $\varphi = \mathbf{b}_k$ along the surface $\|\mathbf{b}_k\| = 1$ and therefore it is good for eigenvalues. We performed a number of numerical experiments with different choices of α, including values changing from iteration to iteration. The simplest choice $\alpha = E_0$ proved to be reasonably effective as concerns convergence rate and we never observed numerical instabilities. Therefore we decided to stick to this choice $\alpha = E_0$ in our computations. To the vector $\mathbf{r}$ obtained by either rule a) or b), we apply the Davidson preconditioner D_σ^{-1} according to:

$$\mathbf{r} \leftarrow \{Diag(\mathcal{H}^{FCI} - \sigma\}^{-1} \mathbf{r} = D_\sigma^{-1} \mathbf{r} \tag{5.11}$$

where σ is a parameter; a sensible choice is $\sigma = E_0$: the preconditioner is positive definite and enhances the components close to E_0 in energy. However, we loose the orthogonality of the Lanczos scheme and the new vector $\mathbf{r}$ must be orthogonalized to $\mathbf{b}_0, \mathbf{b}_1, \ldots, \mathbf{b}_n$. This implies that all the basis vectors should be stored on disk. Davidson's

D_σ preconditioner equation depresses the high energy components and enhances those lying near σ as required by a method to compute an eigenvector of energy close to σ. In our case we rather need to span all the low energy region of the Full CI Hamiltonian. The Davidson's σ preconditioner may depress too much the lower lying excited states with high transition multipole. This can be avoided by defining a new diagonal preconditioner $\mathbf{S}_t$ which leaves unaltered the components of energy up to a given value and acts as the Davidson's one for higher values. The (nonzero) matrix elements of this preconditioner are:

$$S_{t_i i} = \begin{cases} 1 & E_0 < H_{ii}^{FCI} \leq -\frac{E_0}{2} \\ \frac{\frac{1}{2}E_0}{DiagH^{FCI}-\sigma} & -\frac{E_0}{2} \leq H_{ii}^{FCI} \end{cases} \tag{5.12}$$

In this way only the components with energy higher than $\frac{E_0}{2}$ are depressed. This preconditioner, called STEP, is intermediate between Lanczos and Davidson and it proved to be better than pure Davidson for the present purpose.

5.2.1 Description of the algorithm

The present form of the FCI algorithm for a fully diagonal matrix element is the following:

1. set $k = 0$, $\mathbf{b}_0 = \frac{-(E_1-\hat{Q})|\Phi_0\rangle}{\|-(E_1-\hat{Q})|\Phi_0\rangle\|}$
2. write $\mathbf{b}_k$ on disk
3. perform FCI FO $\mathbf{h}_k = \mathcal{H}\mathbf{b}_k$
4. compute the kth row and column of the reduced Hamiltonian matrix $\mathbf{H}_{ij}^k = \mathbf{b}_i^\dagger \mathbf{h}_k$ with $i = 1, 2, \ldots, k$
5. diagonalize $\mathbf{H}^k$ to get transition energies ε_i and multipoles R_i
6. compute the London formula $S_{k,k}$. If $|S_{k,k} - S_{k-1,k-1}|$ is less than convergence criterion stop
7. compute $\mathbf{r}$ using either a) or b)rule
8. precondition $\mathbf{r} \leftarrow \mathbf{S}_t\mathbf{r}$
9. Schmidt orthogonalize $\mathbf{r}$ to all the previous vectors $\mathbf{b}$
10. set $k = k + 1$, $\mathbf{b}_k = \frac{\mathbf{r}}{\|\mathbf{r}\|}$ and go back to point 2

The computationally demanding step is as always 3, where we perform, in a direct way, the FCI Hamiltonian by vector multiplication. The resulting vector $\mathbf{h}k = \mathcal{H}^{FCI}\mathbf{b}_k$ is used to compute the matrix elements needed to add a new row and column to the reduced Hamiltonian matrix of the previous iteration. At step 5 the eigenvectors of the reduced Hamiltonian matrix provide a set of pseudostates and the first row of the eigenvector matrix multiplied by $\|((E_1 - \hat{Q})|\Phi_0\rangle\|$ provides transition multipoles R_i needed to compute $S_{k,k}$ at step 6. A failure of the algorithm may result at step 9, if the new direction $\mathbf{r}$ is lying in the iterative subspace. We did not attempt a stability analysis of the procedure, but limited ourselves to monitor the behavior of the sequence $S_{k,k}$ and the norm at step 9. The present algorithm was denoted by the acronym LSDK for London-Step-Davidson-Krylov. The procedure is able to compute a fully diagonal matrix element and takes advantage of the monotonous character of the associated sequence S_k to terminate if a stable value is reached. At the end we also have an approximation to the solution of the first order perturbative equation that can be exploited to compute nondiagonal matrix elements by scalar multiplication with appropriate vectors (see later). A diagonal matrix element $\langle\hat{Q}_A\hat{Q}_B|\hat{Q}_A\hat{Q}_B\rangle$ where $\hat{Q}_A \neq \hat{Q}_B$ may however be computed from the transition multipoles and excitation energies obtained from two separate and converged computations on the fully diagonal matrix elements.

5.3 Diagonal Matrix Elements: Results for Be

The previous computational procedure providing diagonal matrix elements is appropriate for interacting systems of high symmetry like two atoms. The results of our computations on Be are shown in Table 5.1, where we compare the results of our LSDK method with the 16 points numerical quadrature of the Casimir Polder. We used three different AO bases:

- the 126 AO B_3 basis of Papadopoulos et Al. [67]
- the 9s9p5d basis used by Graham et Al. [69]
- a 9s9p5d3f2g derived from the 9s9p5d3f basis used in a previous work [59] by adding two g functions with exponents 0.3 and 0.05.

The threshold for stopping is $h = 0.5 \cdot 10^{-7}$. Pre Full CI computations were performed with the MOLPRO code version 2000.1 [85] The data reported show that the LSDK method is capable of reproducing the Casimir Polder results with high accuracy. Convergence of the LSDK values depends upon the multipole operator involved and the

Table 5.1: Dipole (α) and quadrupole (C_Q) polarizabilities, C_6 and C_8 dispersion coefficients for Be

AO basis	B_3	9s9p5d	9s9p5d3f2g
FCI dim.	$8.0 \cdot 10^6$	$0.8 \cdot 10^6$	$3.1 \cdot 10^6$
FCI energy	-14.665498	-14.656662	-14.656767
α	37.4705	37.5790	37.8066
C_Q	95.4440	94.6803	99.3500
Method	C_6		
CP-16	211.9030	213.1272	214.6724
LSDK a	211.9019	213.1270	214.6723
LSDK b	211.9030	213.1272	214.6724
Method	C_8		
CP-16	4859.216	4863.328	5111.085
LSDK a	4859.176	4863.314	5111.091
LSDK b	4859.216	4863.328	5111.085

AO basis and it was achieved in 40 (dipole) to 60 (quadrupole) iterations. In any case, at least in our implementation,the computational cost is much less, than that to compute the 16 values of the polarizability at imaginary frequency needed by the Casimir Polder integration. Indeed each iteration in the complex field involves two multiplications $\mathcal{H}^{FCI}\mathbf{b}$, one for the real and one for the imaginary part of the vector. We estimate on average 10-12 iterations for each imaginary frequency to get convergence of 10^{-6} in the residual norm of polarizability perturbative equation; therefore 40-60 LSDK iterations are the equivalent of 2-3 imaginary frequencies. However, it should be noticed that other implementations of the perturbative equation solution claim higher efficiency than ours. Another advantage of LSDK is the variational bounding property of the diagonal matrix elements. As concerns the AO bases, the reported values of the quadrupole polarizability C_Q and the C_8 coefficient show the importance of the g functions. Comparison with the values of quadrupole polarizability given by Komasa [70] ($\alpha = 37.755$ and $C_Q = 100.32$) indicate that our C_8 coefficient is probably of good quality.

5.4 Nondiagonal Matrix Elements: LiH Results

For two interacting molecules we need to compute also nondiagonal matrix elements, where $\hat{Q}'_A \neq \hat{Q}_A$ or $\hat{Q}'_B \neq \hat{Q}_B$, or both. Let us consider the case $\hat{Q}_A = \hat{Q}_B$; at step k of the iterative process we implicitly define an approximate solution

$$\Phi^k_{AB} = -\sum_{i,j=1}^{k} \frac{R^A_i|i\rangle \otimes R^B_j|j\rangle}{\varepsilon^A_i - E^A_0 + \varepsilon^B_j - E^B_0} \tag{5.13}$$

we can therefore compute non diagonal matrix elements by scalar multiplication of the previous by the vectors $(E_1^{A'} - \hat{Q}'_A)|\Psi^A_0\rangle$ and $(E_1^{B'} - \hat{Q}'_B)|\Psi^B_0\rangle$. Suppose we want to determine $\langle\hat{\mu}_x\hat{\mu}_x|\hat{Q}_{xz}\hat{Q}_{xz}\rangle$ the first idea is to use the solution obtained from the same iterative subspace as for the diagonal matrix elements. However, our experience shows that, in general, the scalar product does not show a convergent behavior like a diagonal element. The problem arises when there are two different operators on both molecules. In particular we find that the iterative subspace generated by the starting vector $(E_1^x - \hat{\mu}_x)|0\rangle$ gives good results e.g. for $\langle\hat{\mu}_x\hat{Q}_{xz}|\hat{Q}_{xz}\hat{Q}_{xz}\rangle$ (besides $\langle\hat{\mu}_x\hat{\mu}_x|\hat{\mu}_x\hat{\mu}_x\rangle$), but not for $\langle\hat{Q}_{xz}\hat{Q}_{xz}|\hat{\mu}_x\hat{\mu}_x\rangle$. On the other hand if we start from $(E_1^x - \hat{Q}_{xz})|0\rangle$ we get convergent behavior for $\langle\hat{\mu}_x\hat{Q}_{xz}|\hat{Q}_{xz}\hat{Q}_{xz}\rangle$ and again not for $\langle\hat{Q}_{xz}\hat{Q}_{xz}|\hat{\mu}_x\hat{\mu}_x\rangle$. We also tried iterative subspaces generated by taking as starting vector a linear combination of $(E_1^x - \hat{\mu}_x)|0\rangle$ and $(E_1^x - \hat{Q}_{xz})|0\rangle$: we found always poor results. A satisfactory procedure is the following. We start two parallel subspace iterations, one from $(E_1^x - \hat{\mu}_x)|0\rangle$, another from $(E_1^x - \hat{Q}_{xz})|0\rangle$ and use the sum of the two subspaces $IS_x + IS_{xz}$ to expand the solution of the perturbative equation. The iterative subspace has double dimension, but only minor modifications in the code are required. In our actual implementation, at each step we have an orthonormal basis of IS_x, another for IS_{xz}, but we have a mixed overlap matrix $\mathbf{S}$ between them. The overall metric and reduced Hamiltonian matrices have the following structure:

$$\textbf{overlap}: \quad \begin{bmatrix} \mathbf{I}_{xx} & \mathbf{S} \\ \mathbf{S} & \mathbf{I}_{xzxz} \end{bmatrix} \tag{5.14}$$

$$\textbf{hamiltonian}: \quad \begin{bmatrix} \mathbf{H}_{xx} & \mathbf{H}_{xxz} \\ \mathbf{H}^\dagger_{xxz} & \mathbf{H}_{xzxz} \end{bmatrix} \tag{5.15}$$

Compared to the independent computation of the diagonal elements, at each step we have to compute some extra scalar products between FCI vectors to update the off diagonal blocks $\mathbf{S}$ and $\mathbf{H}_{xxz}$. This involves no significant additional computational cost because the time consuming operations are the same as those required for the two diagonal elements. As concerns more general matrix elements, i.e., with three or four

Table 5.2: Comparison of dispersion constants for LiH computed with various methods and the 109 AO basis

	LSDK	CP-16	FM
Dispersion Constants for $n = 6$			
A	17.785928	17.7398033	17.738885
$B = C$	20.081013	20.0240612	20.010608
D	22.714491	22.6457958	22.612709
Dispersion Constants for $n = 7$			
A	-77.476380	-77.3059769	-77.397927
B	-63.112078	-62.9895401	-63.017266
C	-87.458787	-87.2575912	-87.276522
D	-71.211737	-71.0742487	-71.030147

different operators, we expect that three or four parallel subspace iterations are needed. We did not investigate further this point.

5.4.1 Results for LiH

The computations were performed at fixed internuclear separation of 3.015 bohr, the z-axis being parallel to the bond; the origin of axes was taken in the center of mass. A first set of results concerning the comparison of different methods is displayed in Table 5.2. We report the so called elementary dispersion constants A, B, C, D, directly connected to the matrix elements of perturbative equation, as illustrated many time during this thesis. The methods used are: LSDK, 16 points numerical integration CP-16 and the 4 points interpolative method of Figari and Magnasco, FM [53]. These results were obtained using the 109 AO basis used in a previous work [58, 57]. The data show the degree of agreement between the various procedures. It should be remarked that the LSDK values for the A and D constants of $n = 6$ are variational lower bounds and therefore they are closer to the exact FCI values than Casimir Polder or Figari Magnasco. All other constants involve nondiagonal matrix elements, and therefore are not variationally bound. As concerns the computational cost, at least in our implementation, LSDK is again cheaper than CP-16 and also cheaper than 4 points FM. The second set of results was obtained using the sp, spd and spdf AO bases of Tunega et Al. [60] and the LSDK method. In order to reduce the dimension of the Full CI space, the largest (11s8p6d3f/9s8p6d2f) was contracted to (11s8p6d1f/9s8p6d1f) as follows. A RHF calculation on LiH was performed and the

Table 5.3: Energy and static electrical properties of LiH with Tunega Noga bases [60]

Basis	sp (11s8p/9s8p)	spd sp+(6d/6d)	spdf spd+(1f/1f)
AO/FCI dim.	$68/1.5 \cdot 10^6$	$128/17.1 \cdot 10^6$	$163/44.5 \cdot 10^6$
Energy	-8.0630127	-8.0685194	-8.0693359
μ_z	2.3081	2.2942	2.2935
Θ_{zz}	3.1914	3.0969	3.0929
α_z	26.81718	25.99266	25.93219
α_x	27.81325	29.54676	29.56438
Az, zz	-107.56880	-108.77857	-108.59122
$A_{x,xz}$	-81.209588	-75.1877857	-75.116286
C_{zz}	208.7490	213.7072	213.3282
C_{xx}	52.3572	103.0669	103.0434
C_{xz}	103.4504	116.3757	117.0246

contraction coefficients on Li and H were taken from the coefficients of the f functions in the HOMO. Energy and static electrical properties are reported in Table 5.3, dispersion constants A, B, C, D in Table 5.4. From the values of dispersion constants we computed the dispersion coefficients displayed in Table 5.5 for the largest spdf basis. The latter are reported in view of their interest as values obtained by an AO basis of higher quality than previously reported data e.g., in [57]. It should be remarked that considerable loss of significant figures occurs in the computation of $C_6^{L_A L_B M}$ and $C_7^{L_A L_B M}$ for high values of $L_A L_B M$.

5.5 Final Remarks

We have described the iterative technique LSDK to compute dispersion constants in the framework of direct CI or similar methods. The technique expands the London formula in a set of pseudostates recursively generated and incorporates ideas taken from the well known Lanczos and Davidson methods for eigenvectors. LSDK proved to be capable to produce results of quality comparable to numerical quadrature of the Casimir Polder integral with less computational cost. The diagonal matrix elements computed by LSDK enjoy variational bounding properties. Finally we applied LSDK to the computation of dispersion constants of Be and LiH using AO bases of high quality.

Table 5.4: Dispersion Constants for LiH computed with Tunega Noga bases [60] and LSDK

	sp (11s8p/9s8p)	spd sp+(6d/6d)	spdf spd+(1f/1f)
Dispersion Constants for $n = 6$			
A	18.195133	17.624843	17.578319
$B = C$	19.515589	19.939737	19.918115
D	20.951796	22.603497	22.614698
Dispersion Constants for $n = 7$			
A	-76.824019	-75.972149	-76.717534
B	-68.268604	-63.238170	-63.152191
C	-82.433586	-86.980019	-86.917175
D	-73.273160	-70.551389	-71.528631

Table 5.5: Expressions of the dispersion coefficients $C^{L_A L_B M}$ for $n = 6; 7$ (a.u.) for LiH computed with Tunega Noga spdf bases

L_A	L_B	M	$C_6^{L_A L_B M}$
0	0	0	125.140
0	2	0	-5.1553
2	0	0	-5.1553
2	2	0	0.7136
2	2	1	-0.1586
2	2	2	0.0200
L_A	L_B	M	$C_7^{L_A L_B M}$
0	1	0	1458.5
0	3	0	78.244
2	1	0	-59.299
2	1	1	9.8832
2	3	0	-2.9532
2	3	1	-0.4922
2	3	2	-0.0352

Chapter 6

Variational CI technique for Dispersion Constants

In this Chapter we will again focus on the first order perturbative equation, we have talked about many times. We can anyway rewrite this equation in a slightly different way as [71]:

$$[(\mathbf{H}_A - E_A^0) \otimes \mathbf{I}_B + \mathbf{I}_A \otimes (\mathbf{H}_B - E_B^0)]\mathbf{\Theta}_{AB} = -\mathbf{q}_A \otimes \mathbf{q}_B \tag{6.1}$$

where $\otimes$ is the matrix Kronecker product $\mathbf{H}_A$ is the matrix of the FCI Hamiltonian of molecule A (and B correspondely), $\mathbf{I}_A$ is the identity matrix of FCI space, and $\mathbf{q}_A$ is the vector of FCI coefficients of $(\hat{Q}_A - E_A^1)|\Phi_A\rangle$ of dimension N_A, Θ_{AB} is the coefficient vector of first order solution in $\otimes$ product space, and consequently $\mathbf{q}_A \otimes \mathbf{q}_B$ is a column vector of dimension $N_A \times N_B$. The previous equation represents a set of linear equations which could, in principle, be treated by standard methods. The main difficulty is due to its dimension, equal to the product of the FCIs of the interacting molecules. In this case, not even a single vector of the $FCI_A \otimes FCI_B$ space can be kept in the computer memory. One can anyway express the solution as

$$\mathbf{\Theta}_{AB} \approx \sum_{ij} c_{ij} \mathbf{z}_{Ai} \otimes \mathbf{z}_{Bj} \tag{6.2}$$

where $\mathbf{z}_{Ai} \in FCI_A$ and $\mathbf{z}_{Bj} \in FCI_B$ are expansion vectors, therefore we overcame the difficulty connected with the vectors dimensions by handling only vectors belonging to the CI space of a single molecule. Next, we may compute the coefficients c_{ij} by some variational criterion of the type used for solving large linear systems, but now applied in a subspace of $FCI_A \otimes FCI_B$. The main criteria to come to a solution are

- projection of the perturbative equation to be solved in that subspace (i. e. Galerkin)

- minimization of the residual norm (least squares)

At this point it is useful to remark that numerical Casimir Polder with integration point $i\omega_k$ and weights w_k may be considered as a particular case of the previous approximate solution, where the expansion vectors are the real part of the solution for the imaginary frequencies $i\omega_k$ perturbative equations and the matrix of the coefficients is assumed to be diagonal and given by

$$c_k = \frac{w_k}{2\pi} \tag{6.3}$$

Therefore, when the Casimir Polder integral is approximated by a numerical quadrature, the coefficients are, in general, nonoptimal, although it is well known that this technique provides good results using 8-16 Gaussian points. This also suggests using the real part of the solution vectors of perturbative equation at the Gaussian points $i\omega_k$ as an effective expansion set. In our variational scheme, we can also include the imaginary parts of the solutions, which is discarded in classical Casimir Polder method. Similarly, another effective expansion set is suggested by the Pade' techniques using the Cauchy moments [62]

$$\mathbf{z}_{Ai} = (\mathcal{H}_A - E_A^0)^{-i}(E_A^1 - \hat{Q}_A)|\Phi_A\rangle \quad i = 1, 2, \ldots, n \tag{6.4}$$

The vectors defined by the previous equation are obtained by solving recursively a set of linear perturbative equations at zero frequency, by plugging the solution of the $i-1^{th}$ equation into the i^{th}. We will consider here only these two types of expansion sets; other types of expansion sets could however be considered.
Once the expansion vectors are given for molecules A and B, we are dealing with four kinds of vector (sub)spaces:

1. FCI spaces of molecules A and B, FCI_A, FCI_B; their dimensions N_A and N_B are large, but vectors belonging to them can be handled by the standard techniques of direct CI

2. Subspace $\mathcal{S}_A$ of FCI_A spanned by the vectors $\mathbf{z}_{Ai}$, $i = 1, \ldots, kA$, with $k_A \ll N_A$. Similarly, for FCI_B

3. Tensor product space $FCI_A \otimes FCI_B$ of dimension $N_A \times N_B$

4. Subspace $\mathcal{S}_A \otimes \mathcal{S}_B$, of dimension $k_A \times k_B \ll N_A \times N_B$, spanned by the tensor products $\mathbf{z}_{Ai} \otimes \mathbf{z}_{Bj}$

6.1 Variational equation for the coefficients

To work out the algebra, it is convenient to adopt a matrix notation for vectors in the tensor product space. Given two ordinary vectors $\mathbf{x}$, $\mathbf{y}$ with components $x_i, \quad i = 1, \ldots, m$ and $y_j, \quad j = 1, \ldots, n$, their tensor product is a two-index object with components $x_i \cdot y_j$ that can be written either as a column of length $m \cdot n$ or as an $m \times n$ matrix. The same holds for a general vector in tensor product space, as it can always be expanded in tensor products. Accordingly, the first-order PT equation in tensor product space can be written in two forms. The first is the one we draw in the previous Section, and the second is the following Sylvester equation:

$$\mathbf{X}_{AB}(\mathbf{H}_A - E_A^0) + (\mathbf{H}_B - E_B^0)\mathbf{X}_{AB} = -\mathbf{q}_B\mathbf{q}_A^\dagger \tag{6.5}$$

where $\mathbf{X}_{AB}$ is $\mathbf{\Theta}_{AB}$ rearranged as a $n \times m$ matrix. The matrix notation suggests a way to compute the residual norm associated with our approximate $\mathbf{X}_{AB}$ via traces of matrices of small dimensions. The Euclidean scalar product between vectors in tensor product space goes into the trace product $Tr(A^\dagger B)$ between the corresponding matrices, and one can exploit the invariance of the trace under cyclic permutation of the factors. Let $k_A \ll N_A$ be the number of expansion vectors $\mathbf{z}_{Ai}$ in space FCI_A and collect them in a matrix $\mathbf{Z}_A$ of dimension $N_A \times kA$; therefore the coefficient equation may be rewritten as:

$$\mathbf{X}_{AB} = \mathbf{Z}_B\mathbf{c}\mathbf{Z}_A^\dagger \tag{6.6}$$

where $\mathbf{c}$ is the $k_A \times k_B$ matric of the coefficients. The associated residual in matrix notation is

$$\mathbf{R} = \mathbf{Z}_B\mathbf{c}\mathbf{Z}_A^\dagger\mathbf{H}_A + \mathbf{H}_B\mathbf{Z}_B\mathbf{c}\mathbf{Z}_A^\dagger + \mathbf{q}_B\mathbf{q}_A^\dagger \tag{6.7}$$

While the residual is a dense matrix of the same dimensions as the FCI Hamiltonians, its square norm $\|\mathbf{R}\|^2$ can be computed as a sum of traces of small matrices. The key point is to exploit the well-known property of the trace:

$$Tr(\mathbf{ABC}) = Tr(\mathbf{BCA}) = Tr(\mathbf{CAB}) \tag{6.8}$$

The norm therefore becomes:

$$\begin{aligned} \|\mathbf{R}\|^2 &= \mathbf{q}_B^\dagger\mathbf{q}_B\mathbf{q}_A^\dagger\mathbf{q}_A + 2Tr(\mathbf{q}_{HZB}^\dagger\mathbf{c}\mathbf{q}_{ZA}) + 2Tr(\mathbf{q}_{ZB}^\dagger\mathbf{c}\mathbf{q}_{HZA}) \\ &+ Tr(\mathbf{H}_{2ZB}\mathbf{c}\mathbf{S}_A\mathbf{c}^\dagger) + Tr(\mathbf{H}_{2ZA}\mathbf{c}^\dagger\mathbf{S}_B\mathbf{c}) + 2Tr(\mathbf{q}_{ZB}^\dagger\mathbf{c}\mathbf{H}_{ZA}\mathbf{c}\dagger) \end{aligned} \tag{6.9}$$

where $\mathbf{S}_A = \mathbf{Z}_A^\dagger\mathbf{Z}_A$ is the overlap $\mathbf{H}_{ZA} = \mathbf{Z}_A^\dagger\mathcal{H}\mathbf{Z}_A$ is the outprojection of $\mathcal{H}_A$ in $\mathcal{S}_A$, $\mathbf{H}_{2ZA} = (\mathcal{H}_A\mathcal{Z}_A)^\dagger(\mathcal{H}_A\mathcal{Z}_A)$ is the outprojection of $\mathcal{H}^2$ in $\mathcal{S}_A$, $\mathbf{q}_{ZA} = \mathbf{Z}_A^\dagger\mathbf{q}_A$ and $\mathbf{q}_{HZA} =$

$\mathbf{Z}_A^\dagger \mathcal{H} \mathbf{q}_A$ (and similarly for B). All matrices are obtained by performing scalar products of FCI vectors available in any code for the computation of second order properties at FCI level. The relative residual norm

$$\frac{\|\mathbf{R}\|}{\sqrt{\mathbf{q}_B^\dagger \mathbf{q}_B \mathbf{q}_A^\dagger \mathbf{q}_A}} \tag{6.10}$$

can be used to check convergence. Unfortunately, the matrices have mixed signs and loss of accuracy can occur in the computation of $\|\mathbf{R}\|^2$.

6.1.1 Coefficient from Galerkin Projection

The projection or Galerkin condition requires the residual $\mathbf{R}$ to be orthogonal to the subspace $\mathcal{S}_A \otimes \mathcal{S}_B$ spanned by the products of expansion vectors; consequently one has to deal with the following equations

$$\mathbf{Z}_A^\dagger \mathbf{R}^\dagger \mathbf{Z}_B = 0 \tag{6.11}$$

$$\mathbf{S}_B \mathbf{c} \mathbf{H}_{ZA} + \mathbf{H}_{ZB} \mathbf{C} \mathbf{S}_B + \mathbf{q}_{ZB} \mathbf{q}_{ZA}^\dagger = 0 \tag{6.12}$$

The second equation is a small Sylvester equation for the coefficients $\mathbf{c}$, the same equation could be obtained by the Hylleras variational principle in the subspace $\mathcal{S}_A \otimes \mathcal{S}_B$ (see [71]). As concerns the methods of solution, a first possibility is via diagonalization of the matrices $\mathbf{H}_{ZA}$, $\mathbf{H}_{ZB}$, in the metrics $\mathbf{S}_A$, $\mathbf{S}_B$ respectively. However, this works only when the metrics are well conditioned; in practice, this applies only to a very small number of expansion vectors. After some experiments, the following procedure was adopted: we orthonormalize the basis within each subspace $\mathcal{S}_A$, $\mathcal{S}_B$ and then compute the matrices $\mathbf{H}_{ZA}$, $\mathbf{H}_{ZB}$ by performing a FO $(\mathcal{H} - E^0)\mathbf{z}_i$ in the FCI space for each (orthogonalized) expansion vector. Compared with the numerical integration, this is an additional computational cost, but much smaller than that needed to compute the expansion vectors. The latter equation is reduced to an ordinary Sylvester equation and we can use one of the well-known methods for small Sylvester equations, e.g., the Bartels and Stewart algorithm [68]. Alternatively, we transform the (small) Sylvester equation in a system of $k_A k_B$ linear equations. Thus, we are able to include many more expansion vectors, and therefore to approach more closely the exact solution of the perturbative equation.

6.1.2 Coefficients from the Least Square Condition

The Least Square (MinRes) condition requires the residual norm $Tr(\mathbf{R}^\dagger \mathbf{R})$ to be minimal, in this case however the residual vector $\mathbf{R}$ will no longer be orthogonal to the subspace

$\mathcal{S}_A \otimes \mathcal{S}_B$, the equation for the coefficient will be:

$$\mathbf{S}_B\mathbf{c}\mathbf{H}_{2ZA} + 2\mathbf{H}_{ZB}\mathbf{c}\mathbf{H}_{ZA} + \mathbf{H}_{2ZB}\mathbf{c}\mathbf{S}_A + \mathbf{q}_{ZB}\mathbf{q}^{\dagger}_{ZA} + \mathbf{q}_{HZB}\mathbf{q}^{\dagger}_{HZA} = 0 \tag{6.13}$$

By the use of this expression we still obtain an upper bound to the exact FCI solution and we have

$$Exact \leq \mathbf{c}^{Galerkin} \leq \mathbf{c}^{MinRes} \tag{6.14}$$

as a consequence of the Hylleras principle. As concerns the numerical aspects of the solution, the same consideration applied to the Galerkin equation apply in this case, and once the expansion bases are orthonormalized the solution can be obtained via the use of a system of $k_a k_B$ linear equations.

6.2 Result for BH and Comparison of the Methods

Our variational method has been used in the FCI determination of dispersion coefficients for the BH molecule, in the same study a comparison with the interpolative method was also performed. To perform the study we used two atomic basis sets the first one being the so called b5 basis (89 A.O.) [71] and the second one the double augmented v5Z (daug-v5Z) of Dunning and coworkers [80, 81, 82] (268 A. O.), the latter in particular was retrieved by EMSL [83].

6.2.1 The b5 basis

As concerns the b5 basis we acted as follows:

- Frozen Core ($1s^2$) FCI computations, FCI space $3.7 \cdot 10^6$ determinants in C_{2v} symmetry group, (part of the computations at this level have allready been performed in [71])
- String Truncated CI computation [86], CI space $104 \cdot 10^6$ determinants, using the following truncation scheme:
  - 2 molecular orbital (MO) are kept in core allowing double excitations
  - 11 MO are kept fully active
  - 19 MO are allowed to undergo double excitations
  - 57 MO are allowed to undergo single excitations
- Frozen Core Coupled Cluster at CCSD level

Table 6.1: BH energies and static electric properties computed using b5 basis. E is the energy, μ is the dipole moment, $\alpha_{\parallel}$ and $\alpha_{\perp}$ the parallel and perpendicular component of the polarizability respectively.

	String Trunc. CI	Froz. Core FCI	Full Elect. CCSD	Froz. Core CCSD
E	-25.2490099	-25.23565361	-25.2514139	-25.2327909
μ	0.54382346	0.543885412	0.55914219	0.55399204
$\alpha_{\parallel}(0)$	23.016370	23.1779437	22.800214	22.8732838
$\alpha_{\perp}(0)$	20.637134	20.7647977	21.0325375	20.9871151

- Full Electron Coupled Cluster at CCSD level

Results for energies and static electric properties obtained at this level of theory are collected in Table 6.1 As a first evidence one can see how the frozen core effect for the energy appears to be quite important for this particular system, while first and second order electric properties are affected to a much lesser extent, this fact justify our choice to subsequently perform a Frozen Core FCI calculation with a larger expansion basis set. CCSD dipole moments are larger than the corresponding CI values, on the other hand the parallel component of the polarizability is greater at CI level while the perpendicular components shows an opposite behavior. Our electric properties values can be compared with the ones given by Halkier and coworkers [72, 73]. At Coupled Cluster level we determined the values of imaginary frequencies polarizabilities by the $[3,4]$ Pade' approximants [62] using the Cauchy moments calculated with the Dalton code [19]. Results are collected in Table 6.2. The frequency dependent polarizabilities have also been determined at Frozen Core FCI level and String Truncated CI level with perturbation theory formalism and by $[3,4]$ Pade' approximants in the case of Frozen Core CI, these results are collected in Table 6.3. Frequencies $i\omega$ were chosen in such a way to fulfill the empirical criterion for interpolative method we gave in [57]. Using the Pade' approximants to the dynamic polarizabilities obtained at CCSD and Frozen Core FCI level we computed the BH Dispersion Constants via the interpolative procedure [53, 57], results are presented in table 6.4 Finally The Dispersion Constants were computed using the variational method at Frozen Core FCI and String Truncated CI level. In particular as expansion vectors we used the Real and Imaginary solution of the perturbative equations for the polarizability (the frequencies being the ones chosen for the interpolative technique) results are displayed in Table 6.5 for Frozen Core FCI and 6.6 for String Truncated CI together with the value of the Dispersion Constants

Table 6.2: BH CCSD frequency dependent polarizabilities from [3, 4] Pade' approximants and Cauchy moments

$i\omega$	$\alpha_{\parallel}(i\omega)$	$\alpha_{\perp}(i\omega)$	$\alpha_{\parallel}(i\omega)$	$\alpha_{\perp}(i\omega)$
	FULL CCSD		Froz. Core CCSD	
3.000000	0.39722	0.31415	0.39375	0.31273
1.000000	2.91887	2.39986	2.90452	2.39330
0.333333	11.81269	9.56384	11.81726	9.57000
0.000000	23.01637	20.63713	23.17794	20.76480

Table 6.3: BH Frozen Core FCI and String Truncated CI frequencies dependent polarizabilities

	String Trunc CI		Frozen Core			
	Directly Computed		Directly Computed		Pade'[3,4]	
$i\omega$	$\alpha_{\parallel}(i\omega)$	$\alpha_{\perp}(i\omega)$	$\alpha_{\parallel}(i\omega)$	$\alpha_{\perp}(i\omega)$	$\alpha_{\parallel}(i\omega)$	$\alpha_{\perp}(i\omega)$
3.000000	0.440486	0.415979	0.41777	0.397691	0.39406	0.35895
1.000000	2.977717	2.643298	2.9312	2.62848	2.90626	2.57833
0.333333	11.886704	9.571361	11.87538	9.56055	11.87524	9.55989
0.000000	23.016370	20.637134	23.17794	20.76480	23.17794	20.76480
7.000000	0.093441	0.090328	//	//	//	//
1.666667	1.266689	1.163044	//	//	//	//
0.600000	6.244658	5.314824	//	//	//	//
0.142857	19.289442	15.227911	//	//	//	//

Table 6.4: CCSD and Frozen Core FCI Dispersion Constants computed from Pade' approximant to the polarizability by the interpolation approach

	Full Elect. CCSD	Frozen Core CCSD	Frozen Core FCI
$D_{\parallel,\parallel}$	23.0307	23.1790	23.2947
$D_{\parallel,\perp}$	19.1660	19.2608	19.7090
$D_{\perp,\perp}$	15.9755	16.0309	16.7013

Table 6.5: BH Frozen Core FCI Dispersion Constants. M.F. stands for Magnasco Figari interpolative technique, Int. J. stands for our variational technique, 4 pt. indicates that only the first subset of the frequencies dependent polarizability has been used, [Re] indicates the use of the real part of the perturbative equation solution, [Im] the use of the imaginary part and [Re] + [Im] the use of both, $\|\mathbf{R}\|$ is the residual norm

	M.F. 4 pt	Int. J. 4 pt [Re]		
		Low. Bound	$\|\mathbf{R}\|$	Upp. Bound
$D_{\parallel,\parallel}$	23.3763	23.2497	$0.4 \cdot 10^{-2}$	23.4680
$D_{\parallel,\perp}$	19.9263	19.1895	$0.1 \cdot 10^{-1}$	20.4240
$D_{\perp,\perp}$	17.01171	15.88715	$0.2 \cdot 10^{-1}$	18.6087

	//	Int. J. 4 pt [Re]+[Im]		
		Low. Bound	$\|\mathbf{R}\|$	Upp. Bound
$D_{\parallel,\parallel}$	//	23.1635	$0.8 \cdot 10^{-5}$	23.1639
$D_{\parallel,\perp}$	//	19.16325	$0.6 \cdot 10^{-5}$	19.1636
$D_{\perp,\perp}$	//	15.88935	$0.4 \cdot 10^{-5}$	15.8896

obtained with the application of the interpolative technique itself. In table 6.5 and 6.6 we have indicated upper and lower bound values of Dispersion Constants, lower bound has to be intendended as the value directly obtained from the variational method, while upper bound is the value obtained from Temple's VP extended to perturbation theory [74]

$$Exact_{FCI} \leq < {\mu_1}^A {\mu_2}^B | {\mu_1}^A {\mu_2}^B > + \frac{\|\mathbf{R}\|^2}{E_{exc} - E_0} \tag{6.15}$$

where E_{exc} is the $1^s t$ excited level (of appropriate symmetry), and $\|\mathbf{R}\|$ is the residual norm of the variational equation. As a first approximation we used only the Frozen Core FCI excitation energies for state Σ ($\hat{\mu}_\parallel$ operator) and Π ($\hat{\mu}_\perp$) which are respectively

- $E_\Sigma - E_0 = 0.21287256$
- $E_\Pi - E_0 = 0.10652291$

Rigorously speaking lower and upper bound should be referred to Temple's VP and variational value respectively, but because the value of the dispersion constants would have negative sign we have exchanged the two terms in order to avoid confusion. From the

Table 6.6: BH String Truncated CI Dispersion Constants. M.F. stands for Magnasco Figari interpolative technique, Int. J. stands for our variational technique, 4 pt. indicates that only the first subset of the frequencies dependent polarizability has been used, [Re] indicates the use of the real part of the perturbative equation solution, [Im] the use of the imaginary part and [Re] + [Im] the use of both, $\|\mathbf{R}\|$ is the residual norm

	M. F. 4 pt	Int. J. 4pt [Re]		
		Low Bound	$\|\mathbf{R}\|$	Upp. Bound.
$D_{\parallel,\parallel}$	23.2972	23.1627	$0.5 \cdot 10^{-2}$	23.4347
$D_{\parallel,\perp}$	19.8795	19.1603	$0.1 \cdot 10^{-1}$	19.6388
$D_{\perp,\perp}$	16.9892	15.8848	$0.2 \cdot 10^{-1}$	17.3760

	//	Int. J. 4 pt [Re]+[Im]		
	//	Low. Bound	$\|\mathbf{R}\|$	Upp. Bound
$D_{\parallel,\parallel}$	//	23.1635	$0.1 \cdot 10^{-2}$	23.2179
$D_{\parallel,\perp}$	//	19.1633	$0.2 \cdot 10^{-2}$	19.2833
$D_{\perp,\perp}$	//	15.8893	$0.2 \cdot 10^{-2}$	16.0385

previous data it easy to see how dynamic polarizabilities computed by the Pade' approximants differs from the analytical perturbative values by some percents, expecially for values of $i\omega$ far from the real axes. (At Frozen Core FCI level the error on the perpendicular component of the polarizabilities goes from $6.0 \cdot 10^{-3}\%$ at $i\omega = 0.333$ to 10% at $i\omega = 3.0$). As the Dispersion Constants are concerned the values computed by the interpolative method using the Pade' approximants and using the analytical polarizabilities at the same level of theory the error ranges from 0.5% for $D_{\parallel,\parallel}$ to 1.8% for $D_{\perp,\perp}$. Finally we may underline that between the 4 points interpolative and variational methods there is a substantial agreement if one excludes the value of the total perpendicular constant $D_{\perp,\perp}$, moreover the inclusion of the imaginary part of the solution vector in the variational expansion basis has little influences on the value of the constant itself, but has an important effect on the residual norm.

6.2.2 The v5Z basis

As the v5Z (268 AO) basis is concerned we performed the following computation

- Frozen Core ($1s^2$) FCI giving rise to $316 \cdot 10^6$ determinants in C_{2v} symmetry group.

Table 6.7: BH v5Z basis Frozen Core FCI and CCSD energies and static electric properties, E is the energy, μ is the dipole moment and $\alpha_{\parallel}$ and $\alpha_{\perp}$ are the parallel and perpendicular component of the polarizability respectively

	Frozen Core FCI	CCSD	Frozen Core CCSD
E	-25.236833	-25.263980	-25.234065
μ	0.546760	0.563512	0.556943
$\alpha_{\parallel}(0)$	23.18200	22.75254	22.86952
$\alpha_{\perp}(0)$	20.54835	21.04137	21.01354

Table 6.8: BH v5Z Frozen Core FCI frequencies dependent polarizability

$i\omega$	$\alpha_{\parallel}(i\omega)$	$\alpha_{\perp}(i\omega)$
3.000000	0.417679	0.425199
1.000000	2.927977	2.791326
0.333333	11.86931	9.99817
0.000000	23.18200	20.54835

- Frozen Core and Full Electron CCSD

In table 6.7 we collected energies and static electric properties obtained from this basis. In Table 6.8 and 6.9 we present the frequency dependent polarizabilities obtained analytically at Frozen Core FCI level, and as the Frozen Core and Full Electron CCSD [3, 4] Pade' approximants by the Cauchy moments respectively. Again the frequencies $i\omega$ have been chosen in such a way they respect our empirical formula [57], but due to the dimension of the CI space, and to the computational cost required for each iteration we limited only to the first 4 frequencies subgroup. Finally in Table 6.10 we reported the Dispersion Constants computed at Frozen Core FCI level by the interpolation method and by the variational method using the solutions of the polarizability perturbative equations as the expansion basis; while in table 6.11 dispersion constants obtained by the interpolative method at CCSD and Frozen Core CCSD are shown too. As concerns the derivation of the Temple's upper bound to the dispersion constants we did not calculate the actual value of the BH excitation energy with the v5Z AO basis, we used instead the values of excitation energies obtained at Forzen Core FCI with the b5 AO basis. This choice is due to the very high computational cost of Frozen Core FCI

Table 6.9: BH v5Z Frozen Core and Full Electron CCSD [3,4] Pade' approximants to the frequencies dependent polarizability

$i\omega$	$\alpha_{\parallel}(i\omega)$	$\alpha_{\perp}(i\omega)$	$\alpha_{\parallel}(i\omega)$	$\alpha_{\perp}(i\omega)$
	Full Electrons		Frozen Core	
3.000000	0.39629	0.31388	0.39262	0.31243
1.000000	2.91416	2.39838	2.89972	2.39209
0.333333	11.79640	9.55320	11.81187	9.56683
0.000000	22.75254	21.04137	22.86952	21.01354

Table 6.10: BH v5Z Frozen Core FCI dispersion constants. M.F. stands for Magnasco Figari interpolative technique, Int. J. stands for our variational technique, 4 pt. indicates that only the first subset of the frequencies dependent polarizability has been used, [Re] indicates the use of the real part of the perturbative equation solution, [Im] the use of the imaginary part and [Re] + [Im] the use of both, $\|\mathbf{R}\|$ is the residual norm

	M. F. 4 pt	Int. Journ. 4 pt		
		Low. Bound	$\|\mathbf{R}\|$	Upp. Bound
$D_{\parallel,\parallel}$	23.3676	23.2384	$0.5 \cdot 10^{-3}$	23.2657
$D_{\parallel,\perp}$	20.3078	19.6496	$0.2 \cdot 10^{-2}$	19.7696
$D_{\perp,\perp}$	17.6658	16.6541	$0.8 \cdot 10^{-3}$	16.7161

with the v5Z AO basis, and is however justified by the fact that this approximation will lead to a (probably negligible) overestimation of the upper bound.

6.2.3 Concluding Remarks

Coupled Cluster and FCI (or string truncated CI) calculations of the BH dispersion coefficients have been performed with a very high level basis set (268 A.O.). In the meantime two innovative methods, derived or commonly applied in our laboratory, have been tested and validated. In particular as concerns the variational method it enjoys bounding properties both on the upper and lower side. By expanding the solution as a linear combination of tensor products of CI vectors of the isolated molecules, we are able to work in the huge dimensional tensor product space of the interacting molecules. A convenient matrix notation makes the algebra easier and suggests a way to compute

Table 6.11: BH v5Z CCSD Dispersion Constants from [3, 4] Pade' approximants and 4 points interpolative method

	Full Electron CCSD	Frozen Core CCSD
$D_{\parallel,\parallel}$	22.7450	22.8706
$D_{\parallel,\perp}$	19.1470	19.1908
$D_{\perp,\perp}$	16.1590	16.1406

the residual norm in order to check convergence. The present calculations as well as the results presented in [71] indicate that this new techniques allow for better accuracy than with numerical Casimir Polder or interpolative procedures for a comparable computational cost.

Chapter 7

The BSSE: A test study on the Neon dimer

We will present in this Chapter a detailed study [75] of the influence of BSSE in the determination of Long Range Dispersion Coefficients, comparing this approach with the perturbative one. In particular we will examine how the use of Counterpoise Correction affect the behavior of CI and CC methods, expecially in connection with size consistency problem.

7.1 Introduction

On both the theoretical and the experimental sides, the interest of chemists and physicists in clusters involving rare-gas atoms increases [76, 77, 78]. In order to be able to perform simulations on medium-size clusters, very accurate two-body potentials are needed. These potentials can be conveniently computed by using high-level quantum-chemistry algorithms on Rare-gas (Rg) dimers, Rg_2. Because of the smallness of the interaction, a very accurate value of the asymptotic limit of the potential energy curve is extremely important. Since Rg_2 dimers are closed-shell systems that dissociate into two closed-shell atoms, a single determinant gives a qualitatively correct description of the dimer for any value of the internuclear distance. For this reason, single-reference methods can be successfully used even in the dissociation region, contrary to what happens for most chemical systems. In this context, one must be very cautious towards truncated Configuration-Interaction (CI) methods, as they suffer from the well known Size-Consistency (SC) problem. On the other hand, Coupled-Cluster methods are Size Consistent and therefore they are not affected by this kind of problems.

In order to obtain accurate values of the potential-energy curves, it is absolutely necessary to take into account the Basis-Set Superposition Error (BSSE), and to accordingly modify the energy values. BSSE arises because the Wave Function (WF) of the dimer at finite internuclear distance is better described than the WF of the separated atoms, since the orbitals *of the two atoms* are simultaneously used. For this reason, BSSE is particularly important for small or medium-size basis sets, while it goes to zero in the limit of complete basis sets.

As we said previously, the most diffuse procedure to overcome this problem is the use of the Counterpoise Correction, proposed by Boys and Bernardi [16]. In this procedure, a series of atomic energies are computed, by using a basis set ($\mathbf{b}_t$) composed of the atomic orbitals of all the atoms of the system, and the differences between these energies and the atomic values are subsequently used to correct the energy surface of the system. In other words, the energy $E(\mathbf{b}_t)$ of the complex, computed by using the basis set $\mathbf{b}_t$ is corrected by adding a geometry-dependent energy shift Δ, which is given by

$$\Delta \;=\; \sum_I \Delta_I \tag{7.1}$$

where I labels the atoms in the complex

$$\Delta_I \;=\; E_I(b_I) - E_I(b_t) \tag{7.2}$$

Here $\mathbf{b}_I$ represents the atomic basis set of the atom I, while $\mathbf{b}_t$ is the total LCAO basis, given by the union of all the atomic basis sets. This procedure, although not an exact one, give a satisfactory approximation and leads to a satisfactory approximation to the BSSE In the present Chapter, the effect of the BSSE on the calculation of Dispersion Coefficients at Configuration-Interaction (CI) and Coupled-Cluster (CC) level is investigated. As already well known, the BSSE must be corrected in order to obtain reliable potential-energy curves of van der Waals (VdW) systems. However, although the BSSE-corrected curves obtained by the different methods are at first sight qualitatively rather similar, CI and CC methods show very different behaviors as far as the Long Range Dispersion Coefficients are concerned [75]. Indeed, we found that, while CC approaches are well adapted for this type of calculations, the corresponding truncated-CI values are completely useless. The reason for this striking difference can be traced back to the lack of Size Consistency of the truncated-CI methods.

Our dimer calculations were compared with Full-CI (FCI) results obtained on a single atom by means of our perturbative scheme we have diffusely illustrated in the previous Chapter. In our largest FCI calculation, the CI space contains more than one billion of partly symmetry-adapted and spin-adapted Slater determinants. This represents, to the

best of our knowledge, by far the largest calculation of second-order properties ever done at Full-CI level.

7.2 Computational Details

In the present section, the basis sets and computational methods, that have been used in [75], are described. The use of the interface Q5COST between different computational codes is also illustrated and discussed.

7.2.1 Basis sets

As already stated several times in this thesis the computation of molecular dispersion interaction is very sensitive to the quality of the computed polarizabilities of the constituent atoms. These properties are, on their turn, critically dependent on the quality of the basis sets, and in particular on the presence of diffuse atomic orbitals. For this reason, diffuse orbitals are usually added to the standard atomic basis sets in these circumstances. Unfortunately, this fact can have the consequence of an even larger effect on the BSSE. Some authors [79] report the use of the so called mid-bond functions, instead of diffuse ones for the computation of Neon dimer potential energy curve; we decided to discard this possibility mainly in order to use the same basis set in supramolecular and long range perturbative approach. The calculations are performed with the Correlation Consistent basis sets, optimized by Dunning and coworkers [80, 81, 82]. In particular, the following two basis sets, retrieved from the Pacific Northwest Laboratory basis set library EMSL [83] have been used: triply-augmented valence double-zeta (taug-vDZ). and quadruply-augmented valence triple-zeta (qaug-vTZ). Since these are valence basis sets, it does not make sense to correlate core electrons, and in all the correlated computations the $1s$ orbitals of the two Neon atoms have been kept frozen at Hartree Fock level. This fact presents also the advantage of a considerable saving in computation time.

7.2.2 Computational Methods

The following methods have been used in the present study:

1. Long Range Perturbative Approach (LRPT) where the atom-atom interaction [1] is treated by perturbation theory starting from the product of isolated fragments wave functions.

   The adopted computation strategy was the following: Using Full or String Truncated CI formalism it is possible to immediately get the values of the Dispersion

Coefficients via the use of our laboratory's innovative perturbation-variational formalism [71]. Note that this technique involves only the use of isolated atoms wave functions, so values obtained can be considered as BSSE free and size consistent by construction. Moreover values of Neon atom dipole and quadrupole polarizabilities are obtained as byproducts. The formalism involved implies solving the perturbative equations for the dispersion interaction by expanding the solution as a linear combination of tensor products of suitable FCI vectors. In the present computation the latter where chosen to be the so called Cauchy vectors [71] strictly related to the FCI computation of Cauchy moments. An expansion set of ten Cauchy vectors provided satisfactory convergence. Both Full-CI (FCI) and string-truncated CI calculations were obtained with the use of the program VEGA [84] Molecular orbitals and their integrals were computed with the MOLPRO2000 code. [85]

In the String-truncated CI formalism [86], the determinants formed by strings having up to a given level of excitation are retained in the CI space: single excitations (CIS), single and double excitations (CISD), single, double and triple excitations (CISDT). Notice that, if up to quadruply excited strings are considered (CISDTQ), in the case of the Neon atom, one gets Frozen-Core FCI.

2. Supramolecular Approach. In this approach potential energy curves for the Ne_2 dimer are computed using:

   (a) Single-and-Double Truncated CI, CISD, program CASDI [87].

   (b) Single-and-Double Truncated CC, CCSD, DALTON package [19].

   (c) Single-and-Double Truncated CC with non iterative triple correction, CCSD(T), DALTON package [19].

At CISD, CCSD, CCSD(T), the energy curve has been obtained performing energy computation at various values of interatomic separation, the curve has been subsequently counterpoise corrected, and linearized as described in the next Section in order to get the values of Dispersion Coefficients. From the energy curves we also derived values of minimum energy distance, well depth energy, zero points energy and anharmonic vibrational frequency. As concerns the vibrational levels, the computations were performed by the Numerov method [88] in matrix form as formulated by Lindberg [89] implemented in a code described in [90]

7.2.3 The use of Q5Cost wrappers

CASDI program used for the computation of CISD energy curves was originally interfaced with Molcas [91] program suite via the wrapper MOLCOST. In order to perform such a computation in the same environment as CC ones we decided to interface CASDI with DALTON, using the new developed Q5Cost data format [92] and library [93]. Q5Cost, as we will diffusely illustrate in the next part of this thesis, is a new data format and Fortran libraries developed by us, that allows the easy exchange of the so called "Quantum-Chemistry Binary Data" (mainly molecular integrals) among different codes. In particular, for this work, atomic basis integral produced by Dalton [19] after SCF calculations were processed with a four indices transformation to get them in molecular orbitals basis and written in Q5Cost format. Subsequently an interface or wrapper (Q5MOLCOST) was designed and written in order to write molecular orbitals in a MOLCOST format directly accessible by CASDI program.

7.3 Results

In Figure 7.1 (a and b), the potential energy curves are reported, for the different correlated methods and obtained by using the two basis sets. The CISD, CCSD, and CCSD(T) curves are rather similar. It can be seen that the position of the minimum is not strongly affected by the BSSE correction, while the energy-well shape and depth are completely changed by the BSSE.

The curves obtained by using the VDZ (Figure 7.1.a) and VTZ (Figure 7.1.b) are extremely similar, a fact that indicates that the BSSE converges very slowly to zero as a function of the basis-set size, probably due to the presence of diffuse functions [94] (we remind that BSSE vanishes for a complete basis set). In Table 7.1, BSSE incorrect and correct equilibrium distance and energy well depth are reported together with the zero point energy, the number of vibrational bound states and the anharmonic vibrational frequency, determined after counterpoise correction. Again this parameters show the same behavior as the ones previously described.

In Figure 7.2 (a and b), the same curves are displayed, relatively to the asymptotic region (from 12.0 to 20.0 Bohr). Again, the curves obtained by using the VDZ (Figure 7.2.a) and VTZ (Figure 7.2.b) are very similar, but it appears now that the behavior of CI is extremely different than CC.

As discussed in this Chapter's introduction, the leading terms of the asymptotic energy are given by the equation

$$E(R) = E_\infty + C_6 R^{-6} + C_8 R^{-8} \tag{7.3}$$

By multiplying this expression by R^8 and rearranging the different terms, one gets

$$(E(R) - E_\infty)R^8 = C_6R^2 + C_8 \tag{7.4}$$

This means that, if one plots the quantity $(E(R) - E_\infty)R^8$ as a function of R^2, the result should be a straight line for large values of R. The results of these plots are shown in Figure 7.3, for four different cases: uncorrected CI and CC (7.3.a), and BSSE-corrected CI (7.3.b) and CC (7.3.c). It is clear that, in the case of uncorrected energies, either CI or CC, the long range curves are far from being straight lines. This implies that the BSSE completely masks the correct long-range behavior of the potential energy for this VdW species. On the other hand, once the BSSE has been corrected, the CC results (either CCSD or CCSD(T)) have a correct linear behavior. Rather surprisingly, however, this is not true for the CISD results, as it could have been guessed from the long-range tail of the potential, Figure 7.2. Using a linear least square regression it was possible to obtain values of the Dispersion Coefficients from the Coupled Cluster, BSSE correct, potential curves: results are collected in table 7.2. These values can be compared with the results obtained from LRPT treatment, and with experimental ones, reported again in table 7.2. Moreover in table 7.2 computed or experimental values of polarizabilities are presented too.

7.4 Discussion

Two main aspects can be underlined from the analysis of the data: The long range behavior of the potential energy curves with the determination of Dispersion Coefficients, in particularly for the failure of CISD; and the determination of spectroscopic properties from the analysis of the equilibrium region of the curves.

7.4.1 Dispersion Coefficients: The failure of CISD

The remarkable difference in the long-distance part of potentials that are overall substantially similar is rather unexpected. The reason can be traced back to a subtle interplay between two different sources of error that affect CI calculations: Basis-Set Superposition Error and Size-Consistency Error (SCE). SCE originates from the fact that, in truncated CI calculation, determinants that are present in the product of monomer WF are absent in the dimer WF. For this reason, the CISD energy of two fragments separated by such a large distance, that they are physically non-interacting is different from the sum of the CISD energies of the isolated fragments. The SC error is far from being negligible: in fact, the CISD energy of two non-interacting neon atoms is about 0.15

hartree higher than the sum of the corresponding energies of isolated atoms. However, the SCE depends only weakly on the geometry: once the BSSE has been taken into account via the counterpoise correction, the CISD values for the equilibrium distance and dissociation energy are in a reasonable accord with the corresponding CCSD values (which are SC-error free) and also in a reasonable accord with the experimental [95, 96] and previously computed values [97, 98]. For this reason, CISD can be used to compute the spectroscopic quantities of a VdW dimer as Ne_2, although the results are certainly less accurate than those obtained from CCSD, and much less accurate than CCSD(T). As expected the use of diffuse functions appears to be of great importance to improve the computation of dispersion interactions, as an example we can consider the Ne_2 CISD BSSE corrected energy well depth computed with vDZ basis set during a preliminary study: in that case a value of about 30 μh was obtained to be compared with 83.5 μh for taug-vDZ (experimental value 134 μh).

Let us consider now the dispersion coefficients. Before being corrected to take into account the BSSE, the long-range tail of the potential-energy curves gives absolutely unreliable results. Once the BSSE has been taken into account via the CP correction, the CC curves fit very well into the long-range expression, and the values of the dispersion coefficients are in a good agreement with both the FCI and experimental ones. The situation is completely different for the CISD calculations, that cannot be fitted with the theoretical expression at large distance. In this case, the CP correction overcorrects the energy values, that become even higher than the corresponding asymptotic values. This is because the CP correction is extracted from **atomic** calculation, while it is used to correct **molecular** energies. The (relatively small) error due to the lack of size consistency of CI results has a dramatic effect on the long-range tail of the potential-energy curves. In fact, the sum of the atomic energies is larger than the energy of non-interacting atoms, giving therefore a too large correction. For this reason, the CP correction **overestimates** the effect of BSSE, thus giving a long-range tail of the potential that is completely unnatural.

7.4.2 Spectroscopic Properties

As the spectroscopic properties are concerned, as already stated, our values can be compared with a recent experimental work by Wüest and Merkt [96]. In that paper the authors determine the position of rovibrational energy levels of the Ne_2 dimer using vacuum ultraviolet laser spectroscopy. The potential curve for the ground electronic state was subsequently determined by means of a nonlinear fitting of a model interaction potential to the measured position of the rovibrational levels. It is quite interesting to see how the zero point energy level lies very high in energy, in fact it accounts for

about 40% of the well depth, leading to a very low binding of the complex; this fact is anyway confirmed by experimental results. Moreover Wüest and Merkt [96] observe only two vibrational levels, in agreement with our results, but from the analysis of the potential they predict the existence of a third vibrational level with a very low binding energy. The existence of this level is anyway still uncertain and depends strongly from the energy well depth and from the form of the long range tail of the potential due to the high diffuse nature of the vibrational Wave Function. The computed spectroscopic properties can be improved towards the basis set limit using a two point basis set extrapolation formula [99]. Applying this formula to the CCSD(T) BSSE corrected results we obtain $E_{min} = -130\mu h$, $R_{min} = 5.82 bohr$, $\Delta E_0 = 12.38\mu h$ and $\omega = 13.5 cm^{-1}$

7.5 Final Considerations

It has been shown that the BSSE plays a key role in the numerical calculation of the dispersion coefficients of VdW species. No reasonable value of Dispersion Constant or equilibrium properties can be obtained for the Ne_2 dimer if one does not take into account the BSSE correction. The use of Counterpoise Correction allows to obtain satisfactory results provided one uses size consistent methods for the computation of the potential energy curves of the dimer. Values obtained in such a way with CCSD or CCSD(T) agree quite well with experimental values and with the BSSE-free LRPT values. On the other hand, the application of the Counterpoise Correction to curves obtained with non size consistent methods gives quite good values for the equilibrium properties but totally wrong Dispersion Coefficients. This fact is due to a subtle interplay between Basis-Set-Superposition and Size-Consistency Errors. By using the potential energy curves obtained at CI and CC level, we computed the Zero-Point energy and the anharmonic vibrational frequency for the fundamental electronic state of Ne_2, showing the existence of two bound vibrational states, our results agree quite well with spectroscopic experiments.

Table 7.1: CISD, CCSD, CCSD(T), BSSE counterpoise uncorrected and corrected Minimum and vibrational frequencies: R_{min}^{uncorr} interpolated value of the BSSE uncorrected energy curve minimum (a_0 bohr); E_{min}^{uncorr} BSSE uncorrected potential energy well depth (μE_h); R_{min}^{corr} interpolated value of the BSSE corrected energy curve minimum (a_0 bohr); E_{min}^{corr} BSSE corrected potential energy well depth (μE_h); N_{bs} number of bound states for BSSE corrected curves; ΔE_0 Zero point energy calculated from the BSSE corrected well depth (cm^{-1}); ω anharmonic vibrational frequency from BSSE corrected curves (cm^{-1}).

	R_{min}^{uncorr}	E_{min}^{uncorr}	R_{min}^{corr}	E_{min}^{corr}	N_{bs}	ΔE_0	ω
taug-VDZ							
CISD	5.7025	-456.71	6.3037	-52.675	1	7.2243	//
CCSD	5.6862	-475.50	6.2454	-70.022	2	8.2618	6.6990
CCSD(T)	5.6527	-540.83	6.1741	-83.488	2	9.1751	8.3160
qaug-VTZ							
CISD	5.7514	-461.30	6.0995	-71.563	2	8.5749	6.9332
CCSD	5.7188	-490.46	6.0157	-93.766	2	9.9941	9.4897
CCSD(T)	5.6518	-521.52	5.9269	-116.44	2	11.430	11.960
Experiment							
[95]			5.84	-134	//	//	//
[96][1]			5.85	-134	2	12.56	13.76

Table 7.2: Ne atom, taug-VDZ and qaug-VTZ basis set: Full and String-Truncated CI Properties and Dispersion Coefficients. Dispersion Coefficient interpolated from BSSE corrected potential energy curves. N_{CI} is the number of CI determinants in D_{2h} symmetry point group; E is the total energy of the atom (E_h hartree); α_{dip} is the dipole polarizability (atomic units a_0^3 where a_0 bohr); α_{quad} is the quadrupole polarizability (atomic units a_0^5); C_6 and C_8 are the R^{-6} and R^{-8} dispersion coefficients, respectively ($E_h a_0^6$, $E_h a_0^8$). When available, the experimental, or previous computed best values are also reported.

	N_{CI}	E	α_{dip}	α_{quad}	C_6	C_8
taug-vDZ						
CIS	$2.929{\cdot}10^3$	-128.663720	2.436792	3.097065	-5.9899	-7.2528
CISD	$1.926{\cdot}10^6$	-128.708024	2.649742	3.605931	-6.3270	-19.4611
CISDT	$1.319{\cdot}10^8$	-128.709878	2.680308	3.666439	-6.3996	-19.7892
FCI	$1.044{\cdot}10^9$	-128.709923	2.680788	3.667532	-6.4008	-19.7955
qaug-vTZ						
CI-sd	$7.100{\cdot}10^7$	-128.810697	2.649	7.005	-6.354	-35.550
Interpolated	taug-vDZ					
CCSD	//	//	//	//	-5.8849	-21.9760
CCSD(T)	//	//	//	//	-6.5433	-28.4863
Interpolated	qaug-vTZ					
CCSD	//	//	//	//	-6.1717	-37.4064
CCSD(T)	//	//	//	//	-7.1054	-37.8797
Experiment[100, 101]	//	//	2.669	7.52	-6.383	//

Figure 7.1: The CISD, CCSD, CCSD(T) potential-energy curves as a function of the inter-nuclear distance. 1a: taug-vDZ, 1b: qaug-vTZ. Units: distances in bohr and energies in hartree

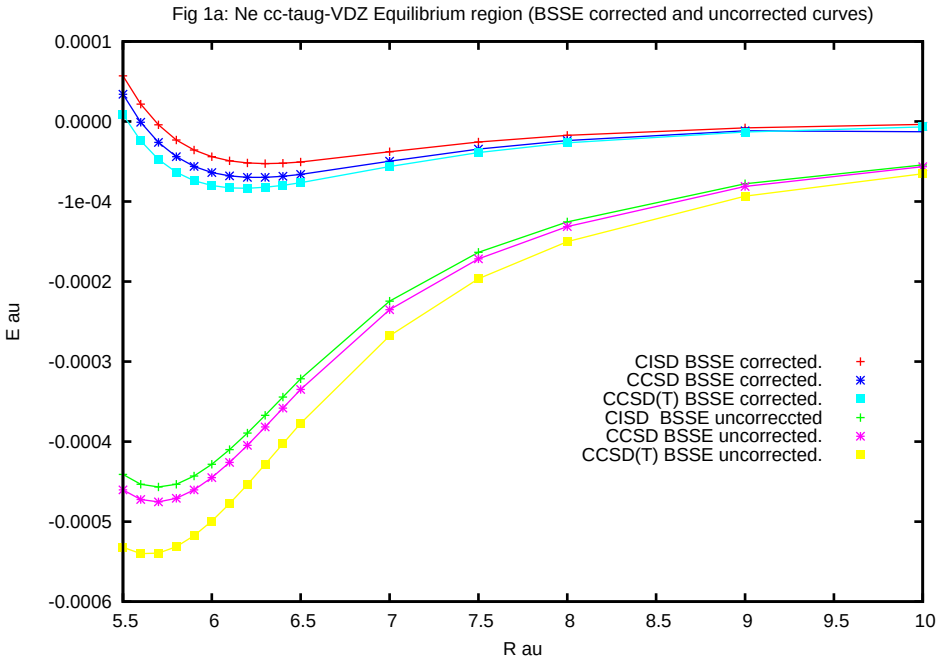

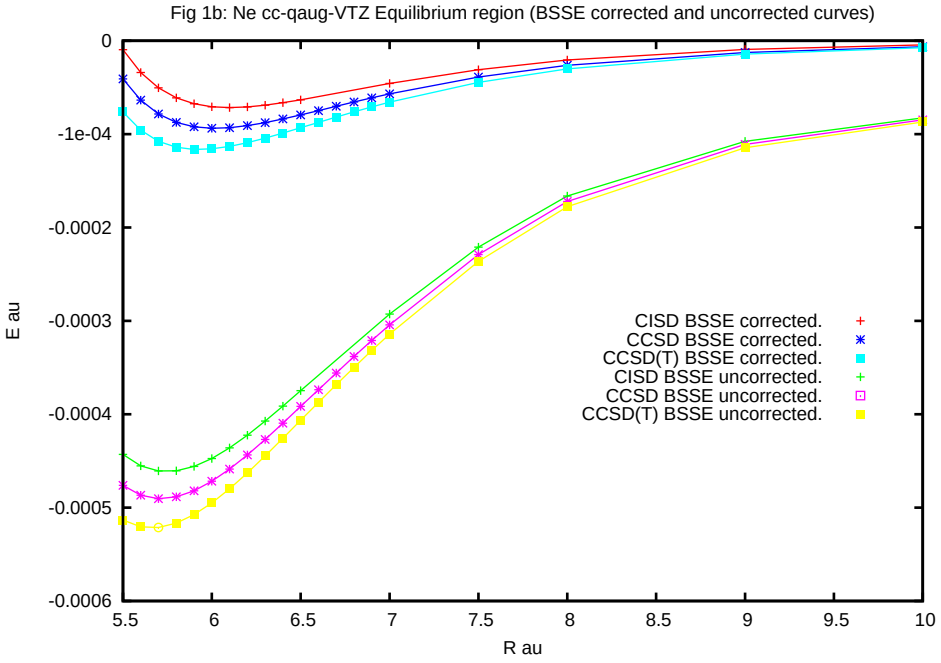

Figure 7.2: The CISD, CCSD, CCSD(T) BSSE corrected potential-energy curves in the asymptotic region. 2a: taug-vDZ, 2b: qaug-vTZ. Units: distances in bohr and energies in hartree.

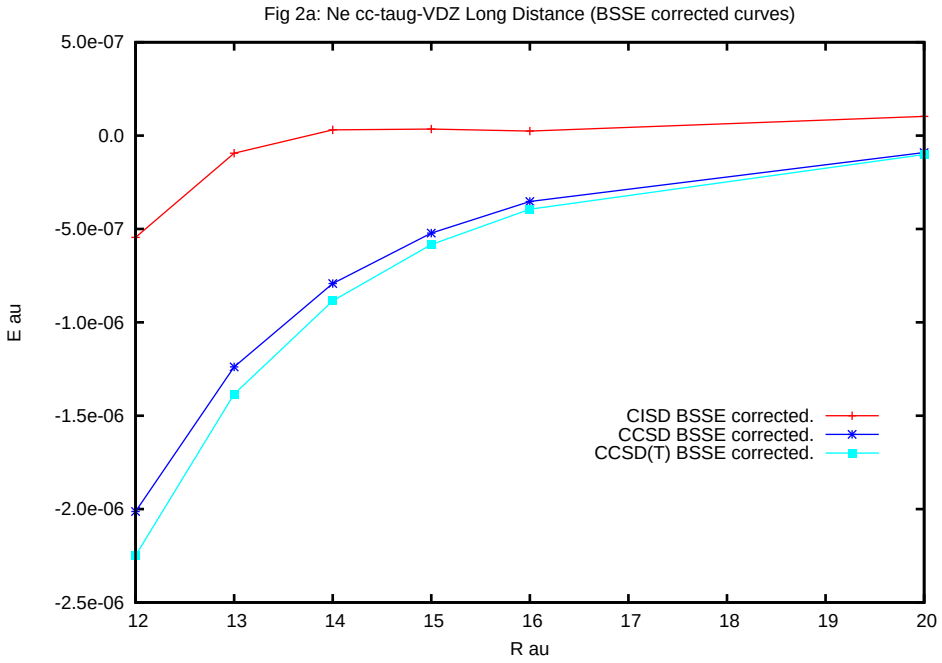

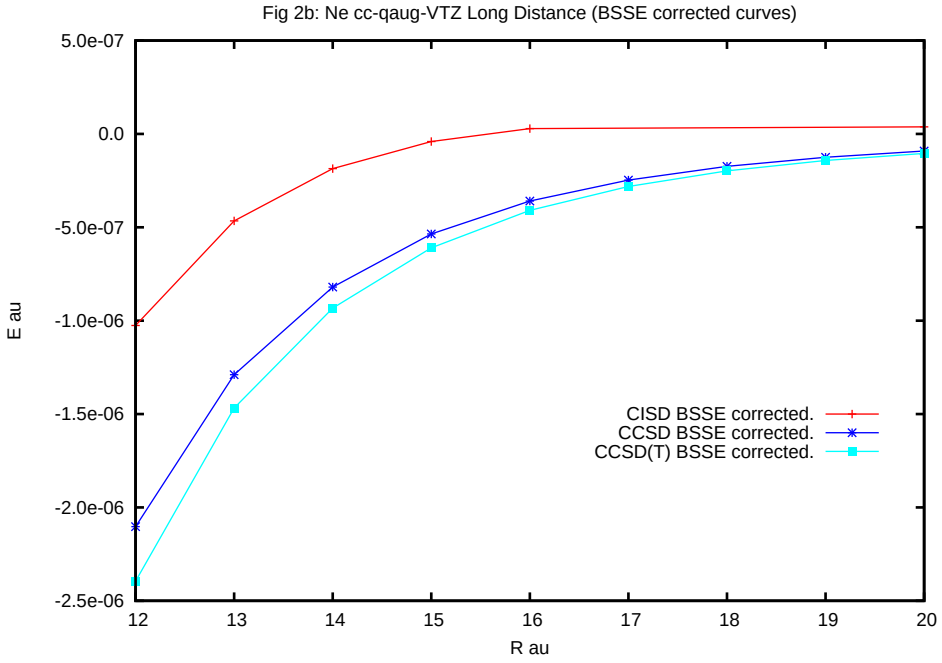

Figure 7.3: ER^8 as a function of R^2 (see text), in the asymptotic region. 3a: taug-vDZ and qaug-VTZ CISD, CCSD, CCSD(T) BSSE-uncorrected; 3b: taug-vDZ and qaug-VTZ CCSD, CCSD(T) BSSE-corrected; 3c: taug-vDZ and qaug-VTZ CISD, BSSE-corrected. Units: bohr^2 versus hartree·bohr^8.

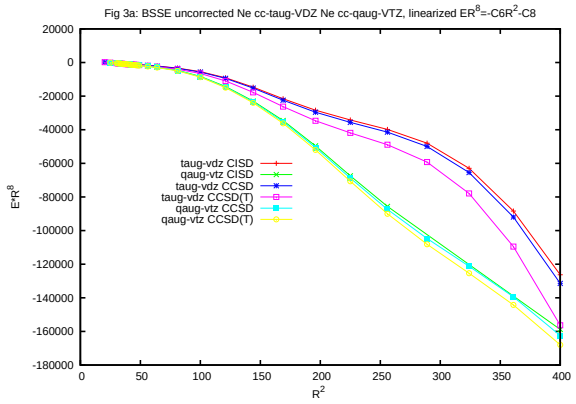

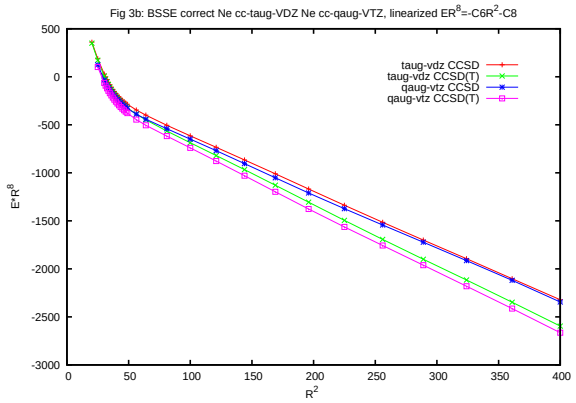

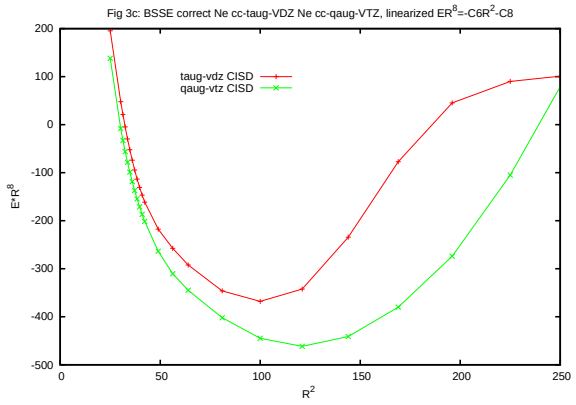

Figure 7.4: The computed points and the corresponding interpolated curves, in the asymptotic region. 4a: taug-vDZ; 4b: qaug-vTZ. Units: distances in bohr and energies in hartree.

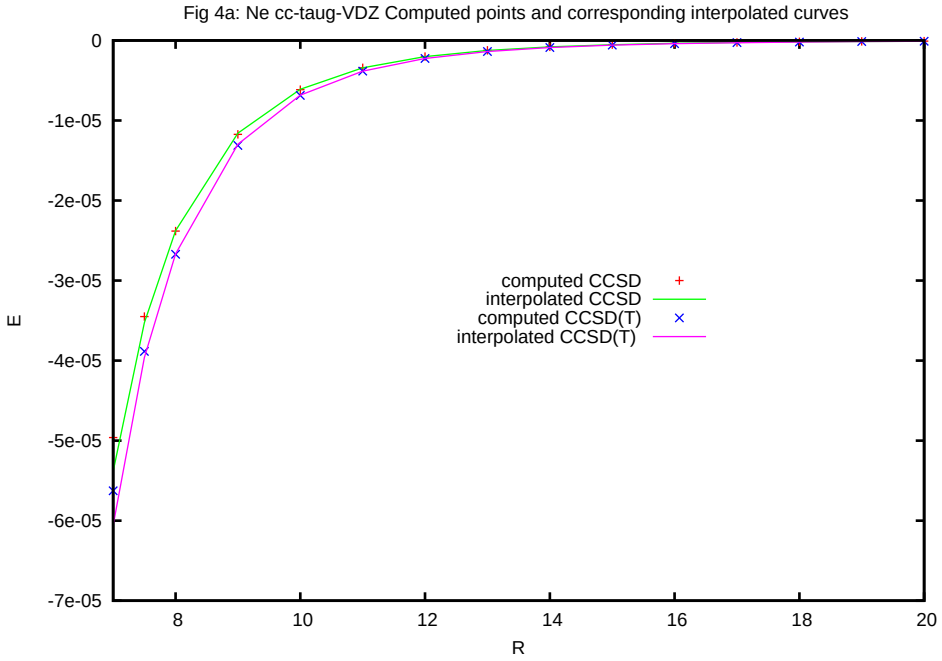

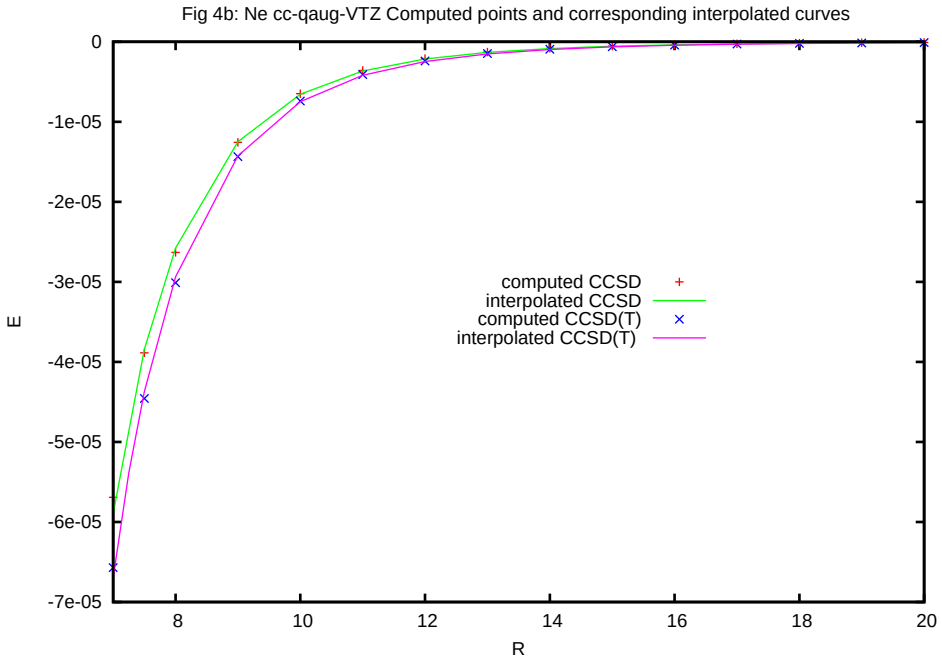

Chapter 8

R_{12} Coupled Cluster computation of electric properties

In the present Chapter we will discuss the implementation and the first applications of the analytical computation of electric properties at R_{12} CCSD level. In particular preliminary results for first order properties (i.e. dipole moments) will be shown.

8.1 Coupled Cluster First Order Properties

The first order properties [102, 103] can be seen as first derivatives of the energy

$$\begin{aligned} Q_\chi &= \frac{\partial E}{\partial \chi} \\ &= \langle 0|\hat{Q}_\chi|0\rangle \\ &= \langle 0|\frac{\partial \mathcal{H}}{\partial \chi}|0\rangle \end{aligned} \tag{8.1}$$

where $|0\rangle$ represents a ground state wave function in Dirac notations. At Coupled Cluster level we may obtain the value of the previous observable by straightforward differentiation of the Coupled Cluster energy equations considering the exponential Ansatz e^T

$$\begin{aligned} Q_\chi &= \frac{\partial E}{\partial \chi} \\ &= \langle 0|\frac{\partial}{\partial \chi} e^{-T}\mathcal{H}e^T|0\rangle \\ &= \langle 0|e^{-T}\frac{\partial \mathcal{H}}{\partial \chi}e^T|0\rangle + \langle 0|\overline{H}\frac{\partial T}{\partial \chi}|0\rangle \end{aligned} \tag{8.2}$$

where $\overline{H} = e^{-T}\mathcal{H}e^{T}$ represents the similarity transformed Hamiltonian. Inserting a resolution of the identity $|\mathbf{h}\rangle\langle\mathbf{h}|$ between the derivative cluster amplitudes and the similarity transformed Hamiltonian one obtains

$$Q = \langle 0|\overline{H}^{\chi}|0\rangle + \langle 0|\overline{H}|\mathbf{g}\rangle\langle\mathbf{g}|\frac{\partial T}{\partial \chi}|0\rangle \tag{8.3}$$

where we used the notation $\overline{H}^{\chi} = e^{-T}\frac{\partial \mathcal{H}}{\partial \chi}e^{T}$ while $|\mathbf{g}\rangle$ represents an excited state obtained as usual by the application of an appropriate excitation operator. Although strategies for first order properties calculations based on this equation have been advocated [104], it should be emphasized that such a strategy is unwise. The problem is the perturbed amplitude T are required for all the degrees of freedom under consideation. Since the computational scaling associated with the determination of $\frac{\partial T}{\partial \chi}$ is the same as that encountered in solving the non linear equations for the unperturbed amplitudes, the cost of such a calculation scales linearly with the number of perturbation. An alternative derivation can be obtained by differentiating the coupled cluster amplitude equations

$$\langle\mathbf{g}|e^{-T}\mathcal{H}e^{T}|0\rangle = 0 \tag{8.4}$$

and inserting a resolution of the identity. Following this procedure the linear equation system becomes

$$\langle\mathbf{g}|\frac{\partial T}{\partial \chi}|0\rangle = (\langle\mathbf{g}|E - \overline{H}|\mathbf{g}\rangle)^{-1}\langle\mathbf{g}|\overline{H}^{\chi}|0\rangle \tag{8.5}$$

inserting the previous in the first order property equation one gets

$$\begin{aligned} Q &= \langle 0|\overline{H}^{\chi}|0\rangle + \langle 0|\overline{H}|\mathbf{g}\rangle + (\langle\mathbf{g}|E - \overline{H}|\mathbf{g}\rangle)^{-1}\langle\mathbf{g}|\overline{H}^{\chi}|0\rangle \\ &= \langle 0|\overline{H}^{\chi}|0\rangle + \langle 0|\Lambda|\mathbf{g}\rangle\langle\mathbf{g}|\overline{H}^{\chi}|0\rangle \end{aligned} \tag{8.6}$$

where Λ represents the solution to the perturbation independent linear equation

$$\langle 0|\Lambda|\mathbf{g}\rangle = \langle 0|\overline{H}|\mathbf{g}\rangle(\langle\mathbf{g}|E - \overline{H}|\mathbf{g}\rangle)^{-1} \tag{8.7}$$

Moreover Λ is a deexcitation operator and the form of its parametrization is identical to that of the adjoint T

$$\Lambda = \Lambda_1 + \Lambda_2 + \ldots + \Lambda_n \tag{8.8}$$

$$\Lambda_k = \frac{1}{k!^2}\sum \lambda^{i_1 i_2 \ldots i_k}_{a_1 a_2 \ldots a_k} a^{\dagger}_{i_1} a_{a_1} a^{\dagger}_{i_2} a_{a_2} \ldots a^{\dagger}_{i_k} a_{a_k} \tag{8.9}$$

in the previous equation we used the notation a for virtual and i for occupied spin orbitals. It should be noted that practically the same expression can be obtained if one

adopts the matrix eigenvalue perspective [105]. In that case, in fact, we have $\Phi\rangle = e^T|0\rangle$ which can be considered as the right eigenvector of $\overline{H}$, but due to the non hermitian nature of the similarity transformed Hamiltonian the left eigenvector will in general be different and can it be shown to be equal to

$$\langle\Phi^\dagger = \langle 0|e^{-T}(1+\Lambda) \tag{8.10}$$

As usual with this notation case the expectation value for the first order property will simply be

$$Q = \langle\Phi^\dagger|\hat{Q}|\Phi\rangle = \langle 0|e^{-T}(1+\Lambda)|\hat{Q}|e^T|0\rangle \tag{8.11}$$

8.1.1 Application: Dipole Moments of Small Molecules

The previous formalism was implemented in the Bratislava R_{12} [52] code, allowing for the determination of first order electric properties at CCSD-R_{12} level. Practically the T amplitudes were computed fully exploiting the R_{12} theory, while Λ, and hence Q were obtained using the previous R_{12} amplitudes but a conventional similarity transformed Hamiltonian. The determination of the deexcitation operators Λ was actually the bottleneck, both from a computational and from a coding point of view. The first applications were performed by computing CCSD-R_{12} dipole moments for some of the systems for which Klopper reported, in a recent work [106], computation at MP2-R_{12} level. In Table 7.1 we present CCSD and CCSD-R_{12} results for the NH_3 molecule; in this case, as well as in the next ones, geometry is taken from [106], while AO basis set are retrieved from [107]. The latter have been expecially optimized for R_{12} calculations, therefore they are specifically designed to provide the appropriate approximation to the resolution of the identity embedded in R_{12} environment. As previously stated, in order to fulfill this particular requirement basis sets for molecules need, to be saturated at least for angular momenta $\ell = 3 \cdot \ell_{occ}$, i.e. up to angular momenta three times bigger than the highest angular momentum of occupied orbitals. In Table 7.2 and 7.3 results for H_2O and HF are also reported. From these data it is easy to understand that as far as the energy is concerned the introduction of R_{12} allows to speed up the converge towards the basis set limit (using R_{12} one gets approximately the same value obtained with a conventional CCSD performed with a basis saturated for two more angular momenta) for the dipole moment the same behavior can be evidenced, even if the effect is somehow less pronounced (the gain being of approximately one angular momentum).

Table 8.1: NH_3 CCSD and CCSD-R_{12} energy and dipole moments computed with different basis

	$CCSD$		$CCSD-R_{12}$	
	spdf	*spdfg*	*spdf*	*spdfg*
AO	224	320	224	320
E a.u.	-56.3790	-56.3877	-56.3935	-56.3948
μ a.u.	0.5599	0.5609	0.5610	0.5619

Table 8.2: H_2O CCSD and CCSD-R_{12} energy and dipole moments computed with different basis

$CCSD$			
	spdf	*spdfg*	*spdfgh*
AO	197	273	348
E a.u.	-76.4087	-76.4185	-76.4211
μ a.u.	0.7292	0.7314	0.7321
$CCSD-R_{12}$			
	spdf	*spdfg*	*spdfgh*
AO	197	273	348
E a.u.	-76.4258	-76.427	-76.4277
μ a.u.	0.7304	0.7325	0.7329

Table 8.3: HF CCSD and CCSD-R_{12} energy and dipole moments computed with different basis

CCSD			
	spdf	*spdfg*	*spdfgh*
AO	170	226	280
E a.u.	-100.38140	-100.3918	-100.3946
μ a.u.	0.6523	0.6568	0.6579
$CCSD-R_{12}$			
	spdf	*spdfg*	*spdfgh*
AO	170	226	280
E a.u.	-100.3946	-100.4013	-100.4029
μ a.u.	0.6568	0.6599	0.6605

8.2 Future developments: Equation of Motion Second Order Properties

Using standard techniques of perturbation theory, elements of frequency dependent polarizability may be expressed as

$$\alpha_{q_i q_j}(\omega;-\omega) = -\langle\widetilde{\Phi}_0|[q_i - \langle q_i\rangle][\mathbf{R}_0^{\pm} + \mathbf{R}_0^{\mp}][q_j - \langle q_j\rangle]|\Phi_0\rangle \tag{8.12}$$

the resolvent operator $\mathbf{R}_0^{\pm}$ may be defined as

$$\mathbf{R}_0^{\pm} = |\mathbf{h}\rangle\langle\widetilde{\mathbf{h}}|E_0 - H_0 \pm \omega|\mathbf{h}\rangle^{-1}\langle\widetilde{\mathbf{h}}| \tag{8.13}$$

where $|\Phi_0\rangle$ and $\langle\widetilde{\Phi}_0|$ are the ground state wave function and its dual obtained from the field free Hamiltonian H_0, $\langle q_i\rangle$ and $\langle q_j\rangle$ are the ith and the jth components of the dipole moment $\langle\widetilde{\Phi}|\hat{Q}|\Phi\rangle$, and finally $\langle\widetilde{\mathbf{h}}|$ and $|\mathbf{h}\rangle$ are functions that compose the complementary space and satisfy the orthogonality restrictions $\langle\widetilde{\mathbf{h}}|0\rangle = 0$ and $\langle\widetilde{0}|\mathbf{h}\rangle = 0$, with $|0\rangle$ and $\langle\widetilde{0}|$ representing a reference state and its dual. Obviously the suitability of any approach for calculating second and higher order properties is related to the accuracy of the perturbed wave functions. In a sum over state (SOS) procedure, analogous to the one we presented in Chapter 1, the perturbed wave functions are considered as linear combinations of the unperturbed (zero field) states. For systems having ground states that may be represented adequately by a single reference function, one approach which has been shown to provide an accurate prediction of singly excited state is the equation

of motion CC (EOM-CC) method in which wave functions and energy level are obtained by diagonalizing the similarity transformed Hamiltonian $\overline{H} = e^{-T} H_N e^T$ (H_N being the normal ordered Hamiltonian). Because this similarity transformation is nonunitary, the resultant transformed Hamiltonian is non hermitian. Therefore the bra and ket wave functions are not related by hermitian conjugation but rather form a biorthogonal basis in which a state i is defined through

$$\langle \widetilde{\Phi}_i^{CC}| = \langle 0|\mathcal{L}_i e^{-T} \tag{8.14}$$

and

$$|\Phi_i^{CC}\rangle = e^T \mathcal{R}_i |0\rangle \tag{8.15}$$

fullfiling the normalization condition

$$\langle \widetilde{\Phi}_i^{CC}|\Phi_j^{CC}\rangle = \delta_{ij} \tag{8.16}$$

where $\mathcal{R}$ and $\mathcal{L}$ are the right and left hand eigenvectors of $\overline{H}_N$ respectively. As we said in the previous section the ground state left eigenvector will be

$$\langle \widetilde{\Phi}_0^{CC}| = \langle 0|(1+\Lambda)e^{-T} \tag{8.17}$$

while $\mathcal{R}_0$ is simply the unity.
The total similarity transformed Hamiltonian in the presence of an electrical field ε directed along $\mathbf{q}$ will become [108]

$$\overline{H}_N = \overline{H}_N^0 + \varepsilon \mathbf{q} \tag{8.18}$$

where, obviously $\overline{H}_N^0$ represents the unperturbed transformed Hamiltonian in normal order. With this choice of the Hamiltonian and the convenient computational partitioning in which $|0\rangle$ represents the reference Slater determinant and $|\mathbf{g}\rangle$ the set of excited determinants the equation for the frequency dependent polarizability may be written as

$$\alpha(\omega;-\omega) = \sum_{l=0}^{1} \langle 0|(1+\Lambda)[\mathbf{q}_i - \langle \mathbf{q}_i\rangle]|\mathbf{g}\rangle[\langle \mathbf{g}|\overline{H}_N - E_{CC} + (-1)^l\omega]^{-1}\langle \mathbf{g}|[\mathbf{q}_j - \langle \mathbf{q}_j\rangle]|0\rangle \tag{8.19}$$

where E_{CC} represents the coupled cluster energy and $\mathbf{q}$ the involved dipole moments components, moreover the first order property's expectation value $\langle \mathbf{q}\rangle$ appearing in the right hand side does not contribute to the polarizability, because of the biorthogonality relation therefore the previous equation becomes:

$$\alpha(\omega;-\omega) = \sum_{l=0}^{1} \langle 0|(1+\Lambda)[\mathbf{q}_i - \langle \mathbf{q}_i\rangle]|\mathbf{g}\rangle[\langle \mathbf{g}|[\overline{H}_N - E_{CC} + (-1)^l\omega]|\mathbf{g}\rangle]^{-1}\langle \mathbf{g}|\mathbf{q}_j|0\rangle \tag{8.20}$$

which will represent our working equation. Implementation of the present equation requires a small amount of code beyond that needed to solve Coupled Cluster equation and compute first order property. In particular it will be necessary to solve the Cluster equations equation

$$\langle \mathbf{g}|X_{k^{\pm}}|0\rangle = [\langle \mathbf{g}|[\overline{H}_N - E_{CC} \pm \omega]|\mathbf{g}\rangle]^{-1}\langle \mathbf{g}|\mathbf{q}_k|0\rangle \tag{8.21}$$

Our planned computational strategy can therefore be summarized as follows:

1. Solve the Coupled Cluster R_{12} equations
2. Compute Λ with the equations given in the previous Section (Compute also first order properties if needed)
3. Form the matrix elements $\langle 0|(1+\Lambda)\mathbf{q}_k|\mathbf{g}\rangle$ and $\langle 0|\mathbf{q}_k|\mathbf{g}\rangle$
4. Solve the equation for the $X_{k^{\pm}}$ amplitudes
5. Evaluate the polarizability as

$$\alpha_{q_i q_j}(\omega;-\omega) = [\langle 0|(1+\Lambda)\mathbf{q}_k|\mathbf{g}\rangle - \mathbf{q}_i\langle 0|\mathbf{q}_k|\mathbf{g}\rangle]\langle \mathbf{g}|X_{j^{\pm}}|0\rangle \tag{8.22}$$

6. If the static polarizability is needed simply scale the previous value by a factor 2, otherwise come back to point 4, reverse the sign of ω and accumulate the results

The present method has not been fully implemented yet in the Bratislava CC-R_{12}, but we are anyway planning to have it working correctly in the near future. This will allow us to determine not only real frequencies dependent polarizabilities (important, for instance, to study Raman spectroscopy intensities) but also the imaginary frequencies polarizabilities which are needed for the determination of intermolecular dispersion coefficients via Casimir Polder or related methods.

Part III

Code Interoperability in Quantum Chemistry: Qcml/Q5Cost A Grid Oriented Common Format

Chapter 9

A Grid Oriented Common Format for Quantum Chemistry data

"Computational Grids are the equivalent to the electrical power Grid" [109]

"With Web Services we allow a thousand flowers to bloom. With a Grid we organize the planting and growth of a crop of plants to make harvesting easier. [110]"

9.1 The grid technology: an overview

The popularity of the Internet as well as the availability of powerful processors and high-speed network technologies as low-cost commodity components is changing the way we use computers today. These technological opportunities have bring the possibility of using distributed computers as a single, unified computing resource, leading to what is popularly known as Grid computing. The term Grid was chosen as an analogy to a power Grid that provides consistent, pervasive, dependable, transparent access to electricity irrespective of its source; a detailed analysis of this analogy can be found in [109, 110]. This rather new approach to network computing is popularly known by several other names, such as metacomputing, scalable computing, global computing, Internet computing, and more recently peer-to-peer (P2P) computing. Grids, in practice, enable the sharing, selection, and aggregation of a wide variety of resources including supercomputers, storage systems, data sources, and specialized devices that are geographically distributed and owned by different organizations for solving large-scale computational

and data intensive problems in science, engineering, and commerce. Therefore they act in such a way to create a sort of virtual organizations which can be thought as a temporary alliance of subjects that come together to share resources and skills, core competencies, or computational power in order to better face the requirements of large-scale processes and eventually better exploit business opportunities, and whose cooperation is supported by computer networks. The concept of Grid computing, at the beginning, started as a project to link geographically dispersed supercomputers, but now it has grown far beyond its original intent. The Grid infrastructure can, in fact, help many applications, including collaborative engineering, data exploration, high-throughput computing, and distributed supercomputing. In this context a Grid can be viewed as a seamless, integrated computational and collaborative environment. The users interact with the Grid resource broker to solve problems, and the latter on its turn performs resources discovery, scheduling, and the applications of jobs on the distributed Grid resources. From the end-user point of view, Grids can be used to provide the following types of services:

- Computational services. These are concerned with providing secure services for executing, individually or collectively, applications on distributed computational resources. In this case the so called Resources Brokers provide the services for collective use of the distributed resources network. This kind of Grids are often simply referred as Computational Grids. Some examples include: NASA IPG, the World Wide Grid, and the NSF TeraGrid.

- Data services. These are concerned with providing secure access to distributed datasets and to their management. In order to provide a scalable storage and access to the datasets, the latter may be replicated, cataloged, and eventually be stored in different locations to create an illusion of mass storage. The datasets are processed using computational Grid services and this combinations are commonly called Data Grids. Applications that need Data Grid to manage, share, and process large datasets are, for instance, high-energy physics and drug design.

- Application services. This kind of Grid is used for the management of applications and for the transparent access to remote software and libraries. Obviously this service is, nowaday, mostly accomplished by web services.

- Information services. They are concerned with the extraction and presentation of meaningful informations by using outputs provided by computational, data, and/or application services. The low-level details in this case are related to the way information is represented, stored, accessed, shared, and maintained.

- Knowledge services. These are concerned with how the knowledge is acquired, used, retrieved, published, and maintained to assist users in achieving their particular goals and objectives. Knowledge, in this context, should be thought as the informations one needs to solve a problem, or execute a decision. An example of this kind of service may be data mining.

To build a Grid, the development and deployment of a number of services is required. These include security, information, directory, resource allocation and, in some cases, payment mechanisms in an open environment. Moreover it is often necessary to build high-level services for application development, execution management, resource aggregation, and scheduling. Grid applications, in fact, usually refer to multidisciplinary and large-scale processing applications, often coupling resources which cannot be replicated at a single site, and which may be globally delocalized for whatever practical reason. The latter are anyway some of the main driving forces behind the success of global Grids. In this light, the Grid unquestionably allows users to solve larger or new problems by exploiting resources that before could not be easily coupled. Hence, the Grid should not only be considered a computing infrastructure for large applications, it is, indeed, a technology that can bond and unify remote and diverse distributed resources providing pervasive services to all the users that need them.

9.1.1 Grid Applications

A Grid platform could be used for many different types of applications. Grid-aware applications are usually categorized into five main classes:

- distributed supercomputing (e.g. compute *ab initio* energies to build a potential surface);
- high-throughput (e.g. quantum or molecular dynamic);
- on-demand (e.g. smart instruments);
- data intensive (e.g. data mining);
- collaborative (e.g. developing different high level codes to solve a complex problem).

A new emerging class of application that can benefit from the Grid is:

- service-oriented computing (e.g. application service built in such a way to provide the users' requirements driven access to remote software and hardware resources).

There are several reasons for moving applications on a Grid, for example:

- to exploit the inherent distributed nature of an application;
- to decrease the total response time of a huge application;
- to allow the execution of an application which is outside the capabilities of a single (sequential or parallel) architecture;
- to exploit the affinity between an application component and Grid resources with a specific functionality.
- to easily interface different codes and algorithm one needs to solve a complex problem (this represents our main concern)

It is now clear how, although wide-area distributed supercomputing has been a popular application of the Grid, a large number of other applications coming from science, engineering, commerce, and education, can benefit from it. Grid distributed supercomputing may, on its turn, benefit from the existing applications developed using the standard message-passing interface (e.g. MPI) for clusters. Many of them can, in fact, run on Grids without change, since an MPI implementation for Grid environments is available. Many of the applications exploiting computational Grids are, anyway, embarrassingly parallel in nature. The Internet computing projects, such as SETI@Home and Distributed.Net, for instance, build Grids by linking multiple low-end computational resources, such as PCs, across the Internet to detect extraterrestrial intelligence and crack security algorithms, respectively. The nodes in these Grids work simultaneously on different parts of the problem and pass results to a central system for postprocessing. But we are nonetheless, witnessing an impressive transformation of the ways computational research is performed. Research is becoming increasingly interdisciplinary; in many cases research start to be conducted in virtual laboratories in which scientists and engineers routinely perform their work without regard to their physical location. They are able to interact with colleagues, access instrumentation, share data and computational resources, and access information in digital libraries. This exciting development has a direct impact on the next generation of computer applications and on the way they will be designed and developed. The complexity of future applications is expected to grow rapidly, therefore increasing the movement towards component frameworks, which enable the rapid and widespread construction and use of cooperative environment. But this fact will also imply grid architectures will be much more crucial in the closest future and technological research, on its side, will be much more concerned about the easy interface of different

applications, and about the use and development of on demand services and cooperative environment.

9.2 A Common Format: Motivation

The activity reported in this Part has been carried out during the last few years within a COST in Chemistry funded project (action D23 AbiGrid) [111, 112]; the same action is now going on under a new COST project (action D37 DeciQ). The aim of the project named [92], A meta-laboratory for code integration in ab-initio methods, is to build a grid distributed laboratory where researchers would be able to use several codes, running on different platforms, without worrying about boring details like file transfers, accounting, format translation and so on.
All the partners of the proposal have been developing quantum chemistry codes for internal use for many years. These codes are complementary and their combined use is very important for the new collaboration. Moreover "general purpose" programs are needed in the workflow in order to compute some general and standard quantities that will be used by the specific programs. The idea was to integrate all these codes in a single meta-system for Post-SCF calculations, including heterogeneous computers, geographically distributed at the partners site. In fact, it is important to leave each code on the platform it was originally designed for, under the responsibility of its owner for maintenance and production, hence avoiding duplication of effort and the need for porting. The first problem faced by the project was the different formats adopted by every code in the chain, for this reason we report the work done on this very topic, i. e. how to enable different programs, relying on different data formats, to communicate with each other In general, one can imagine two different ways to make programs communicate. The first one is to write interfaces converting the output of the first program into the input of the second program. This means that we need a converter for each pair of communicating codes. The second possibility, and the one we have chosenhere, is to design a "common format" and to write a converter for each program in the set. In this case only one converter is needed for each code we are interested in. Of course, in order to avoid inventing "yet another format", we have made great efforts to design a format as general as possible and to coordinate with other similar initiatives in Europe and elsewhere. First of all we can identify two different kinds of information in quantum chemistry calculations: small data quantities, mainly ASCII coded, like atom labels, geometry, symmetry, basis sets and so on large datasets, normally binary, like integrals and expansion coefficients. The data format we are interested in is mainly conceived for interchange. We do not think it should be used as an internal format within programs, so we are more interested in func-

tionality (it has to be general and complete) than in high performance and efficiency. As far as the first type of data is concerned, several initiatives are active nowadays and include CML [113] (Chemistry Markup Language) and the activities carried out within the E-science project in UK In all these projects, the choice for describing chemistry related quantities relies upon an XML [114] based format that allows both human readability and machine comprehension. We have adopted the same approach and spent some time and effort in the definition of such a format. We called it QC-ML (Quantum Chemistry Markup Language) and its description is reported. For an easy processing of QC-ML files inside a QC program, we also need a specific library accessible from FORTRAN programs, since FORTRAN is the most common language used in the QC environment. No such library was available when we started this activity, so we devoted some effort for producing it. The description of the library (f90xml) is reported subsequently. For the second type of data, large binary ones, XML is not convenient, mainly due to its verbosity. For several reasons HDF5 [115] was considered the best technology for designing the large binary data format. A description of the data format (Q5cost), of the HDF5 technology and a discussion about its use in the data format is reported. A description of the library used to access Q5 files will also be presented in the proceeding. Our main idea is to have a sort of central repository containing all information about the chemical system under investigation. The data in the repository are based on standard formats (Q5cost and QC-ML). When a specific program has to be run on these data, a code specific input-wrapper will translate the data from the repository into the code specific input files. Then the program can be executed. The output data produced, through the output-wrapper, will be used to update the central repository. In Figure 9.1 we show a possible scheme for several codes running in sequence on the same data contained in the central repository. In order to realize this vision we will need a common language for describing the workflow and in addition, legacy and commercial licensed software will need to be integrated in the infrastructure. The final infrastructure must satisfy both grid requirements (fault tolerance, reliability) and human interface requirements (web-based interfaces, user-friendly environments).

9.2.1 The QC Context: Intermolecular Forces and Linear Scaling

As all the researchers in the present COST working group we share a common interest in the implementation of QC ab initio algorithms for the treatment of molecular systems. A peculiarity of the group is that most of the implemented codes concern nonstandard algorithms, proposed and developed by the same persons that will take care of the imple-

Figure 9.1: A Schemating representation of the integrated system

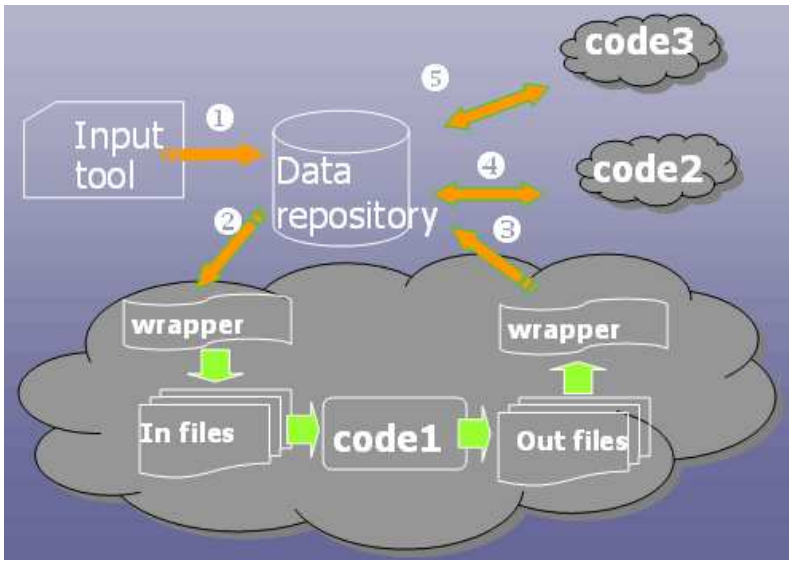

mentation. In fact, although many highly efficient QC commercial codes are presently available, the development of new techniques requires a huge programming work. In particular, the attention is focused on algorithms and programs, for the treatment of the electronic correlation. Nine Universities belonging to six different European countries are and have been involved in the code development work:

- Bologna (Italy) a FCI [34] package, with calculation of energy and first and second order properties;
- Budapest (Hungary) [116] participation to the COLUMBUS project: a general purpose abinitio chain (SCF, CASSCF,CI);
- Budapest (Hungary): implementation of a direct MRCC [117] algorithm;
- Ferrara (Italy) NEVPT [118]: a MR perturbative algorithm;
- Toulouse (France) CASDI [87] a MR CI algorithm;
- Lille (France) EPCISO [119]: a spin orbit code;
- Valencia (Spain) PROP [120]: evaluation of molecular properties;
- Zurich (Switzerland) GAMESS US [121] a general ab initio package and Gemstone [122] a grid architecture environment for QC;
- Tromsø (Norway): participation to the DALTON [19] project;

In recent years the interest has been particularly focused on the treatment of large systems via the use of local orbitals, although not in an exclusive way (see the discussion in the next section). These different codes are in many cases complementary, and the interaction between different chains is extremely important. At the same time, the flexibility and the experimental character of the single codes must be preserved, since these are research products subject to a permanent evolution. For this reason, the merging of these different codes into a single chain was not a viable solution. The need for a closer integration among different codes, while keeping the independence of the individual chains, was one of the reasons that motivated the activity of our WG.

9.2.1.1 The treatment of large systems

The computational complexity of typical quantum chemistry methods is very high starting for instance, from N^4 for Density Functional Theory (DFT) up to N^7 in the case

of the highly sophisticated Coupled-Cluster with the contribution of triple excitations (CCSD(T)) method (here N is the number of atomic orbitals used in the calculation, and hence is proportional to the system size). The Full Configuration Interaction (FCI) method, which gives the "exact" result for a given orbital basis, has an even faster growth, with a factorial dependence. It is clear that, due to such fast computational complexity, the application of QC methods to large realistic systems is extremely problematic. Unfortunately, large systems are precisely the most interesting ones for most technological applications, like drug design, material science, catalysis, etc. In the last decade new computational techniques have emerged, that enable the reduction of the complexity of the algorithms to a linear behavior [123, 124, 125] as a function of the system size. These are called Linear-Scaling (LS) methods and take advantage of the locality of the molecular interactions to neglect all those contributions involving pairs of atoms which are far apart in the molecule. LS methods use orbitals (either atomic or molecular) that are localized as much as possible in a given region of the molecule. Due to the fact that interactions between local orbitals in general decay very quickly as a function of their separation, they can be neglected as soon as the distance reaches a given cutoff. (The long-range two-center Coulomb interaction is an exception to this behavior, and the corresponding integrals require a special treatment). For this reason, the use of local orbitals in calculations is becoming a standard choice in modern QC. In fact this has been the only successful way of achieving LS in the DFT, SCF, MP2, and CC approaches. Current LS methods are of the Single-Reference (SR) type, which means that there exists a particular Slater determinant that gives a reasonable zero-order approximation of the wave function, and this determinant plays a special role in the theory. However, SR methods give in general accurate results for closed-shell systems only, and therefore are limited to describing molecules in their ground state and close to the equilibrium geometry. Different situations of chemical or physical interest often require a Multi-Reference (MR) approach. These include the treatment of electronic spectroscopy, chemical reactivity, transition-metal complexes and, more generally, magnetic systems, charge/excitation processes and many others. For these reasons, it is clear that MR approaches play a central role in QC and related areas, like material science, nanotechnologies and biochemistry. At the same time, the extremely steep increase of their computational complexity as a function of the system size limits these approaches to quite small systems. MR algorithms that directly produce local orbitals, and that can work on a local basis, can represent a first important step towards the development of MR Linear-Scaling methods. The possible development of LS codes is far from being the unique advantage of localization. As far as MR approaches are concerned, there can be a significant benefit in using localized orbitals. Indeed the use of delocalized orbitals often

allows a quite poor flexibility, for instance in choosing the active orbitals in CASSCF calculations. In the case of many aromatic compounds, for instance, the complete π system should often be taken as the active one. In large molecules, such an approach is impossible. On the contrary, with localized orbitals, the effort may be focused on the part of the system where the interesting phenomenon takes place. Moreover the use of localized orbitals allows the interpretation of a MR wave function in terms of clear and well defined electronic structures which are familiar to all Chemists.

9.3 Qcml: an Xml format for Quantum Chemistry

Each chemical system can be described, at the Quantum Chemistry level, by a collection of data of very different kinds. A first and easy classification is to define them either as:

- Base facts: a fact that is given in the world and is remembered (stored) in the system
- Derived facts: created by an inference or a mathematical calculation from terms, facts, other derivations, or even action assertions

In this case, Base facts are the initial data for describing the physics of the system, like stoichiometry, geometry, symmetry and basis set information. Derived facts are all those quantities computed from the previous ones using QC algorithms, like different types of energies, properties, integrals, coefficients, and so on. In the first category, we can devise three different classes of data, describing respectively:

- Symmetry: the symmetry of the system in terms of group name and other symmetry data;
- Geometry: the atomic composition of the system and its cartesian coordinates;
- Basis: the basis set information, either given by name or fully defined.

All these data are rather "small" and can be effectively described using a mark-up language for enhancing readability and standardization. A hierarchical scheme of Quantum Chemistry objects was designed and described [92] with a XML based specific language, that we called Qcml (Quantum Chemistry Mark-up Language). Qcml is defined by a XML-Schema that can be found on the WEB
(http://sirio.cineca.it/abigrid/QCMLSchema.xsd)
together with the proper html documentation

http://sirio.cineca.it/abigrid/workArea/QCMLdoc.html every Qcml file needs to be validated against this schema. A brief description of XML and the motivation for using it for describing QC data are reported in the next subsection. The first part of a Qcml file is devoted to the description of Base Facts, grouped under the tag `<molecule>` containing as attributes the number of electrons, the electric charge, the spin multiplicity and the space symmetry of the (ground) state wave function. Inside the `<molecule>` tag three sub-sections are present, describing respectively the spatial symmetry (`<symmetry>`) of the molecular skeleton, the atomic composition and geometry (`<geometry>`) and the atomic basis set (`<basis>`). In our present implementation these quantities are constant under the run and are left untouched by any program in the chain. Here we show a schemating represention of the basic format of the first section of a Qcml file:

```
<molecule nElectrons charge spinMultiplicity spaceSymmetry>
   <symmetry ... />
   <geometry ... />
   <basis    ... />
</molecule>
```

The system symmetry is described using the group name that references a repository containing all possible Abelian Symmetry Groups described with their generators. The system geometry is described by a list of atoms and their Cartesian coordinates; the user can choose whether to list all atoms or only those unique by symmetry. In the second case the Cartesian coordinates of the missing atoms are internally generated using the group generators referenced by Symmetry tag. Atoms are described by their atomic symbol; symbol `Du` can be used for special pseudoatoms of zero charge and mass, necessary in most cases for using special bond functions. The system basis is described by means of Gaussian type basis functions for each unique atom, with their exponents and contraction coefficients. The user can explicitly introduce these quantities for each angular momenta by means of tags `<angularMom>` for specifying basis function angular type (s, p, d, etc..) and orbital `<exponents>` and `<contractions>` to write down actual parameters. As an alternative it is possible to define a basis for each atom by means of standard names (for instance vDZ, Sadlej, etc...); in this case exponents and contraction coefficients are retrieved from the EMSL database, and can therefore be made available to wrappers if needed for the specific QC program input.
The second section of the Qcml file is intended to contain Derived Facts , e.g. data that are produced and computed as an effect of running a QC program. It is clear that while the first section of the Qcml file is kept untouched once one has defined the QC problem and system under investigation, the second one is constantly modified or upgraded during

the QC runs. The fundamental tag defining this section is <computedData> which may contain three fundamental subtags: energy, properties and file. Again we present the structure of this second part of the Qcml file:

```
<computedData>
 <energy unit levelOfTheory quality value>
    <state spaceSymmetry spinMultiplicity excitationLevel />
 <property unit levelOfTheory quality value>
    <state "bra" spaceSymmetry spinMultiplicity excitationLevel />
    <state "ket" spaceSymmetry spinMultiplicity excitationLevel />
    <operator order name/>
 <file address URL/>
</computedData>
```

The tag <energy> is used to store the computed values of molecular energies. It requires the definition of the level of theory, and the specification of the electronic state to which it refers by means of symmetry class, spin multiplicity and ordinal number within the specified symmetry and spin subspace. Note that in each Qcml file more than one tag <energy> can be present, each of them referring to different levels of theory on a single state, or to different states. The tag <property> is used for storing properties of (at least theoretically) any order, in the usual perturbation theory sense. It requires the same qualifiers as the <energy> tag but more child tags: the left hand ('bra' in the Dirac notation) state and the right hand ('ket') state, as well as the operators involved. For first order properties only one operator will be defined, otherwise more than one operator is needed (for instance two for second order properties and so on). If 'bra' and 'ket' states are not the same, the stored property value is considered a transition matrix element between the two states, like e.g. a transition dipole. The tag <file> contains the linking information to a separate binary file that stores all the computed "large" binary data, like one and two electron integrals and MO coefficients. This file is identified by its name (if stored on the same platform) or, more generally, with its Uniform Resource Location (URL) that is a standard and unique way to identify a file over the network. The file data format is Q5cost based on HDF5 and whose structure is described later. The information described up to now is not sufficient to completely describe a Computational Chemistry system. Still missing are all those specific directions necessary to actually run a QC program chain and safely perform the given computation. Thus, we plan a final section in the Qcml file containing the so-called work flow parameters of the computational chain. We have not devised this section yet, since it is strongly connected to the choice of specific grid architectures and techniques, while it adds little or nothing to the physical

description of the problem. In order to use and change the Qcml file we need a program, specifically designed for each QC code in the chain, capable of retrieving information from, and writing information to, the file in accordance with the Xml syntax. For a given QC code, the input wrapper reads data from the Qcml file and converts them into the QC code specific input, while the output wrapper reads data from the QC code specific output and adds them to the Qcml file. Many informatics tools with many language bindings are nowadays available for performing such a task. Some of them are object oriented (for instance DOM [128]) or events oriented (SAX), and libraries to manipulate Xml files are quite common for JAVA, C++ or scripting languages like Python or Perl. Even if today a limited number of FORTRAN libraries are available (xmlf90, xml-fortran) [129], at the time we started this work there were no libraries usable for the FORTRAN language. Since FORTRAN is the most common language used by QC programmers we decided to write down a specific FORTRAN 90-XML library, to be used for producing the wrappers. Specific details about the library will be given later, here we just want to mention that the library is based on a publicly available C binding (gdome2) [130], it implements a DOM [128] model and it allows users to write or read any specific Xml element (tag and attributes), using a FORTRAN Application Programming Interface (API). The library is completely general and does not contain any "chemical" concepts. It can be used for general programming involving Xml and FORTRAN. It is available under the open-source license on the web address reported.

9.3.1 Xml: why the best choice?

A complete and exhaustive description of the Xml meta-language and its applications will be far beyond the scope of this thesis, and will require a consistent amount of time, but we think it is convenient to recall briefly its main feature justifying its choice as the base for our Qcml. Extensible Markup Language (Xml) is a simple, very flexible text format derived from SGML (ISO 8879). Originally designed to meet the challenges of large-scale electronic publishing, XML is also playing an increasingly important role in the exchange of a wide variety of data on the Web and elsewhere. Each XML document has both a logical and a physical structure. Physically, the document is composed of units called entities. An entity may refer to other entities to cause their inclusion in the document. A document begins in a "root" or document entity. Logically, the document is composed of declarations, elements, comments, character references, and processing instructions, all of which are indicated in the document by explicit markups. The logical and physical structures must nest properly. Each XML document contains one or more elements, the boundaries of which are either delimited by start-tags and end-tags, or, for

empty elements, by an empty-element tag. Each element has a type, identified by name, sometimes called its generic identifier (GI), and may have a set of attribute specifications. Each attribute specification has a name and a value. Xml Schemas express shared vocabularies and allow machines to implement rules made by people. They provide a means for defining the structure, content and semantics of XML documents. Each XML document should be validated against a proper Xml Schema. The main reason that led us to the choice of Xml is its high versatility and its hierarchical structure, two features that allow the definition of an high organized, self-consistent and self-describing file format, i.e. a file format being in turn robust enough to allow easy exchange among different codes, and flexible to be adapted to research codes under constant development. It is also important to recall in Europe and abroad there is a large number of projects intended to build Xml chemical languages, e.g. Xml based file formats to describe chemical entities. Although most of these project are aimed to describe structural chemistry (consider for instance Cml in the U.K.) it is very important to build a communication channel between them and our quantum chemistry based project, allowing the ease implementation of future integration and cooperation.

9.4 Q5Cost: a HDF5 format for Quantum Chemistry

For the large binary data distinctive of quantum chemistry, we need to find a suitable technology that can merge characteristics like portability, efficiency, FORTRAN binding, data compression, and easy access to information. Usability is also important but not critical since it was our intention to build a new data model based on QC concepts and a new library to access it. HDF5 was considered the best technology for designing our abstract model. In fact, using it several important features come for free, like portability across different hardware platforms, efficiency and data compression and tools for file inspection. The main characteristics of the HDF5 technology is reported in the next section and a complete discussion about the Q5cost library is reported in the next Chapter. In this section we will present the abstract data model for large binary data in QC. It is targeted toward computational chemical entities, which are mapped onto the appropriate subroutines in the Q5cost library. Starting from a preliminary analysis among the involved research groups, an extensible data model has been proposed based on some firm criteria: The first criterion in this model is that many different types of simple data must be handled (nuclear energy, molecular orbital labels, molecular symmetry and so on). We will refer to these data as "metadata", in order to distinguish them from the

real large information on the chemical system, the integral values. Metadata represent well known chemical entities and belong to three generic data classes: scalars, vectors and n-index arrays. For example, the nuclear repulsion energy is a floating point scalar, molecular orbitals are an (N, M) floating point 2-indices array, the associated orbital energies are a floating point vector, the molecular orbital labels are a vector of strings and so on. The library should provide an interface for accessing these data both as generic or specialized entities. The second criterion is that in quantum chemistry large matrices with an arbitrary number n of indexes (rank-n arrays) are common data structures. This is the case for entities like two-electron integrals ($n = 4$), but also for other more application-specific information, like the four particle density matrix ($n = 8$). These data usually scale aggressively with the system size, and they are normally accessed with a chunked approach. For the sake of simplicity we have chosen for the moment to store only non-zero elements, each one associated to n indexes in the case of a rank-n array.

These large data arrays share common features:

- they usually are integrals, whose evaluation involves one or more operators and a given (large) number of functions. These functions are referred by the indices of the matrix. For example, two-electron integrals on the molecular orbital basis are stored as a rank-4 array with indices referring to the molecular orbitals; in the case of atomic basis set overlap integrals, the indices refer to the atomic basis set orbitals. the rank of the matrix depends on the operator involved, a n-particle operator giving rise to a rank-2n array. Atomic basis set overlap is described by two indices, and can be stored as a rank-2 array, two-electron integrals has four indices imposing a rank-4 array and the four particle density matrix has eight indices, requiring a rank-8 array.

- additional information is needed to identify the operator involved. The latter is in general a tensor in the physical space, so we also need to specify the component (cartesian/spherical) for each matrix. The electron-electron repulsion is a scalar two-body operator and generates the usual 4 index array of the two-electron integrals; the dipole is a one-body vector operator and needs three rank-2 matrices, one for each component; the quadrupole needs six matrices and so on. Moreover for each operator component one has to specify the spatial symmetry and real/imaginary nature of the stored values (e.g. magnetic dipole). Symmetry may also reduce the number of matrices to be stored.

This means that all these data objects could be described as one "generic property", provided we give the matrix rank and the definition of the involved operator(s) and

functions. Since some of these "properties" are well known chemical entities and chemists are used to refer to them by name, we chose to provide a specific library access to most of them (e.g. overlap, one-electron integrals, two-electron integrals, etc), in addition to a general interface to handle the "generic property". This should ensure both ease of use and flexibility of the library. The last point to be taken into account is that all these chemical objects are related within a hierarchical structure and logical containment relations can be defined for them. A first (root) container, named System, represents the molecular system as defined by its structural information (chemical composition and spatial geometry). Multiple Systems make it possible to handle different molecular geometries. To this container we can associate all the metadata that are invariant at the level, mainly information about the spatial reference frame. A System can contain several "Domains". The role of the Domain is to group together Property entities whose indices conceptually refer to the same kind of functions. Three Domains have been recognized as fundamental: AO for Atomic Orbitals, MO for Molecular Orbitals and WF for wave functions. Each Domain can contain other containers, one for each actual property. Moreover a set of invariant metadata, different for each type of domain, is associated to it and stored as Scalar, Vector and Matrix entities.

- The AO Domain holds properties referring to the atomic basis set functions: overlap, one-electron and two-electron integrals on the atomic basis set, in addition to the generic property. The invariant metadata consist of information on the Atomic orbitals, such as their number, labels and symmetry features.

- The MO Domain holds properties referring to molecular orbitals: one-electron and two-electron integrals on the MO basis set, in addition to the generic property. The descriptive metadata for the domain refer to the MO basis description: their number, labels and symmetry, the AO basis, the method/wavefunction they were derived from (SCF, MCSCF, ...), the coefficient matrix, orbital energies, classification and occupation numbers (where applicable).

- The WF Domain holds properties referring to the electronic states. Although under development, the complete definition of this container is not available yet, but it is not essential for the first deployment and test of the library and format.

For each of the domains, different occurrences can be defined by means of an identifier (tag) chosen by the user, with a default value if no tag is provided. The aim is to provide storage of multiple entries for each Domain, like in case of multiple molecular orbitals in the MO Domain, or multiple basis sets in the AO Domain. The bottom level of the hierarchical scheme defines the property container. Even if at the user level different

Figure 9.2: The abstract model of the Q5Cost file system

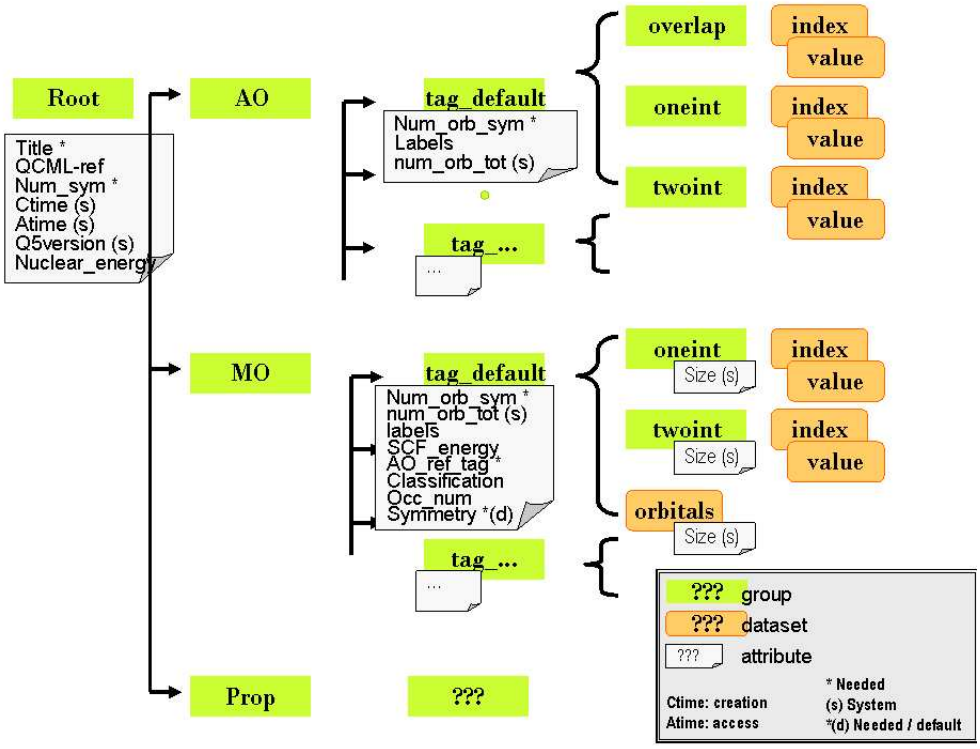

"properties" are available, and as we said all of them are different instances of the same "generic property" object. This object holds the true data, i.e. the integral values and the corresponding index values. Also here, in order to fully define the nature of the actual property, some metadata are needed: name, rank, symmetry and type (i.e., real, imaginary or complex). In ab-initio codes, the two-electron integrals, either on the atomic or the molecular basis set, are among the largest data set. For this reason, an efficient management of these integrals is crucial for obtaining a good performance. The whole set of N integrals, with the corresponding indices, therefore can be stored within a linear structure like that reported below:

```
(val1; i1, j1, k1, l1)
 ...
(valN; iN, jN, kN, lN)
```

where `val` is the floating point integral value and `i,j,k,l` are the corresponding integer indices. As already said the simplest solution is to store both the integrals and the four indices, so the order of the records does not matter. Moreover, null or small integrals can be simply omitted from the list, a fact particularly important when working with local orbitals. For this reason, at the moment, this is the only strategy that was adopted in the Q5cost data format. The price one has to pay is the additional storage of the four integer orbital labels, leading to a memory/disk occupation that could be three times larger than the one if only integrals were stored (in the common case of `REAL*8` integrals and `INTEGER*4` indices). In the case of very large integral files, this overhead can be extremely heavy. For this reason, in many QC programs the integrals are stored in a well defined order, the standard order, so that the orbital labels can be omitted without loss of information. (In the presence of spatial symmetry, a large number of zero integrals are present, and the standard order can be modified in order to take this fact into account). At present only the simplest solution has been implemented in Q5cost. This representation of the data, although not the most efficient solution in terms of space occupation, is well known by the interested parties, easy to debug and already integrated in the current library. Other strategies for storing integrals, for instance without indices but with a given order, should be easy to implement. Of course we are aware that, for the sake of generality, it is important to provide for the possibility to store integrals also in the other way, allowing the choice among one or more definite orders.

9.4.1 HDF5: Why the best choice?

The Hierarchical Data Format (HDF) is a general purpose library and file format for storing scientific data. HDF5 was created to address the data management needs of

scientists and engineers working in high performance, data intensive computing environments. As a result, the HDF5 library and format emphasize storage and I/O efficiency. For instance, the library is tuned and adapted to read and write data efficiently on parallel computing systems. HDF5 is developed and maintained by NCSA/University of Illinois (http://hdf.ncsa.uiuc.edu). It consists of an abstract model for managing and storing data, and a library (with bindings for several programming languages) to implement the data model. The HDF5 library provides a programming interface to a concrete implementation of the abstract model. HDF5 can easily handle data described by conventional data structures such as multidimensional arrays of numbers, tables or records, and images, in addition to more complex data structures such as irregular meshes and highly diverse data types. Other important issues are heterogeneous computational environments, parallel data access and processing, the diversity of physical file storage media, and varying notions of the file itself. It also addresses the issues of efficient data access and storage, file portability and supports very large data volumes (practically unlimited). Its flexible data model is extremely useful in multidisciplinary science applications. Some HDF5 features that led us to the choice of this technology are:

- Unlimited file size, extensibility, and portability
- General data model
- Flexible, efficient I/O
- Unlimited variety of data types

An HDF5 file has a hierarchical structure and appears to the user as a directed graph, conceptually similar to the UNIX type file system. The nodes of this graph are the higher-level HDF5 objects that are exposed by the HDF5 Application Programming Interfaces (APIs):

- Groups (corresponding to directories)
- Datasets (corresponding to files)
- Attributes (or metadata: low dimensional data describing the other data)

All the components of an HDF5 file can be easily managed by means of the HDF API. Moreover HDF5 is unique in its ability to physically and conceptually separate data from metadata (Attributes), even if they are stored in the same file. The available HDF5 software tools consist of a number of libraries for each supported programming language

(Fortran 90 is one of them) and several utilities for managing data files (inspecting, copying, merging, and so on). It is open source and freely downloadable from the HDF5 web site. Using this technology several specific data formats and applications were created in different contexts. A wide list of tools (both commercial and open source) based on HDF5 can be found on the web (http://hdf.ncsa.uiuc.edu/whatishdf5.html).

Chapter 10

Accessing the file: Fortran APIs

As previously stated in order to implement the easy access to the Qcml/Q5Cost file format we designed and wrote two APIs: F77/F90Xml [126] and Q5cost [93]. In particular the previous is a general library to provide read/write access to any Xml file regardless of its specific, i.e. "chemical", significance. The latter, on the contrary, is an higher level library intended to provide specific access to Q5Cost file, therefore its istances and objects are logically bound to quantum chemical entities.

10.1 Q5cost a FORTRAN API to handle Quantum Chemistry large datasets

The Q5Cost library provides read and write access to files defined in accordance with the data model described before (Q5cost data model). It provides a specifically designed high-level access for quantum chemistry developers. The rationale is to provide a FORTRAN interface based on well known chemical entities, rather than groups or datasets like in the original HDF5 interface. HDF5 takes care of the low level management of the file, and Q5Cost provides the high-level Application Programmer Interface for storage and retrieval of chemical entities.

The library is written in FORTRAN 95 and consists of several modules, each one providing different facilities. The most important modules are

- **Q5Cost**: defines the high-level API. This module provides subroutines designed to be at the disposal of the final programmer.
- **Q5Core**: provides a wrapping facility for HDF5 routines, in order to perform additional useful services like reference counting and debugging. It also provides

simplified routines to perform frequently used low-level tasks.

- **Q5Error**: provides facilities for high level debugging of library and client codes. This module implements a ring buffer for error messages, different logging levels, generic reference counting for catching memory leaks and a subroutine call stack trace.

The names of the subroutines in each module are identified by an appropriate prefix, and have been chosen to provide an explicit and intention revealing interface to the entities described in the previous section. Although FORTRAN 95 does not allow object oriented (OO) programming, some OO concepts have been used in the development of the library, but taking into account the possible procedural programming background of future developers. The state is preserved in the HDF5 file, and subroutines refer to the file directly through the HDF5 file identifier, an easier concept for FORTRAN programmers more used to file descriptors.
A test suite has been designed and implemented in order to verify the library correctness in a high number of well-known critical situations. At present, more than 250 tests are available, covering most common usage patterns and performing reference counting to prevent leaks of HDF5 references. The test suite provides an effective tool for debugging and bug fixing. Library documentation is embedded into the FORTRAN code as comments, using a custom tag system to provide meta information about each comment. A simple parser, written in the PYTHON programming language, extracts the documentation producing HTML files.

10.1.1 The Q5Cost Module

This module is the main reference for the final user. It provides subroutines to read and write HDF5 files in the Q5cost format with a high level of abstraction. Using this library the users can deal with high level concepts without worrying about low level implementation details. If a finer access is required for the underlying HDF5 file, the Q5Core module provides this type of access in a simpler way with respect to the raw HDF5 routines. All the routines in the Q5Cost module have the `Q5Cost` prefix and they are organized in several classes:

- **Init**: initialize and de-initialize the library within the program.

- **File**: create, open, close the Q5Cost file and write/get root attributes, like creation time, access time and file version.

- **System**: create or check the existence of the System and set/get the specific attributes
- **AO**: create or check the existence of a given occurrence of the AO Domain and set/get its attributes
- **AOOverlap**: create the folder, read and write data for the atomic basis set overlap property
- **AOOneInt**: create the folder, read and write data for the one-electron integrals in atomic orbitals basis
- **AOTwoInt**: create the folder, read and write the data for the two-electron integrals in atomic orbitals basis
- **MO**: create or check the existence of a given occurrence of the MO Domain and set/get its attributes
- **MOOneInt**: create the folder, read and write data for the one-electron integrals in molecular orbitals basis
- **MOTwoInt**: create the folder, read and write the data for the two-electron integrals in molecular orbitals basis
- **WF**: create or check the existence of the WF domain and set/get its attributes
- **Property**: create the folder, read and write data for a generic property. The name, domain, rank and type have to be defined by the user.

Additional routines are available for the generic access to the "Property" class, allowing the management of user defined properties. Subroutines like `AOOverlap`, `MOOneInt` and **MOTwoInt** contain calls to these property routines, passing the specific parameters of the involved property. The routines of the Q5Cost module provide a context-based access to chemical entities. This access is converted into a path-based access, creating an appropriate layout for HDF5 groups, datasets and attributes, and writing the user provided data into the file. Some data are provided automatically by the library, like the creation or access time and the Q5Cost library version. One important aspect of this format is that the user is not forced to enter all the quantities; he can store the quantities that are actually available, or in which he is interested, and add other data later when available. Constraint checks are however mandatory in order to assure basic file consistency. For example, a MO Domain can be created only if a System and an AO

Domain exist, in order to guarantee the presence of fundamental data, like the order of the symmetry group and the number of basis functions for each symmetry class.

10.1.2 The Q5Core and the Q5Error Modules

The Q5Core module is a low level module designed to provide wrapping facilities between HDF5 and Q5Cost. At the moment it is focused on providing additional debug information, reference counting for HDF5 objects, additional low-level API for simplifying common tasks and so on. This module provides path-based management of Scalar, Vector and Matrix entities (in contrast with the context-based approach of the Q5Cost module, which focuses on chemical concepts rather than HDF5 path). It also provides routines for the easy handling of the Property data (indices and values), relative to a CompactMatrix class (CM). End users in general should not access Q5Core module routines. The Q5Core module guarantees the transparency of the Q5cost data model with respect to the underlying technology. In case we decide to use another storage format in place of HDF5, only this module should be modified. The Q5Cost module, i.e. the end user interface, remains unchanged, being independent of the low-level format.

The Q5Error module provides subroutines for debugging and monitoring the behavior of the library and the application code. A ring buffer is provided to keep track of error messages generated by the library. A verbosity level can be set, from totally silent to highly verbose; in the latter case each subroutine call and return is reported in the buffer. Moreover, a stack for backtracking has been implemented to keep track of the call tree. The tree is printed out when an error occurs or when error reporting is requested. Different specific error codes have been provided for, to report anomalous behavior of the application code or of the library itself. The error codes are defined as numeric parameters, and report situations ranging from invalid parameters to non-existence of some information in the file. The presence of an error condition is returned to the application code through the last parameter of each subroutine.

10.1.3 See what you have: The q5dump

In order to facilitate the exchange features of our file format, we wrote a FORTRAN application, miming the existing h5fdump which is distributed with hdf5. The q5dump should be considered a part of the Q5cost library itself, and is capable of retriving the most important metadata stored in a Q5Cost file and print them on the screen. This allows a generic users to get valuable information on the file and on the data stored on

it, but, in the future, it could also be used as a tool for a validation step that should be performed on grid architectures in order to assure file integrity and compatibility.
q5dump makes use of both high level libraries call (basically Q5Cost and Q5Core module's ones), and lower level hdf5 native routines in order to get the most complete, flexible and fast retriving of the information. The Q5Cost files are binary files, therefore the existence of a tool capable of interpreting the informations is of invaluable importance not only in the case of distributed computing but in general situations, and this task would not have been so easily accomplished using standard FORTRAN binary files. Here we present, for the reader convenience, a real example of a q5dump output. The file which has been examined stores molecular integrals computed at SCF level for the LiH molecule in a Sadlej base (33 A.O.) in this case dipole moment integrals have been computed too:

```
************************************
*          Q5Costdump              *
*                                  *
*     a tool for analysis of       *
*           Q5Cost files           *
*                                  *
************************************

Enter the file name:
Creation time 2007/01/12  18.13.55

SYSTEM ATTRIBUTES
Title: Q5 Cost file produced from Dalton
Order of the symmetry group            4
Nuclear Repulsion (Core Energy)   0.995024875621890

Groups present            2
ao           1
tag-default
mo           1
tag-default
-----------------------------------------------------

Properties of AO group <default>

Number of Orbitals          33
Orbital in Symm. Classes   17   7   7   2
```

```
 AO Labels:
Li1sLi1sLi1sLi1sLi1sLi2pzLi2pzLi2pzLi3d0Li3d2Li3d0Li3d2H 1sH 1sH 1sH 2pzH 2pz
Li2pxLi2pxLi2pxLi3d1Li3d1H 2pxH 2pxLi2pyLi2pyLi2pyLi3d1Li3d1H 2pyH 2pyLi3d2
Li3d2

 Property-overlap is present
 -------------------------
 Properties of MO group <default>
 AO REF: <default>

 Number of Orbitals          33
 Orbital in Symm. Classes   17   7   7   2
 AO Labels:
Li1sLi1sLi1sLi1sLi1sLi2pzLi2pzLi2pzLi3d0Li3d2Li3d0Li3d2H 1sH 1sH 1sH 2pzH 2pz
Li2pxLi2pxLi2pxLi3d1Li3d1H 2pxH 2pxLi2pyLi2pyLi2pyLi3d1Li3d1H 2pyH 2pyLi3d2
Li3d2


 XDIPLEN is present

 YDIPLEN is present

 ZDIPLEN is present

 oneint is present

 twoint is present


 ------------------------------------------------------
-----------------------------
```

10.1.4 Performance and efficiency assessment

As we have already discussed, the Q5cost format was intended as a file exchange format between different platforms and codes, and not as an internal format to be used during actual computations. For this reason, performance considerations have been considered to be less important than other features such as transparency or code and file portability. But to ensure that the library does not impose excessive overheads in terms of CPU time

or disk space, we decided to undertake some comparisons with ordinary binary files. All performance tests have been run on a single node of an IBM Linux Cluster 1350 at CINECA (Intel Xeon Pentium IV, 3 GHz 512 Cache). The software was compiled with the Intel FORTRAN Compiler 8.1 and run under Suse Linux SLES 8. In order to perform the tests we wrote a specifically designed code that:

- Creates a proper Q5Cost file with its internal structure (System, AO, MO, ...)
- Opens a normal binary file
- Writes in the Q5Cost file a number of two electron integrals specified by the user with the proper format: a one-dimensional array of reals (values) and a four-dimensional array of integers (indices) using a chunk whose size has been specified by the user.
- Writes the same number of two electron integrals in a binary file together with the four indices. For this operation a buffer of the same size of the chunk specified previously is used
- Computes the time necessary to write the Q5Cost and binary files and calculates their sizes.

In a first test we evaluated the time needed to write a file of approximately 300 Mb, using different chunk sizes; the results are reported in Table 10.1. As it can be seen the time needed to write the Q5Cost file is less than the time needed to write the ordinary binary file for any chunk size. This feature is a direct consequence of the use of the HDF5 library, whose performance characteristics are well documented [115, 127]. Obviously using chunks of high size, hence limiting the number of accesses to the file, decreases rapidly the time needed for the entire process.

In the second test we studied the time needed to write Q5Cost and binary files with a fixed chunk size (16384), and the corresponding size of the file so produced. The results are collected in Table 10.2. It can be seen that the sizes of the Q5Cost files are comparable with the binary file sizes. The Q5Cost files are in fact, only bigger by less than 1% compared with the ordinary binary files. The main problem regarding disk occupation is that all four indices are stored for two electron integrals and this leads to large file sizes. It is possible to avoid storing the indices by using a predefined order; we are currently working on implementing such a mechanism in our library.

Table 10.1: Writing time (in seconds) versus chunk size. Number of integrals 15000064, binary file size 343 Mb, .q5 file size 346 Mb

Buffer size	**Fortran Binary**	**Q5cost**
1,024	265.23	226.62
2,048	121.13	114.53
4,096	62.38	59.02
8,192	34.39	31.46
16,384	18.86	17.04
32,768	8.56	6.09
31,072	6.19	4.86
262,144	5.84	4.08

Table 10.2: Space occupation and writing time (in seconds) versus number of integrals for a fixed chunk size of 16384 integrals

Number of Integrals	**Q5Cost**		**Binary**	
	size	**Write time**	**size**	**Write time**
16,384	397Kb	$5.00\ 10^{-2}$	384Kb	$5.00\ 10^{-2}$
65,536	1.5Mb	$1.00\ 10^{-1}$	1.5Mb	$1.00\ 10^{-1}$
114,688	2.7Mb	0.15	2.6Mb	0.17
507,904	12.0Mb	0.62	12.0Mb	0.68
1,015,808	23.0Mb	1.21	23.0Mb	1.37
5,013,504	115.0Mb	5.88	115.0Mb	6.41
10,010,624	231.0Mb	11.11	229.0Mb	12.12
50,003,968	1.1Gb	56.19	1.1Gb	64.21
100,007,936	2.3Gb	125.32	2.2Gb	148.53

10.2 F77/F90Xml: A Fortran API to handle general Xml file

The present Section describes the design and the implementation details of F77/F90xml, a Fortran 77/90 binding library that provides a DOM interface for accessing XML documents from the Fortran language. Xml (Extensible Markup Language), as already stated, is a well established standard tool for data sharing. Its peculiar structure makes it possible to describe both the data and their meaning in a structured way, by means of a human-readable format which is also machine-parseable. An Xml document is organized as a tree of nested nodes with a single root node including other nodes in a parent-child relationship. Nodes are heterogeneous: they can be elements, comments, text nodes, processing instructions and so on, all of them are indicated in the document by explicit markups and manageable through specific interfaces. In a Xml document elements are delimited by start-tags and end-tags. Each element has a type, identified by its name, and may have a set of attribute specifications. Each attribute specification has a name and a corresponding value. As defined in W3C (World Wide Web Consortium), DOM (Document Object Module) is an interface for accessing and updating an Xml document, and is platform and language independent. DOM builds an in-memory representation of the Xml tree, in terms of elements, attributes, text nodes, and allows basic operations like creation, deletion and retrieval of the nodes. DOM is only an interface specification; specific implementations (also called "bindings") have to be made available for the different programming languages. Since Xml is widely use for commercial applications on the web, several bindings are available for languages like java, python, but not for scientific languages like Fortran. After the definition of Qcml (based on Xml) a Fortran access to XML files was a crucial demand from the involved partners, given the frequent use of the latter by the Quantum Chemistry community, and the development of the F77/F90xml library was, therefore, driven by the lack of an available DOM library for the Fortran binding when the project started. Today several others Fortran interfaces are available, although not always DOM compliant.

10.2.1 The FORTRAN API

The F77/F90xml library is written in C and is designed to provide a Fortran interface to DOM [128]. It is build on top of gdome2 , an open source library that was developed as part of the GNOME project. The gdome2 [130] implementation provides a nearly complete "DOM level 2" interface . The only missing feature is "events", which however is not critical in the target environment. XPath support is available, although not

tested, and therefore it must be considered as experimental. The F77/F90xml library requires libgdome/gdome2 release 0.8.0, glib-1.2.10 and libxml2-2.5.11 . Moreover it requires python 2.3 or above in order to be compiled. The library has been successfully compiled on the Intel/AMD Linux platform, using gcc (C compiler) and the Intel Fortran Compiler. On the IBM p5-575 (with AIX operating system) the compilation has been performed with the XLF compiler suite. The library is released under the terms of the LGPL license and can be downloaded from the web site reported in the References . The F77/F90xml library has been designed with the Fortran 77 backward compatibility in mind. The library provides two interfaces:

- Fortran 77 interface, based on specialized routines called "multiplexers"
- Fortran 90/95 interface, fully DOM Level 2 compliant;

The F77 interface was an initial strong request from the interested parties, since some researchers still work in a pure Fortran 77 environment. The F77 interface is not DOM compliant, and therefore it is quite complex to use and error prone; however, it respects the strict F77 standard rules for routines name length. To respect the standards and to reduce namespace pollution, the library provides specialized routines, called "multiplexers", whose role is to dispatch function calls and parameters to the full DOM API provided by gdome2. Each multiplexer gives access to a different set of DOM routines, grouped by means of their type signature. The F90/95 interface is realized on top of the F77 one and provides a clean and simple access, since in F90 the limitation on the names length is less restrictive. All the gdome2 functions are mapped to Fortran subroutines with similar names and collected into a MODULE. A simple F90 code example is provided:

```
INTEGER :: first, last, elem, err
!
!..<. get elem by some other call ...>
!
CALL f90xml_el_firstChild(first,elem,err)
CALL f90xml_el_lastChild (last ,elem,err)
```

This can be compared with the equivalent C code using the gdome2 library:

```
GdomeElement *elem;
GdomeNode *first, *last;
GdomeException exc;
```

```
/* <... get elem by some other call ...> */

first = gdome_el_firstChild(elem, exc);
last  = gdome_el_lastChild (elem, exc);
```

From the comparison it is easy to get the main features of F90xml library with respect to gdome2. First of all, the standard prefix `f90xml_` replaces `gdome_` in the routine names to provide a correctly name-spaced set. Another important difference is related to the data reference handling. The gdome2 interface is structured in an Object Oriented style, with all the Xml objects (nodes, elements, ...) handled by means of C pointers to dynamically allocated structures. The handling of pointers is not straightforward in Fortran, so an integer token is used to reference a particular pointer corresponding to a given object (for example to GdomeNode, GdomeDomImplementation, GdomeDOMString and so on). The library internally provides a cache space for the token/memory pointer association. It is used for mapping each token with the memory pointer, to store new pointers and to produce the corresponding tokens. A Fortran client program always handles these integer tokens, hereafter named codes, uniquely identifying a particular Xml object. The current implementation makes use of a simple linked list for storing this correspondence. It is kept in memory until the gdome2 object is completely deallocated. Substitution of the linked list with a more efficient hash table can be implemented transparently in a later version of the library. Another major difference is in the routines' arguments layout: in the F77/F90xml library, the first argument is always the corresponding gdome2 function returned value; therefore the F90 interface declares this argument as `INTENT(OUT)`. The following arguments are the same of the corresponding gdome2 routine and in the same order, therefore they are marked as `INTENT(IN)` with the exception of the last one, the returning error condition, that is marked as `INTENT(OUT)`. If the gdome2 function return value is void (no value), the corresponding F77/F90xml subroutine will return in the first integer argument a standard numeric parameter `NullCode`, which evaluates as zero.

String Handling In the F77/F90xml library string objects are handled with a code token referring to a `DOMstring` object. For example, when a name of a Xml element is requested, the subroutine returns a code referencing a `DOMstring` object. In the same way, when an element must be given a name, a `DOMString` has to be allocated and filled with the information, and its code token is then passed to the specific routine. So we need a set of routines to convert Fortran strings to DOMstring objects and vice versa. The following helper routines are available in the library to handle DOMstring objects:

- `f90xml_str_mkref`: creates a new `DOMstring` from a Fortran `CHARACTER` string. It accepts the Fortran string and returns a code referencing the newly created `DOMstring` object.

- `f90xml_str_length`: accepts a `DOMstring` reference and returns its length. This routine is useful to know in advance how many bytes are needed in a Fortran string in order to receive the content of a `DOMstring`.

- `f90xml_str_toFortran`: converts a `DOMstring` object into a Fortran string. This routine's parameters are a `DOMstring`, a Fortran string, an `INTEGER` zero-based offset and a `LOGICAL` return value. The content of the `DOMstring` will be translated to the Fortran string starting at the position provided by the offset. No more characters than the length of the Fortran string will be moved. The `LOGICAL` return value is `.TRUE.` if the `DOMstring` has been extracted up to the last character, otherwise is `.FALSE.`. This routine makes it possible to read long string data in a chunked way, regardless of the actual size of the `DOMstring` and the Fortran string.

- `f90xml_str_print`: prints the `DOMstring` to standard output. Returns "void".

- `f90xml_str_equal`: compares a `DOMstring` with a Fortran string. Returns `.TRUE.` if the strings are equal, otherwise `.FALSE.`

- `f90xml_str_unref`: delete the `DOMstring` object. Returns void

Errors The F77/F90xml library returns the error status in the last `INTEGER` argument of each subroutine. The actual value depends on the kind of error, and a list of possible situations has been foreseen. The `ERR_NO_ERROR` value, which evaluates to zero, is returned when no error occurs. The library checks for various error conditions, such as

- An actual argument is not of the expected type, for example if a `DOMstring` is given where a `DOMelement` is expected;

- A referenced object has not an entry in the cached space;

- A `NullCode` is entered but the routine is unable to handle it;

- Internal errors returned by the gdome2 library.

Library architecture and Fortran 77 interface Standard Fortran 77 expects names limited to 6 characters, although at our knowledge no recent Fortran 77 compilers impose this strict limit. Deploying the complete DOM interface in such limited namespace would have been resulted in names collisions. This problem was solved using Multiplexers, in order to provide access to the complete DOM interface with a reduced namespace footprint. The Fortran 77 interface is based on few multipurpose C functions named multiplexers. The role of multiplexers is to create a many-to-one correspondence between a set of gdome2 routines and a single multiplexer function, on the basis of arguments and return value similarities in terms of number and type. Each C multiplexer is directly mapped in a one-to-one relationship to a Fortran 77 `SUBROUTINE`. Some extra code was realized in order to interface Fortran77 and C, due to the different way they manage strings, memory, routine names and parameters. These multiplexers are the real core of the library. When a multiplexer is called, it dispatches (de-multiplexes) the call to the appropriate function within the subset it describes. In turn, this function performs the actual call to the gdome2 routine. To select which routine to call, a string containing the name of the routine is passed as an argument. Internally, this information is used to invoke the correct function. Each multiplexer routine and its Fortran interface have a conventional name, that refers to the number and type of arguments it accepts. All the Gdome2 routines have been classified in terms of their signature (the number and type of accepted parameters and the returned value) and a short name has been devised for each set. Routines with the same signature are handled by the same multiplexer.

As an example, the gdome2 functions given below:

```
GdomeNode* gdome_el_firstChild(GdomeElement *self, GdomeException *exc);
GdomeNode* gdome_el_lastChild (GdomeElement *self, GdomeException *exc);
```

can be used in a C program in the following way:

```
GdomeElement *elem;
GdomeNode *first, *last;
GdomeException exc;

/* <... get elem by some other call ...> */

first = gdome_el_firstChild(elem, exc);
last  = gdome_el_lastChild (elem, exc);
```

This is how the same functions can be called from a F77 program:

```
   CHARACTER*128 fnName
```

```
       INTEGER first, last, elem, err
!
C <... get elem by some other call ...>
!
       fnName='el_firstChild'
       CALL xp3t1(first,fnName,elem,err)
!
       fnName='el_lastChild'
       CALL xp3t1(last,fnName,elem,err)
```

The function name is case sensitive and has to be exactly the same of the gdome2 function, stripped of the `gdome_` prefix. Since in F90 the restriction on the names length is not so critical, the F90 interface can adhere to the DOM convention and adopt significant and standard names for the routines. The Fortran 90 module is realized simply mapping each subroutine to the corresponding multiplexer. This approach was chosen mainly in order to reduce the development cost, since the library can be created in an automatic way. A second reason was the idea to keep the potential Fortran 77 compatibility. A large part of the library is developed using XML technology. An XML file contains all the information to create the binding routines grouped in the same C multiplexers. The C multiplexers and the Fortran 90 module are automatically generated from this XML file. The file is parsed by a script in Python which collects the needed information, and deploys the C code. The Fortran 77 interface is closely related to the internal implementation of the library, therefore is important by itself, even if not used by client codes.

Chapter 11

Wrappers and Workflow: How we used the libraries

Based on the Q5cost data format and using the library for handling the I/O operations, we wrote some interface programs (wrappers) for converting data from a particular ab-initio program system to Q5cost and vice versa. In general, those wrappers should accomplish a quite simple goal: read quantities stored in a given data format and write them in a different data format using (when possible) the specific I/O library for the two formats. The Q5cost library we propose here can be used to simplify the job of managing data in the Q5cost data format. A schematic representation of the present situation can be seen in the figure. Two zero-level programs (Columbus and Dalton) have been fully integrated, and their integrals can actually be converted into the Q5cost format. The Dalton+FE box refers to the Ferrara four index transformation that can transform the Dalton integrals from the atomic basis to the molecular one.

Moreover a project has started to officially integrate Q5Cost in a MOLCAS module to be distributed with the future versions of the code, the same kind of official integration is scheduled to be done with DALTON and Gamess.

Columbus is one of the most popular ab initio suites, with several important and useful features. It is mainly based on a very efficient implementation of a direct Multi-Reference CI method with evaluation of analytic derivatives and molecular properties in several electronic states. The multi-reference approach makes it possible to describe the interaction of different states, very important for the study of non-adiabatic processes. In addition, Columbus is free and open-source, available to everyone for non-commercial purposes.

The DALTON program allows convenient, automated determination of a large number of molecular properties based on an SCF, MP2, Coupled Cluster, or MCSCF reference

Figure 11.1: A Schemating representation of the integrated system available wrappers

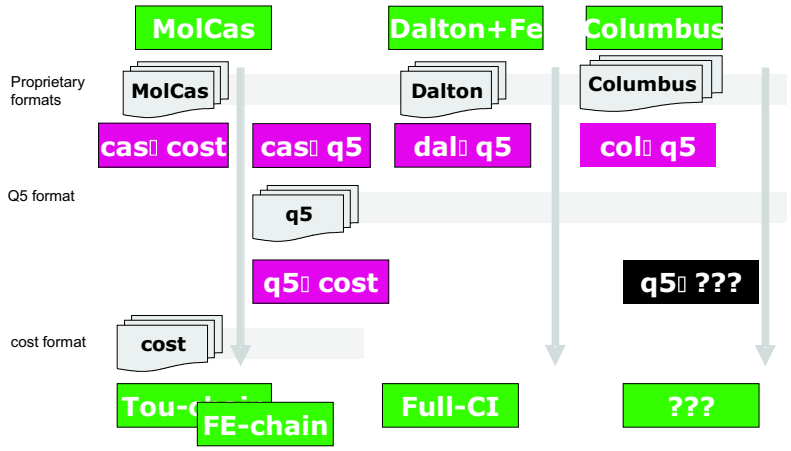

wave function. The program consists of six separate components, developed more or less independently. In particular HERMIT is the integral generator, generating ordinary atomic and molecular integrals appearing in the time-independent, non-relativistic Schrödinger equation, as well as an extensive number of integrals related to different molecular properties. As well as Columbus, Dalton is a free open source program, easily accessible to the scientific community.
Molcas is a quantum chemistry software developed by scientists to be used by scientists. It is a commercial software widely used by the researchers in our groups. For this reason it was among the first to be wrapped even if in a limited way due to the fact that Molcas authors are not directly involved in the project.
Several wrappers have been written in order to take data from these general programs and convert them into a Q5cost file: cas2q5 converts data from Molcas, dal2q5 from Dalton and the Ferrara transformation, col2q5 from Columbus.
FullCI is a program designed to compute energies and eigenvectors at a FCI level, together with first and second order properties (both static and dynamic at real or imaginary frequencies) and transition moments. It requires pre-computed integrals in molecular orbital base, so it has to be interfaced with a zero level program. FCI code originally used MO integrals produced by the 4 index transformation contained in the DYCI-5 suite of programs by A. O. Mitrushenkov; the latter is interfaced with the Molpro 2000.1 code. However presently, it is fully integrated with Q5cost, so it can read data both in its native format and from q5 files, and no wrapper is required.
The Toulouse chain is composed of a set of programs to perform CAS-SCF and MR-CI calculations. Special emphasis is put on the use of local orbitals, and an "a priori" localization procedure has been developed in Toulouse, in collaboration with the Ferrara Group. Using this algorithm, CAS-SCF or quasi-CAS-SCF solutions can be obtained as a combination of orbitals spatially located in a given region of the molecule. This allows a very fine control over the nature of the active space, so avoiding many of the convergence problems that often plague the CAS-SCF algorithms.
The Ferrara Chain mainly consists of a perturbation theory suite of programs based on the NEVPT (second- and third-order, Quasi-Degenerate PT) formalism. It is suitable for the treatment of Multi-Reference problems, and avoids the problem of intruded states that plague other perturbative treatments. A version working with non-canonical orbitals has been developed, allowing the application of this technique to the case of local-orbital descriptions.
The Toulouse and Ferrara chains take integral data from MOLCAS via a common format (MolCost), that was proposed in the past by the same group of researchers as a first attempt to allow code to communicate. It is simply based on a collection of binary files and

a coded file in form of a FORTRAN namelist. The present data format (Q5cost + Qcml) is a further elaboration of this original data model. In this case we decided to write a wrapper (q5_to_cost) to translate the Q5cost format into the MolCost format, so giving access to all the programs in two chains. In the future the two chains will progressively migrate from MolCost toward Q5Cost, so the use of this particular wrapper should be thought only as a temporary solution.

11.1 Final Considerations

Wrapper design, or code direct interfacing, has been demonstrated to be a quite easy and transparent task, and should be performed by the authors of the specific code. Three libraries are required:

- HDF5
- Q5cost
- F77XML (or some other library for managing XML files)

the latter can be either installed at a system level or at user level, ensuring the maximum of flexibility even in third parts supercomputer environment. Moreover a thorough understanding of the program to be wrapped is needed (the source code itself if a direct interfacing is to be done). An input wrapper for a given code needs to read data from the common format (using the Q5cost and F77Xml library) and write those pieces of information in the proprietary format of the code, using an ad-hoc I/O library when available. An output wrapper for a given code reads proprietary data (using ad-hoc I/O libraries in case) and writes them in the common format using the Q5COST and F77XML libraries. We would like to underline how those very first wrappers have given the opportunity of interfacing programs that were not able to communicate before, and we stress that all the tests performed gave correct results. A preliminary application of this interface to the study of dispersion interactions has been performed. The Q5cost library is easy to use and based on chemical concepts. It should be used by chemists for designing the wrappers of their own codes or even for a direct interface as in the case of the FCI code. Further extensions are needed, for example for adding other quantities to the data format. However, we expect this to be a quite simple task, requiring only minor changes in data format and simple additions to the library, due to its high modularity. In fact, some important quantities, like for instance wave function coefficients, and library

features,like the possibility to store the integrals without corresponding indices, are still missing. This may limit the usability of the proposed data format, and we are therefore planning to implement them as soon as possible.

Part IV

Conclusions

Chapter 12

Conclusions

During this thesis two main issues have been taken into account:

- The application of innovative mainly one body (i.e perturbative) methods for the determination of electric properties and intermolecular forces at FCI and Coupled Cluster level
- The development of a Grid Oriented Common Format for Quantum Chemistry

As concerns the first point we showed and described the application of a new interpolative method to compute polarizabilities and intermolecular forces via Casimir Polder formula. This method is based on a rational interpolation of the frequency dependent polarizability equation and allows the determination of dispersion coefficients with reasonable accuracy in the mean time significantly cutting the requested number of computed polarizability values and hence the computational time. It has to be underlined, however that the method is quite sensitive to the choice of the interpolation nodes, i.e. the values of frequency for which polarizability is directly computed. An empirical formula allowing a wise choice of such frequencies has been presented. Using the present method higher order dispersion coefficients (C_7) for LiH were derived for the first time, C_6 dispersion coefficients for the BeH_2 homodimer were derived for the first time too. Moreover we presented a Lanczos Davidson based method (LSDK) which computes dispersion coefficients expanding the London formula in a set of pseudostates iteratively generated. LSDK was applied to the LiH molecule and the Be atom and proved its efficacy producing results of quality comparable to the numerical quadrature of the Casimir Polder formula, both for diagonal and non-diagonal matrix elements. The diagonal elements results moreover, are variationally bounded, even if a strict convergence criterion based on the residual norm is still missing. Convergence test is performed on the value

of the dispersion constant itself, but unfortunately such an approach is not capable to discriminate between actual convergence or stagnation. The total computational time one needs to get sensible results appears to be shorter than that required by classical Casimir Polder and even interpolative method. This is also due to the fact Casimir Polder and interpolative methods require imaginary frequency polarizabilities, hence one has to solve perturbative equations in the complex field, therefore each iteration require twice the time one needs for a real field computation. As the accuracy is concerned we can easily see how the values obtained with LSDK appears to be better (i.e. closer to the Casimir Polder ones) than corresponding values computed by the interpolative method, moreover the dependence on the correct choice of frequencies is eliminated. Finally a variational method based on the resolution of small Sylvester equations has been applied to the computation of dispersion interactions for the BH molecule and for the Ne atom. A convenient matrix notation suggests a straightforward way to compute the residual norm in order to check the convergence. It can, also, be shown that expanding the solution as a linear combination of tensor products of CI vectors of the isolated molecules the classical Casimir Polder quadrature can be reduced to a non optimized solution of the present variational conditions. While this method gives the lower variational bound to the exact solution (exact in the FCI sense), the simple application of Temple's VP extended to perturbation theory allows to obtain the upper bound. We would like to recall the Neon problem involved the resolution of a FCI whose configuration space was bigger than one billion of symmetry adapted determinants, giving rise (to the best of our knoweldge) to the biggest FCI computation of second order properties even performed. As concerns the Ne_2 dimer problem we, also, performed a test study to asses the role of the BSSE and CP correction in the supramolecular determination of long range dispersion interactions. In particular results of dispersion coefficients obtained from a proper interpolation of the interatomic energy potential curve where compared with the ones calculated by our variational method and with experimental DOSD results. This study showed that while CP correction works reasonably well for equilibrium properties both at CI and CC level, the lack of size consistency seriously affects the CI corrected long range tail of the potential curve, making it useless to compute long range dispersion coefficients. In the same study we also obtained as a by product spectroscopic properties of Ne_2 dimer which are in good agreement both with recent experiments and with previous computations. At Coupled Cluster R_{12} level we started the implementation of analytical computation of first and second order electric properties in the Bratislava's code. It has to be underlined that while at conventional CC level many code are able to perform the analytical derivation of electric properties at CC-R_{12} level, to the best of our knowledge, no such code actually exists (the only available code performs these calculations at MP2-

R_{12} level). As concerns the first order properties (i.e. dipole moments) the first results have been shown for some small molecules (about 10 electrons), computations have been easily performed with basis set up to 300 spin orbitals, and they show that the inclusion of R_{12} functions plays an important role in speeding up the convergence towards basis set limit (although for dipole moment the influence is somehow less pronounced than for energies). The implementation of static and dynamic second order properties has not be completed yet.

As far as the second point is considered we designed and wrote an efficient file format for easy file interchange among codes and platforms. The driving force beneath this project is mainly due to the need of an easy interfacing of different QC codes, expecially in the computation of intermolecular forces. Our format is based on Xml (Qcml) for the small dimension data (i.e. geometry, basis set and so on) and HDF5 (Q5Cost) for big dimension data (mainly atomic or molecular integrals and orbital coefficients). Moreover we wrote two FORTRAN libraries to access Q5Cost files (q5cost library) and Xml files (F90Xml). Using these two informatics tools we wrote the first interfaces among different codes and we performed the first scientific applications.

Acknowledgments

There are many and many people that need to be acknowledge to have made possible this work.
First of all many thanks are due to my supervisor Professor G. L. Bendazzoli, for his constant attention and kindness, for the usefull discussions I had with him, and for having taught me quantum chemistry and many other things.
I would like moreover to thank Dr. Elda Rossi for the nice work we had, and we are still having together, and for all the coffees she offered me at CINECA.
Thanks to Prof. Stefano Evangelisti for having invited me in Toulouse, and for having offered me his friendship.
Thanks to Professor Jozef Noga who made possible my visit in Bratislava.
Many thanks to all the other components of my research group: Prof. Paolo Palmieri, Prof. Riccardo Tarroni and the now french-german Dr. Алешандер Олигович (Саша) Митрушенков.

Sincere acknowledgments are due to all the people in our Bologna department, in Toulouse laboratory and in Bratislava institute (I will not cite them name by name but I nonetheless thank them all).

Finally thanks to all the people who share (the Archaeologist Francesca, Gabriele, Ivano il Bombarolo, Enzo Nelson PhD candidate, Giampaolo the Calendar Man), or shared (Roberta, Valentina, Fabrizio, Luca), or actually partially share (Mirko tutor Minzoni) the windowless office with me: they make my days easier and more pleasant even while I deal with my integrals.

And at the very end, as some people would say: last but not least, thanks to all the guys with whom I spent or I am spending pleasant faculty days (Mauro from Transilvania, Lorella, Mr paranoia il Sangi, Claudione, Feffe, il Micio, Gary aka Precoso, Valentina, Willy and many many others) and many thanks to all the fellows who almost every day

share with me the train plus bus journey toward the Faculty (Gabriele from Pracchia with Boozes, Silvia Dr. Mgr. Tozzi, PhD candidate, Nicola Soft Music Low Volume Guy, Federico Chainsaw, Isacco the Train Man, Terry Pure British Capers).

Bibliography

[1] A. J. Stone, "The Theory of Intermolecular Forces", Clarendon Press Oxford (**1996**).

[2] V. Magnasco, R. Mc Weeny in "Theoretical Models of Chemical Bonding", Z. B. Maksic (Ed.) Springer-Verlag (**1991**).

[3] A. D. Buckingham in S. Bratos, R. M. Pick (Ed.s) Vibrational Spectroscopy of Molecular Liquids and Solids, Plenum New York (**1980**).

[4] J. A. Pople, Faraday Discuss. Chem. Soc., 73 (**1982**), 7.

[5] J. H. Van Lenthe, J.G.C.M. Van Duijndevelt, Van de Rijdt, F. B. Van Duijndevelt; Adv. Chem. Phys., 69 (**1987**), 521.

[6] B. Jeziorski, W. Kolos, in H. Ratajcaz, W. J. Orville Thomas (Ed.s), Molecular Interactions vol. 3, Wiley, New York.

[7] A. D. Buckingham, P. W. Fowler, J. H. Hutson ; Chem. Rev., 88 (**1988**), 963.

[8] A.R. Edmonds; Angular Momentum in Quantum Mechanics, (**1957**) Princeton University Press.

[9] R. Loudon, "The Quantum Theory of Light", Oxford University Press (**1973**).

[10] H. C. Longuet Higgins, Proc. R. Soc. London, Ser. A, (**1956**), 235.

[11] J. O. Hirschfelder, W. J. Meath, Adv. Chem. Phys. 12 (**1967**) 3.

[12] F. London; Z. Phys. Chem., B11 (**1930**), 222.

[13] H. B. Casimir, D. Polder, Phys. Rev., 73 (**1948**), 360.

[14] A. Ünsold; Zeit. Phys. A (**1927**) 43, 563.

[15] V. Magnasco, C. Costa, G. Figari; J. Mol. Struct. (Theochem), 206, (**1990**), 235.

[16] S. F. Boys, F. Bernardi; Mol. Phys., 19, (**1970**), 553

[17] I. Mayer; Int. Jour. Quant. Chem., 70 (**1998**), 41.

[18] Amsterdam Density Function a software package:
http://www.scm.com/Welcome.html

[19] DALTON, a molecular electronic structure program, Release 2.0 (2005) see http://www.kjemi.uio.no/software/dalton/dalton.html

[20] R. D. Amos, N. C. Handy, P. J. Knowles, J. E. Rice, A. J. Stone; J. Phys. Chem., 89, (**1985**), 2186.

[21] V. Magnasco, G. Figari; Mol. Phys. 62, (**1987**), 1419.

[22] B. Jeziorski, R. Moszynski, A. Ratkiewicz, S. Rybak, K. Szalewicz, H.L. Williams published in Methods and Techniques in Computational Chemistry: METECC-94, edited by E. Clementi, STEF, Cagliari, (**1993**), Vol. B, p. 79.

[23] G. L. Bendazzoli, S. Evangelisti; published in Computational Chemistry Aspects and Perspectives, edited by G. L. Bendazzoli, P. Palmieri, CNR Milano (**1995**) p. 9.

[24] J. C. Slater; Phys. Rev., 34, (**1929**), 1293.

[25] H. Weyl; The Theory of Groups and Quantum Mechanics, Dover, New York (**1931**).

[26] A. Bongers; Chem. Phys. Lett.; 49, (**1977**), 393.

[27] B. Roos; Chem. Phys. Lett., 15, (**1972**), 153.

[28] N. C. Handy; Chem. Phys. Lett., 74, (**1980**), 280.

[29] P. Saxe, H. F. Schaeferer III, N. C, Handy; Chem. Phys. Lett., 79, (**1981**), 202.

[30] R. J. Harrison, N. C, Handy; Chem. Phys. Lett., 95, (**1983**), 386.

[31] P. E. M. Siegbhan; Chem. Phys. Lett., 109, (**1984**), 417.

[32] P. J. Knowles, N.C. Handy; Comp. Phys. Lett., 95 (**1983**), 386.

[33] J. Olsen, B. O. Roos, P. Jorgensen H. J. A. Jensen, J. Chem. Phys., 89 (**1988**), 2185.

[34] G. L. Bendazzoli, S. Evangelisti; J. Chem. Phys., 98 (**1993**), 3141.

[35] E. R. Davidson; J. Comp. Phys., 17 (**1975**), 87.

[36] G. L. Bendazzoli, S. Evangelisti; Adv. Quant. Chem., 39 (**2001**), 189.

[37] P. O. Löwdin; Int. J. Quant. Chem., II, (**1968**).

[38] J. E. Meyer, M. G. Meyer; Statistical Mechanic, Wiley New York (**1940**).

[39] H.G. Kümmel; A biography of the coupled cluster method, in R.F. Bishop, T. Brandes, K.A. Gernoth, N.R. Walet, Y. Xian (Eds.), World Scientific Publishing, Singapore, (**2002**), pp. 334.

[40] J. Čížek; J. Comp. Phys., 45 (**1966**), 4256.

[41] R. J. Bartlett, C. E. Dykstra, J. Paldus; in Advanced Theories and Computational Approaches to the Electronic Structure of Molecules, C. E. Dykstra, (Ed.), D. Reidel, Dordrecht, (**1984**), pp. 127-159.

[42] F. E. Harris, H. J. Monkhorst, D. L. Freeman; Algebraic and Diagrammatic Methods in Many-Fermion Theory, Oxford Press, New York, (**1992**).

[43] E. Merzbacher; Quantum Mechanics, 2nd ed., John Wiley and Sons, New York, (**1970**).

[44] F. E. Harris, H. J. Monkhorst, D. L. Freeman; Algebraic and Diagrammatic Methods in Many-Fermion Theory, Oxford Press, New York, (**1992**).

[45] G. C. Wick; Phys. Rev., 80 (**1950**), 268.

[46] J. C. Slater; Phys. Rev., 31 (**1928**), 333.

[47] E. A. Hylleras, Z. Phys., 54 (**1929**), 347.

[48] T. Kato; Commun. Pure Appl. Math., 10 (**1957**), 151.

[49] W. Kutzelnigg; Theor. Chim. Acta, 68 (**1985**), 445.

[50] W. Kutzelnigg, W. Klopper; J. Chem. Phys., 94 (**1991**), 1985.

[51] W. Klopper; Chem. Phys. Lett., 186 (**1991**), 583.

[52] W. Klopper, J. Noga; in Explicitly Correlated Wave Functions Methods in Chemistry and Physics. J. Rychlewski (Ed.), Kluwer Academic Press Springer Berlin, (**2003**), 149.

[53] G. Figari, V. Magnasco; Chem. Phys. Lett., 374 (**2003**), 527.

[54] M. Abramowitz, in M. Abramowitz, I. A. Stegueds (Ed.), Handbook of Mathematical Functions, Dover, New York (**1965**), 17.

[55] B.N. Delone, in A. D. Aleksandrov, A. N. Kolmogorov. Ma. A. Lavrent'ev (Eds.). Mathematic, Its Contents, Methods and Meaning, vol. 1, MIT Press, Cambridge (MA), (**1964**), 266.

[56] G. L. Bendazzoli, A. Monari, G. Figari, M. Rui, C. Costa, V. Magnasco; Chem. Phys. Lett., 414 (**2005**), 51.

[57] G. L. Bendazzoli, A. Monari, V. Magnasco, G. Figari, M. Rui; Chem. Phys. Lett., 382 (**2003**), 393.

[58] G.L. Bendazzoli, V. Magnasco, G. Figari, M. Rui, Chem. Phys. Lett.; 300 (**2000**), 146.

[59] G.L. Bendazzoli, in: E.J. Brändas, E.S. Kryachko (Eds.),Fundamental World of Quantum Chemistry: A Tribute Volume to the Memory of Per-Olov Löwdin, Kluwer, Dordrecht, (**2003**) p. 657.

[60] D. Tunega, J. Noga; Theoret. Chim. Acta 100 (**1998**), 78.

[61] A.J. Sadlej; Collect. Czech. Chem. Commun. 53 (**1988**), 1995.

[62] P.W. Langhoff, M. Karplus; J. Chem. Phys. 53 (**1970**), 233.

[63] P.F. Bernath, A. Shayesteh, K. Tereszchuk; R. Colin, Science 297 (**2002**), 1323.

[64] A. Shayesteh, K. Tereszchuk, P.F. Bernath; R. Colin, J. Chem. Phys. 118 (**2003**), 3622.

[65] A. Abdurahman; J. Phys. Chem. A, 107 (**20003**), 11547.

[66] G. L. Bendazzoli, A. Monari; Chem. Phys., 306 (**2004**), 153.

[67] M.G. Papadopoulos, J. White, A.D. Buckingham; J. Chem. Phys. 102 (**1995**) 371.

[68] G.H. Golub, C.F. van Loan; Matrix Computations, North Oxford Academic, Oxford, (**1983**).

[69] R.L. Graham, D.L. Yaeger, J. Olsen, P. Jørgensen, R. Harrison, S. Zarrabian, R. Bartlett; J. Chem. Phys. 85 (**1986**) 6544.

[70] J. Komasa; Phys. Rev. A, 65 (**2001**) 12506.

[71] Bendazzoli G. L., Int. J. Quant. Chem., **2005**, 104, 38-51.

[72] A. Halkier, H. Larsen, J. Olsen, P. Jørgensen, J. Chem. Phys.; 110 (**1999**), 734.

[73] H. Larsen, J. Olsen, C. Hattig; Chem. Phys. Lett., 307 (**1999**), 235.

[74] P. D. Robinson; J. Phys. A, 2 (**1968**), 193.

[75] A. Monari, G. L. Bendazzoli, S. Evangelisti, C. Angeli, N. Ben Amor, S. Borini, D. Maynau, E. Rossi; J. Chem. Th. Comp. in press (available on line at http://pubs3.acs.org/acs/journals/jctcce/index.html)

[76] Clusters of Atoms and Molecules; Springer: Berlin, **1994**.

[77] F. Sebastianelli, Baccarelli, C. Di Paola, F. A. Gianturco; J. Chem. Phys., 119 **2003**, 5570.

[78] F. Filippone, F. A. Gianturco; Europhys. Lett., 44 **1998**, 585.

[79] D. Spelsberg, T. Lorentz, W. Meyer W.; J. Chem. Phys., 99 **1993**, 7845.

[80] T. H. Dunning Jr.; J. Chem. Phys., 90 **1989**, 1007.

[81] R. A. Kendall, T. H. Dunning Jr., R. J. Harrison; J. Chem Phys., 96 **1992**, 6796.

[82] D. E. Woon, T. H. Dunning Jr.; J. Chem. Phys., 100 **1994**, 2975.

[83] Basis sets were obtained from the Extensible Computational Chemistry Environment Basis Set Database, Version 02/25/04, as de veloped and distributed by the Molecular Science Computing Facility, Environmental and Molecular Sciences Laboratory which i s part of the Pacific Northwest Laboratory, P.O. Box 999, Richland, Washington 99352, USA, and funded by the U.S. Department of Energy. The Pacific Northwest Laboratory is a multi-program laboratory operated by Battelle Memorial Institute for the U.S. Department of Energy under contract DE-AC06-76RLO 1830. Contact Karen Schuchardt for further information.
http://www.emsl.pnl.gov/forms/basisform.html.

[84] G. L. Bendazzoli, S. Evangelisti; J. Chem. Phys., 98 **1993**, 3141.

[85] *MOLPRO is a package of ab initio programs written by*, H.J. Werner, P.J. Knowles, J. with contribution from Almlöf, R.D. Amos, A. Berning, M.J.O. Deegan, F. Eckert, S.T. Elbert, C. Hampel, R. Lindh, W. Meyer, A. Nicklass, K. Peterson, R. Pitzer, A.J. Stone, P.R. Taylor, M.E. Mura, P. Pulay, M. Schütz, H. Stoll, T. Thorsteinsson, and D.L. Cooper.

[86] G. L. Bendazzoli, S. Evangelisti; Gazz. Chim. Italiana, 126 **1996**, 619.

[87] CASDI *ab initio* progam, Toulouse University. See also N. Ben Amor; D. Maynau; Chem. Phys. Lett. 286, **1998**, 211.

[88] B. Numerov; Publ. Obs. Central Astrophys. Russ., 2 **1923**, 188.

[89] B. Lindberg; J. Chem. Phys., 88 **1988**, 3805.

[90] F. Passarini, *Tesi di Laurea*, Bologna University.

[91] *Molcas 4 program package*, K. Andersson, M.R.A. Blomberg, M.P. Fülscher, G. Karlström, R. Lindh, P-Å. Malmqvist, P. Neogrády, J. Olsen, B.O. Roos, M. Sadlej, A.J. Schütz, L. Seijo, L. Serrano-Andrés, P.E.M. Siegbahn, and P.-O. Widmark, Lund University, Sweden, (**1997**).

[92] C. Angeli, G. L. Bendazzoli, S. Borini, R. Cimiraglia, A. Emerson, S. Evangelisti, D. maynau, A. Monari, E. Rossi, J. Sanchez-Marin, P. G. Szalay, A. Tajti. *submitted to Int. J. Quant. Chem.*

[93] S. Borini, A. Monari, E. Rossi, A. Tajti, C. Angeli, G. L. Bendazzoli, R. Cimiraglia, A. Emerson, S. Evangelisti, D. Maynau, J. Sanchez-Marin, P. G. Szalay. *submitted to J. Chem. Inform. and Mod.*

[94] H. Hanspeter, B. Kirchner; J. Solca, G. Steinebrunner; Chem. Phys. Lett., 266 **1997**, 388.

[95] R. A. Aziz; M. J. Slamam; Chem. Phys. 130, **1989**, 187.

[96] A. Wüest, F. Merkt F.; J. Chem. Phys. 118, **2003**, 8807.

[97] D. E. Woon; J. Chem. Phys., 100 **1994**, 2838.

[98] R. J. Gdanitz; Chem. Phys. Lett., 348 **2001**, 67.

[99] A. Halkier, T. Helgaker, P. Jorgensen, W. Klopper, E. Koch E., J. Olsen, A. K. Wlison; Chem. Phys. Lett., 286 **1998**, 243.

[100] A. Kumar, W. J. Meath; Can. J. Chem., 63 **1985**, 1616.

[101] A. Nicklass, M. Dolg, H. Stoll, H. Preuss; J. Chem. Phys., 102 **1995**, 8942.

[102] J. F. Stanton, J. Gauss; J. Chem. Phys. 103 (**1995**), 2574.

[103] R. J. Bartlett, J. F. Stanton; in Reviews in Computational Chemistry, K. Lipotwitz D.B. Boyd (Eds.), VCH New York, (**1994**).

[104] P. Piecuch, A. E. Kondo, V. Spirko, J. Paldus; J. Chem. Phys. 104 (**1996**), 4699.

[105] J. F. Stanton, R. J. Bartlett; J. Chem. Phys., 99 (**1993**), 7029.

[106] W. Klopper; J. Chem. Phys., 120 (**2004**), 10890.

[107] P. Valiron, S. Kedzuch; J. Noga, Chem. Pjys. Lett. 367 (**2003**), 723.

[108] J. F. Stanton, R. J. Bartlett; J. Chem. Phys., 99 (**1993**), 5178.

[109] I. Foster, C. Kesselman; The Grid. Blueprint for a new computing infrastructure. Morgan Kaufman, (**1998**).

[110] Madhu Chetty, Rajkumar Buyya; Weaving Computational Grids: How Analogous Are They with Electrical Grids?, Computing in Science and Engineering, (**2002**).

[111] COST in Chemistry Action D23
http://costchemistry.epfl.ch/docs/D23/d23.htm

[112] E. Rossi, A. Emerson, S. Evangelisti, Lect. Not. in Comp. Science, 2658 (**2003**), 316

[113] Cml: Chemical Markup Language http://www.xml-cml.org/

[114] A.Holmer; XML IE5-Programmer's Reference, Wrox Press, Chicago, IL, USA (**1999**);
and http://www.w3.org/XML

[115] HDF5 a general purpose library and file format for storing scientific data
http://hdf.ncsa.uiuc.edu/HDF5/

[116] COLUMBUS, an ab initio electronic structure program, release 5.9.1 (2006). H. Lischka, R. Shepard, I. Shavitt, R. M. Pitzer, M. Dallos, Th. MÃ¼ller, P. G. Szalay, F. B. Brown, R. Ahlrichs, H. J. Böhm, A. Chang, D. C. Comeau, R. Gdanitz, H. Dachsel, C. Ehrhardt, M. Ernzerhof, P. Höchtl, S. Irle, G. Kedziora, T. Kovar, V. Parasuk, M. J. M. Pepper, P. Scharf, H. Schiffer, M. Schindler, M. SchÃ¼ler, M. Seth, E. A. Stahlberg, J. G. Zhao, S. Yabushita, Z. Zhang, M. Barbatti, S. Matsika, M. Schuurmann, D. R. Yarkony, S. R. Brozell, E. V. Beck, and J.-P. Blaudeau.

[117] M. Kàllay, P. G. Szalay, R. Surján; J. Chem. Phys., 117 (**2002**), 980.

[118] C. Angeli, R. Cimiraglia, J-P. Malrieu,; J. Chem. Phys., 117 (**2002**), 9138.

[119] V. Vallet, L. Maron, C. Teichteil, J.-P. Flament; J. Chem. Phys. 113 (**2000**), 1391.

[120] J. M. Junquera-Hernandez, J. Sánchez Marin, D. Maynau. PROP University of Valencia (Spain) and University of Toulouse (France) **2002**.

[121] M. W. Schmidt, K. K. Baldridge, J. A. Boatz, S. T. Elbert, M. S. Gordon, J. H. Jensen, S. Koseki, N. Matsunaga, K. A. Nguyen, S. Su, T. L. Windus, M. Dupuis, J. A. Montgomery Jr; J. Comp. Chem., 14 (**1993**), 1347.

[122] K. K. Baldridge, K. Bhatia, J. P. Greenberg, B. Stearn, S. Mock, W. Sudholt, S. Krishnan, S., A. Bowne, C. Amoreira, Y. Potier; Invited paper: LSGRID Proceedings, (**2005**), in press.

[123] Ph. Ayala, G. E. Scuseria; J. Chem. Phys., 110 (**1999**), 3660.

[124] C. Hampel, H. J. werner; J. Chem. Phys., 104 (**1996**), 6286.

[125] G. E. Scuseria, Ph. Ayala; J. Chem. Phys., 111 (**1999**), 8330.

[126] S. Borini, S. Evangelisti, A. Monari, E. Rossi; "A FORTRAN interface for code interoperability in Quantum Chemistry: 2. The F77/F90xml library", *to be submitted*.

[127] M. Yang, R. E. McGrath, M. Folk; "Performance Study of HDF5-WRF IO", WRF Workshop, (**2004**)

[128] Specification of XML/DOM can be found at the site (http://www.w3.org/DOM).

[129] A. Garcia, xmlf90, (http://lcdx00.wm.lc.ehu.es/ag/xml/index.html);
A. Markus; xml-fortran (http://sourceforge.net/projects/xml-fortran/);
M. Rentmeester, XML (http://nn-online.org/code/xml/).

[130] P.Casarini, L.Padovani; "The Gnome DOM Engine", Extreme Markup Laes 2001 Conference, (**2001**);
see also http://gdome2.cs.unibo.it/